BRNO UNIVERSITY OF TECHNOLOGY

VYSOKÉ UČENÍ TECHNICKÉ V BRNĚ

FACULTY OF CHEMISTRY

FAKULTA CHEMICKÁ

INSTITUTE OF MATERIALS SCIENCE

ÚSTAV CHEMIE MATERIÁLŮ

RHEOLOGICAL EVALUATION OF THERMOSENSITIVE MACROMONOMER PHOTOGELATION IN AQUEOUS ENVIRONMENT

REOLOGICKÉ HODNOCENÍ FOTOGELACE TERMOCITLIVÝCH MAKROMONOMERŮ VE VODNÉM PROSTŘEDÍ

MASTER'S THESIS

DIPLOMOVÁ PRÁCE

AUTHOR Bc. Eva Habánková

AUTOR PRÁCE

SUPERVISOR doc. Ing. Lucy Vojtová, Ph.D.

VEDOUCÍ PRÁCE

BRNO 2017

VYSOKÉ UČENÍ TECHNICKÉ V BRNĚ FAKULTA CHEMICKÁ

Zadání diplomové práce

Číslo práce:	FCH-DIP1084/2016
Ústav:	Ústav chemie materiálů
Studentka:	**Bc. Eva Habánková**
Studijní program:	Chemie, technologie a vlastnosti materiálů
Studijní obor:	Chemie, technologie a vlastnosti materiálů
Vedoucí práce:	**doc. Ing. Lucy Vojtová, Ph.D.**
Akademický rok:	2016/17

Název diplomové práce:

Reologické hodnocení fotogelace termocitlivých makromonomerů ve vodném prostředí

Zadání diplomové práce:

1) Literární rešerše na téma fotosíťování polymerů rozpustných ve vodě a reologie vzniklých gelů
2) Experimentální práce sledující viskoelastické chování termocitlivých makromonomerů fotosíťovaných během reologického měření ve vodném prostředí
3) Vyhodnocení vlivu jednotlivých fyzikálně–chemických parametrů na fotogelační proces
4) Závěr

Termín odevzdání diplomové práce: 19.5.2017

Diplomová práce se odevzdává v děkanem stanoveném počtu exemplářů na sekretariát ústavu. Toto zadání je součástí diplomové práce.

Bc. Eva Habánková
student(ka)

doc. Ing. Lucy Vojtová, Ph.D.
vedoucí práce

prof. RNDr. Josef Jančář, CSc.
vedoucí ústavu

V Brně dne 31.1.2017

prof. Ing. Martin Weiter, Ph.D.
děkan

ABSTRACT

The aim of this diploma thesis is to study the possibility of chemical crosslinking of biodegradable thermosensitive macromonomer α,ω-itaconyl-PLGA–PEG–PLGA in aqueous solutions at ambient and physiological temperature (37 °C). Macromonomer can be crosslinked physically due to hydrophobic interactions between hydrophobic PLGA and hydrophilic PEG. Double bonds from itaconic acid ending the macromonomer provide the possibility of additional chemical crosslinking by photopolymerization. This hybrid network enhances the mechanical stability and lifetime of the hydrogel. Photorheology as a powerful tool for the direct monitoring of the network formation was used to investigate mechanical properties during the irradiation. The possibility to chemically crosslink α,ω-itaconyl-PLGA–PEG–PLGA was initially proved by photopolymerization in bulk. For this purpose organosoluble photoinitiator ethyl (2,4,6-trimethylbenzoyl) phenyl phosphinate (TPO-L) was used. ATR-IR and real time-NIR spectroscopies confirmed double bond consumption. Photorheology showed that photopolymerization leads to higher storage modulus, however, chemical network has not been formed.

It was found that aqueous solutions of α,ω-itaconyl-PLGA–PEG–PLGA have highly time-dependant behaviour due to the thixotropy confirmed by shear rate sweeps. Later it was the reason for different initial modulus in photorheology. On the other hand it could also be an advantage if the material would be used for injecting.

Consequently, very efficient water soluble photoinitiator ethyl (2,4,6-trimethylbenzoyl) phenyl phosphinate (LiTPO) and light in the visible (VIS) range between 400 and 500 nm were used to initiate the reaction in aqueous solutions. It was discovered that the addition of LiTPO increases the pH of aqueous solutions. This results in higher amount of deprotonated carboxylic groups. Repulsive force between negative charges leads to the micelle destruction, when the certain concentration of LiTPO is exceeded. Nevertheless, at higher temperatures micelle structure can be again recovered due to hydrophobic interactions. It was found, that LiTPO shifts the region of gel stability to higher temperatures.

Micelles created by α,ω-itaconyl-PLGA–PEG–PLGA associate double bonds in their middle. This closeness is essential for later chemical crosslinking while hybrid network can be formed. Therefore, at 25 °C the best mechanical properties were achieved with the addition of LiTPO 0.1 wt. % while the addition of 3 wt. % did not lead to any chemical crosslinking. At 37 °C the addition of 0.5 wt. % and 1 wt. % of LiTPO lead to good mechanical properties. In general these hydrogels prepared at 37 °C showed better properties since these thermosensitive copolymers are mainly used as injectable drug delivery systems.

KEYWORDS

Thermosensitive hydrogel, crosslinking, photorheology

ABSTRAKT

Táto práca si dáva za cieľ chemicky zasieťovať biodegradovateľný makromonomér α,ω-itaconyl-PLGA–PEG–PLGA vo vodnom roztoku pri teplote okolia a pri teplote tela (37 °C). α,ω-itaconyl-PLGA–PEG–PLGA makromonomér môže vo vode vytvárať fyzikálnu sieť vďaka hydrofóbnym interakciám medzi hydrofóbnym PLGA a hydrofilným PEG. Vďaka dvojitej väzbe kyseliny itakonovej, ktorá je k makromonoméru pripojená na jeho koncoch sa naskytuje možnosť dodatočného chemického zasieťovania fotopolymerizáciou. Výsledkom je hybridná sieť, ktorá zvyšuje mechanickú stabilitu a životnosť hydrogélu. Na priame sledovanie formovania siete prostredníctvom zmeny mechanických vlastností bola v práci použitá fotoreológia. Možnosť chemicky zasieťovať α,ω-itaconyl-PLGA–PEG–PLGA bola najskôr overená fotopolymerizáciou bulku. Reakcia bola iniciovaná fotoiniciátorom etyl (2,4,6-trimetylbenzoyl) fenylfosfinátom (TPO-L). ATR-IR a Real Time-NIR potvrdili spotrebu dvojitých väzieb po ožiarení. Fotoreologické meranie ale ukázalo, že síce elastický modul rastie, chemická sieť sa netvorí.

Počas fotoreologických meraní vodných roztokov α,ω-itaconyl-PLGA–PEG–PLGA bol problém získať rovnaký počiatočný modul. Bolo zistené, že je to kvôli tixotropii vodných roztokov, ktorá bola neskôr potvrdená reologickými meraniami za postupného zvyšovania šmykovej rýchlosti. Tixotropia však môže byť aj výhodou, ak by bol materiál aplikovaný injekčne.

Fotopolymerizácia vodných roztokov bola uskutočnená v prítomnosti efektívneho vo vode rozpustného fotoiniciátora etyl (2,4,6-trimetylbenzoyl) fenylfosfinátu (LiTPO). Ako zdroj žiarenia bolo použité viditeľné svetlo v rozsahu vlnových dĺžok 400 až 500 nm. Bolo zistené, že prídavok LiTPO zvyšuje pH vodných roztokov makromonoméru, čo vedie k vyššej deprotonácii karboxylových skupín. Odpudivá sila medzi zápornými nábojmi pri určitej zvýšenej koncentrácii LiTPO vedie k deštrukcii micelárnej štruktúry. Napriek tomu môže byť micelárna štruktúra opäť obnovená pri vyššej teplote. Bolo totiž zistené, že LiTPO posúva oblasť stability fyzikálneho gélu k vyšším teplotám.

Micely združujú dvojité väzby pohromade a bolo dokázané, že je to nevyhnutný predpoklad pre následné chemické zasieťovanie a vytvorenie tak hybridnej siete. Preto najlepšie mechanické vlastnosti pri teplote 25 °C boli dosiahnuté pre prídavok LiTPO 0.1 hm.%, zatiaľ čo prídavok 3 hm. % neviedol ku žiadnemu chemickému zasieťovaniu. Pri 37°C prídavky 0.5 % a 1 % viedli k dobrým mechanickým vlastnostiam. Celkovo hydrogély pripravené pri 37 °C vykazovali lepšie mechanické vlastnosti.

KLÍČOVÁ SLOVA

Termocitlivý hydrogél, sieťovanie, fotoreológia

HABÁNKOVÁ, E. *Rheological evaluation of thermosensitive macromonomer photogelation in aqueous environment*. Brno: Brno University of Technology, Faculty of Chemistry, 2017. 82 p. Supervisor assoc. prof. Ing. Lucy Vojtová, Ph.D.

DECLARATION

I declare that the diploma thesis has been worked out by myself and all the quotations from used literature sources are accurate and complete. The content of the diploma thesis is the property of the Faculty of Chemistry of Brno University of Technology and all commercial uses are allowed only if approved by both the supervisor and the dean of the Faculty of Chemistry, BUT.

………………………………
student´s signature

ACKNOWLEDGEMENT

I would like to express the deepest appreciation to my supervisor assoc. prof. Lucy Vojtová and to my consultant Stefan Baudis, Dipl.-Ing.Dr.. Without their willingness and kindness this diploma thesis would not have been possible. I am gratefully indebted to their scientific theories and thoughts they shared with me. Special thanks go to prof. Robert Liska for allowing me to work in his group "Macromolecular chemistry" at Vienna University of Technology giving me a lot of knowledge and experiences. I would also like to thank dr. Lenka Michlovská for synthesis of α,ω-itaconyl-PLGA–PEG–PLGA and its characterization. Finally I would like to express gratitude to my parents for their infinite support during all my studies.

CONTENT

1 INTRODUCTION

Temperature induced sol-gel transition is of a great interest in tissue engineering. Thermoresponsive hydrogels can be used as injectable gels, which undergo gelation at body temperature. Those are very often used in the field of drug release. It is very advantageous especially from toxicological viewpoint, because no other substances are required. Moreover, injection is relatively body-friendly method regarding the incorporation of hydrogel **[1]**. There are also lots of polymer solutions, which are in a sol state at higher temperatures and gel at the body temperature **[2]**. However, this brings other demands and limitations for drugs, because some of them cannot stand high temperatures **[1]**. One of the well-examined drug carriers is PLGA–PEG–PLGA triblock copolymer, commercially known as ReGel®. Its aqueous solutions are in a sol state at lower temperature and create a gel at body temperature due to hydrophobic interactions **[3]**. ReGel® has been already used for the release of insulin **[4]** or under the trade name OncoGel® releasing the paclitaxel drug **[3]**.

In spite of all advantages thermoresponsive hydrogels have, chemical crosslinking is often desirable to enhance mechanical properties and lifetime. Photopolymerization became a common technique of hydrogel preparation. Photopolymerized hydrogels have a wide range of applications in tissue engineering. They have been already used as tissue barriers **[5]**, drug vehicles **[6]** or for cells encapsulation **[7]**, wound treatment **[8]** or even 3D printing **[9]**. To design the structure of photopolymerizable hydrogels, photorheology appears as the proper tool, because it enables direct monitoring of the network formation **[10]**.

The group headed by **assoc. prof Lucy Vojtová** has recently synthetized novel α,ω-itaconyl-PLGA–PEG–PLGA copolymer, which maintain thermoresponsive properties of PLGA–PEG–PLGA and moreover enables either additional chemical crosslinking due to double bonds (DBs) from itaconic acid or binding other molecules through COOH functional groups **[11; 12]**.

2 CURRENT STATE OF THE ART

2.1 Hydrogels

Hydrogel is a 3D elastic network of macromolecules holding together by physical or chemical interactions. Some hydrogels, so-called superabsorbents, are able to swell and retain a voluminous amount of water. However, hydrogels do not dissolve in the water due to the network junctions. When hydrogels are swollen, the content of the polymer is much lower than the content of the water. Water fills voids and the whole space between chains of polymers. The water content is dependent on the density of the network, type of junctions and the environment. Water can be released or absorbed by the change of ambient conditions as pH, temperature or by exposure to an external field **[13-17]**.

According the origin of molecules, hydrogels can be natural or synthetic origin. Natural hydrogels are made either of polypeptides or polysaccharides. Hydrogels created from natural polymers have good biocompatibility and cell adhesion, but their degradation profile and mechanical properties are more difficult to control. Mechanical properties, responses to the environment and lifetime of synthetic hydrogels can be more precisely tailored. They also possess larger water absorption **[15; 18]**.

Regarding the composition, hydrogels can be divided in three main groups. Homopolymeric hydrogels are made of one kind of monomer. Copolymeric hydrogels have chains created from two or more different monomers. Minimally one of the monomers always has to be hydrophilic in order to provide water solubility of pre-polymer and later bind the water within its network. Depending on the crosslinking type they can form physical or chemical network. Sometimes, one copolymer can create both networks at the same time so called hybrid network **[19]**. The third group creates interpenetrating network of polymeric hydrogels. They consist of two polymers, which are crosslinked independently **[15]**.

2.1.1 Hydrogels in Tissue Engineering

There are many reasons why hydrogels are sought-after in tissue engineering. First of all their mechanical properties are very similar to those of soft tissues and they are often biocompatible and biodegradable. The degradation is usually caused by cleavage of groups either hydrolytically or enzymatically **[13; 20]**. Due to the high water content, their consistency is very similar to soft tissues. They have great transport properties. Their network structure is full of voids filled by water, what facilitates the diffusion. This allows cells to penetrate and proliferate. Therefore they are proper material for regenerative templates and encapsulation of cells **[21; 22]**. Hydrogels as wound dressings can transport wound exudate and they are also highly permeable for oxygen. On the other hand they still protect tissues against bacteria and infection **[17]**. Usually they can easily be modified by functional groups which may also increase the cell adhesion. Their hydrophilic nature makes them likely to use as drug carriers since drugs as proteins and oligonucleotides are also hydrophilic. The drug release can be controlled by density of crosslinking and rate of degradation **[23]**.

Another advantage of hydrogels is that some of them can be prepared *in situ* **[1; 6; 23]**. It tends to a better adhesion between hydrogel and tissue. Hydrogel formation *in situ* can be done by change of pH, change of temperature, light irradiation, solvent exchange or by ionic cross-linkage. Thermoresponsive hydrogels are very attractive because no other components are required. This minimizes the cytotoxicity **[1]**. There are some hydrogels which are thermoresponsive and create gels at body temperature. Those may be injected in a liquid state and subsequently create a gel in the body. Injectable materials can nicely fill the defects due to their flowing properties **[1]**. However, *in vivo* polymerization has high demands for biocompatibility, cytotoxicity, pH and released heat **[23]**.

2.1.2 Physical Crosslinking

Hydrogels may arise from chemical or physical gelation. In the case of physical gelation network is created due to junctions, which are based on physical interactions such Van der Waals, Coulombic, ionic, hydrophobic or hydrogen bonds and crystallization **[24]**. Examples of physical interactions are shown in the Figure 1 and Figure 2.

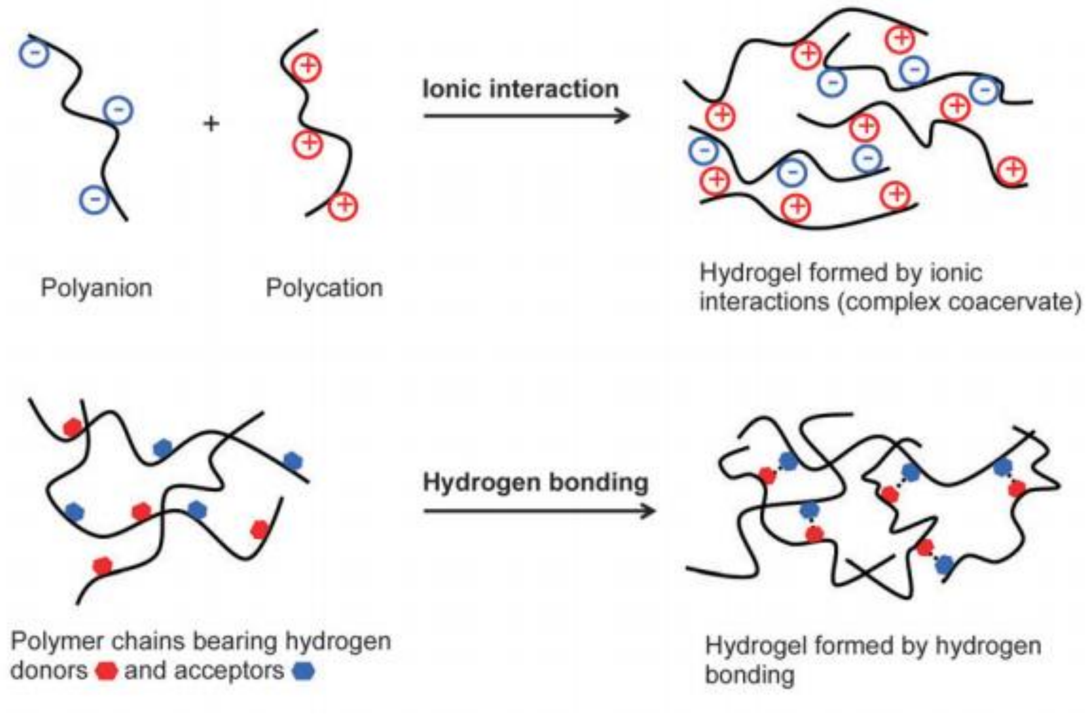

*Figure 1: Schematic examples of physical crosslinking **[25]**.*

Physical network has an advantage that connections can be changed in response to environment (temperature, pH, pressure, magnetic field etc.), what makes this network reversible. After the physical gelation there is no change in molecular weight and gel may be still soluble in the solvent. This is the main difference between physical and chemical crosslinking. Therefore it is more difficult to determine the gel point. Here, the importance of rheology is stressed. It allows to measure an increase in elastic modulus and gelation point can be determined as the cross point of the storage modulus (G') and loss modulus (G'') **[24]**.

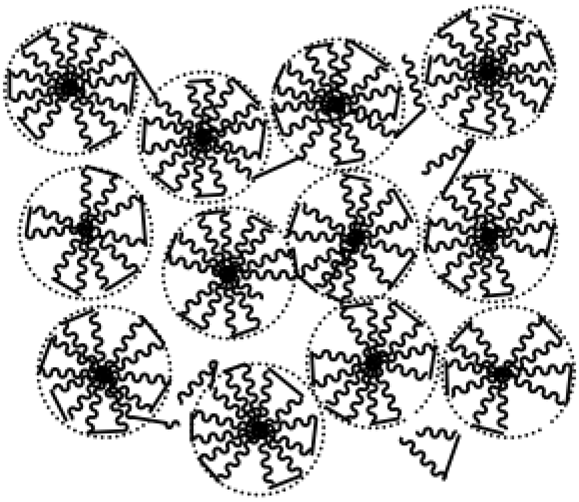

*Figure 2: Hydrophobic interactions of polymer chains lead to a micelle structure **[26]**.*

The point when the critical gel is created differs for different concentrations of polymer **[16]**. At the gel point interactions polymer-polymer and water-water become more preferable than interactions between the polymer and water **[1]**. Gel point can be also defined as the point, when the correlation length starts to change. Correlation length is the distance, in which the relocation of one molecule influences the motion of the other molecule. This effect rises gradually as the physical network is created due to a higher connectivity of the polymer system. It means that the movement of polymer chains correlates over larger distances **[24]**.

2.1.3 Chemical Crosslinking

It is difficult to well-define the physical network and also to secure the sufficient lifetime for the certain application **[24]**. Therefore, mechanical and thermal stability of many polymers can be significantly improved by chemical crosslinking **[13]**. Chemical crosslinking is irreversible because covalent bonds are created. They make hydrogels more resistant to the structural collapse **[27]**. Covalent junctions can be formed by chemical reactions between functional groups (Schiff-base formation, Michael type addition, click chemistry etc.), by radical polymerization and by enzymatic/catalytic reactions. Radical polymerization can be induced either thermally or by the light irradiation and redox reactions **[25; 28]**. Examples of chemical crosslinking are shown in the Figure 3.

Hydrogels can be prepared by the bulk polymerization or the polymerization in solution. In the case of the bulk polymerization, initiator is dissolved in the pre-polymer or the monomer **[23]**. Reaction in bulk produces high amount of heat. Due to a high concentration of DBs viscosity increases rapidly during the network creation. It is often undesirable. One can avoid overheating by polymerization in solution. After the preparation hydrogels have to be cleared from impurities, residual initiators, crosslinking agents, unreacted monomers etc. **[15]**.

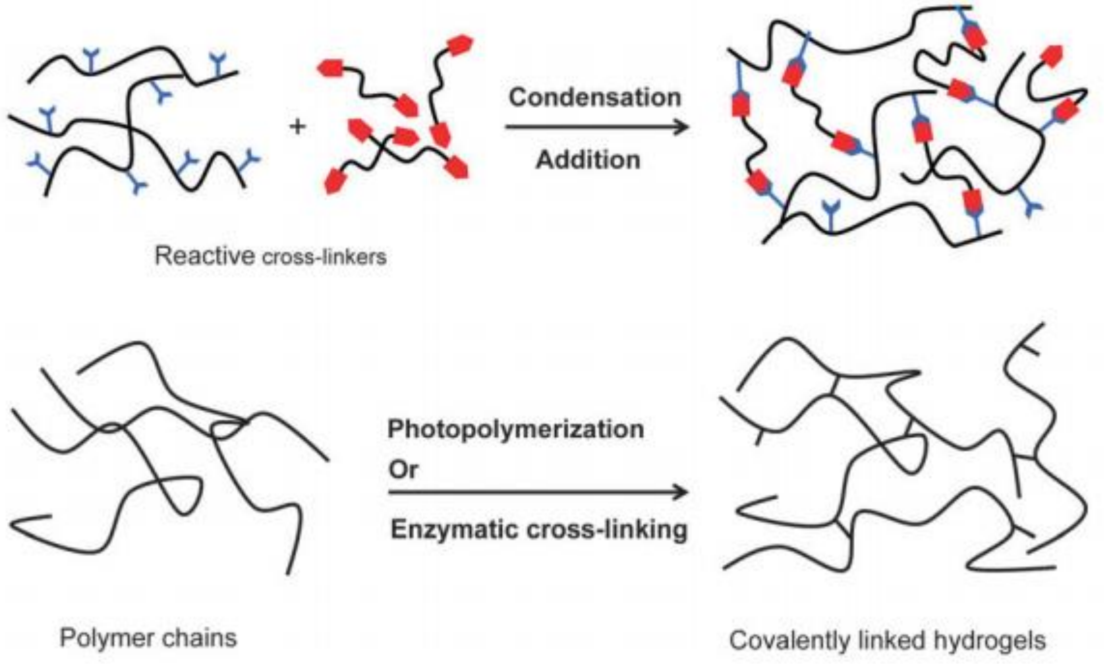

*Figure 3: Schematic examples of chemical crosslinking **[25]**.*

2.1.3.1 Hydrogels Formed by Photopolymerization

Recently, photopolymerization, initiated by UV and visible light irradiation, became a common way for hydrogels preparation. This is performed in the presence of photoinitiators (PIs), which interact with the light and induce the radical polymerization. One of the main advantages is that photo-curing can be done *in situ*. **[13]**. It can have minimal side effects when it is made laparoscopically, using a catheter **[29; 30]** or when transdermal irradiation is applied **[23; 31-33]**. During the transdermal irradiation more than 99 % of the UV light is absorbed by the skin. This may lead to residual unreacted PIs and monomers, which are often cytotoxic **[28]**. Since the light of longer wavelengths may transmit through the skin better, the transdermal photopolymerization is more effective for VIS or IR light irradiation **[23]**. One can directly target the damaged tissue what contributes to the efficiency of the treatment and decreases the contravention of surroundings. Another great advantage of the photopolymerization is the fast curing rate, which is often less than few seconds or minutes **[33]**.

Photocrosslinked hydrogels have quite a wide range of use in biomedicine. According to the literature, polymerized hydrogels have been already tested as drug carriers **[6]**, prevention of thrombosis **[6]**, biosensor coatings **[34; 35]**, post-surgery barriers **[5]** and as templates for cells, scaffolds **[36]**. Moreover, layered matrices have been already produced by photopolymerization. They are prepared layer by layer and can contain different concentration of the drug according to the requirements. Hydrogel layers firmly adhere to each other. One can also design the concentration profile of the drug release by the regulation of the thickness of layers and the rate of the diffusion of dissolved substances **[23]**.

Photopolymerization of monomers is quite well examined. However, monomers may often be cytotoxic. For this reason, pre-polymers, so-called macromonomers, are likely to use for tissue engineering applications **[23; 33]**. In comparison with monomers they cannot diffuse through cell membranes and thus do not influence intracellular processes. Number of DBs within macromonomers is lower and therefore, they do not produce a high amount of heat. Moreover, they can be often photopolymerized by VIS light, which is less toxic than UV light **[37]**.

2.1.3.2 Photocrosslinking of Water Soluble Polymers

There are many papers dealing with water soluble polymers which are befitting for the chemical crosslinking induced by light **[38]**. A lot of water soluble photocrosslinkable polymers are based on poly(ethylene glycol) (PEG), poly(vinyl alcohol) (PVA) or polysaccharides such as hyaluronic acid **[9; 39]**, dextran **[38; 40-43]** and chitosan **[28]**. Those have incorporated reactive groups or more precisely DBs **[23]**. Functional groups as OH, COOH and NH_2 promote the water solubility of polymers **[13]** and DBs enable the photocrosslinking. Pendant functional groups can be modified with vinyl groups. Some water soluble polymers have pendant groups at every monomeric unit and some only at the ends of chains. Schematic examples are shown in the Figure 4. Attachment of the vinyl group mostly decreases water solubility since it usually replaces hydroxyl or carboxylic groups. One has to always compromise between the degree of substitution, which brings better mechanical properties and good water solubility. On the other hand the incorporation of some structures such as maleic acid can enhance the solubility in water. Carbon from carbonyl group of maleic anhydride reacts with hydroxyl group of polymer. This ring opening polymerisation (ROP) leads to one free carboxyl group. This group can either enhance the water solubility or can be used for the attachment of bioactive molecules. For instance **Sin-Hee Kim et al.** synthetized dextran-maleic acid hydrogel precursors and afterwards the hydrogel network was created by the UV irradiation **[38]**. Hydrogels are often non-adherent to cells. This can be changed by incorporation of cell adhesion ligands such as tripeptide arginyl-glycyl-aspartic acid (RGD), which can bring the adhesion for specific kind of cells. Also grow factors can be added to coordinate activity of cells **[23]**.

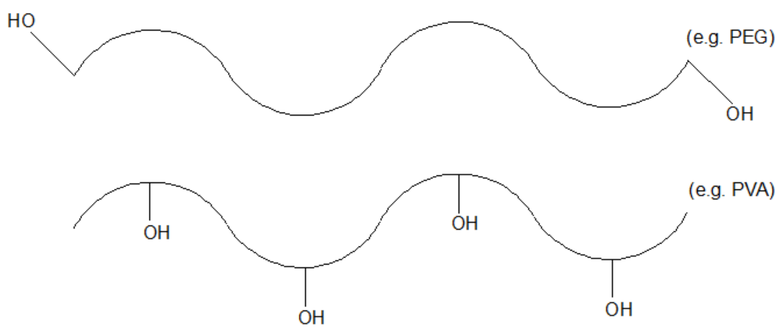

Figure 4: Schematic drawing of water soluble polymers, which have pendant functional groups either only at the ends (PEG) or at every monomer unit (PVA).

Pre-polymers Based on PVA

Commonly prepared hydrogels by irradiation are those based on PVA **[44-49]**. PVA is a hydrophilic and biocompatible material. It has a pendant hydroxyl group at every repeating unit and this enables its modification **[50]**. After the introducing of vinyl groups PVA becomes a crosslinkable polymer and can be used for a wide range of soft-tissue engineering applications **[22]**. The attachment of DBs and subsequent photopolymerization removed the problem with the diffusion of crosslinker during the chemical crosslinking of PVA **[45]**. PVA-based hydrogels are generally non-adhesive, therefore, PVA has to be modified by cell-adhesives peptides to promote cell adhesion and proliferation **[22]**.

Schmedlen et al. evaluated the use of modified PVA in tissue engineering applications. They prepared hydrogels seeded with human fibroblasts. Cells were incorporated to the hydrogel precursor to maintain the homogeneity. More than 80 % of cells stayed viable after the photopolymerization and also after two weeks in the culture media. In this case PVA was modified with methacrylamidoacetaldehyde dimethyl acetal and Irgacure 2959 (I2959) was used as the photoinitiator **[22]**.

Photopolymerizable PVA has been already synthetized using acrylic acid, methacrylic acid **[48]**, glycidyl acrylate **[45]** or acryloyl chloride **[51]**. The biodegradable hydrogel network is often desirable. Therefore, ester-acrylate linkages, which can be easily cleaved by the hydrolysis, are likely to use as crosslinker segments **[46; 47]**.

Pre-polymers Based on PEG

There are lots of works dealing with photocrosslinked hydrogels based on PEG **[52-56]**. PEG is a strongly hydrophilic substance, which can be easily modified at its ends by different reactions **[33]**. PEG is a non-immunogenic polymer, resistant to the protein and cell adsorption and has tissue like elasticity **[6; 33]**.

West and Hubbell prepared photo-crosslinked hydrogels which may be used as drug carriers or even as a prevention of thrombosis. Hydrogels were formed by photopolymerization of aqueous solution of pre-polymer containing PEG and α-hydroxy acid modified at the ends by acrylate. Hydrophilic bioactive molecules were added to the aqueous solution to ensure the homogeneity. Ester bonds are hydrolysed during the polymer degradation. It leads to the increase of pore size and bioactive molecules can be continuously released. Design of drug precursors determines the rate of the drug release. It was found that the drug release at the beginning is faster. It is probably due to a swelling of the hydrogel, which supports the diffusion of the drug. Moreover, hydrogel can be formed *in situ* on the tumour site and the drug can be effectively targeted. Also the formation of the hydrogel on walls of blood vessels can be done to avoid the thrombosis **[6]**. This is called interfacial polymerization. Firstly, the PI, which has a good affinity to the tissue, is absorbed. Afterwards the hydrogel precursor is brought into the contact with PI and during the light irradiation hydrogel is created **[23]**. *In situ* formation also improves the adhesion of hydrogel to the tissue. Otherwise the prepared hydrogel is more or less non-adherent to tissues **[6]**. **Amarpreet S. Sawhney et al.** also designed and synthetized photopolymerized poly(ethyleneglycol)-*co*-poly(α-hydroxyacid) diacrylate macromers. With the content of PEG more than 55 mol. % they ensured the water solubility. Amphiphilic structure of molecules leads to the micelle formation in water. In micelles DBs are oriented and concentrated next to each other, which facilitates the polymerization and increases the rate of propagation. These macromers can be photopolymerized by VIS light in direct contact with tissue. Argon ion laser (514 nm) was used to induce the polymerization. Formation of the heat during the photopolymerization can cause the damage of tissues. In this case there is only low amount of DBs per macromer. Therefore also the amount of released heat is low. PEG based macromers are suitable as burn dressings or they can be used as adhesives in surgery to prevent the formation of scars and organs adhesion **[55]**.

Well-known and well-characterised polymer for the preparation of photocrosslinked hydrogels is poly(ethylene glycol) diacrylate (PEGDA) **[57-60]**. PEGDA is non-adhesive to cells and tissues without the modification. PEGDA hydrogels were first time equipped with RGD peptide by **Hubell et al. [61]**. Structure of PEGDA and its subsequent crosslinking by UV irradiation is shown in the Figure 5.

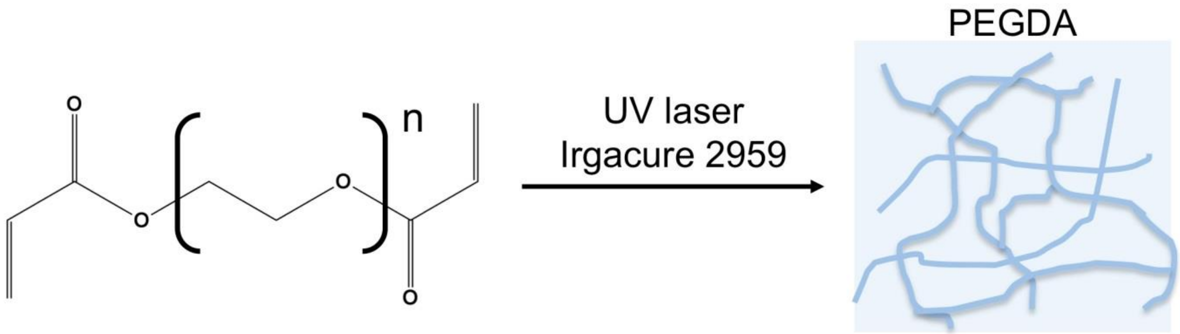

*Figure 5: Schematic crosslinking of PEGDA hydrogels **[62]**.*

It has become very common to combine pre-polymers to create hydrogel networks. For example the combination of dextran and PEGDA is quite well examined **[42; 63]**.

2.1.4 Hybrid Networks

To ensure the immediate gelation and subsequently improve the stability of the hydrogel, the physical and chemical gelation can be coupled in some pre-polymers resulting in hybrid networks **[33]**. This was done for the thermoresponsive triblock copolymer ABA modified by additional methacrylate’s groups on its side chains. B block is made of the hydrophilic PEG and A block is made of poly(N-(2-hydroxypropyl) methacrylamide lactate). Polymer in aqueous solution shows the thermoresponsive behaviour. After the physical gelation mechanical properties and lifetime of the hydrogel can be improved by UV polymerization. **Vermonden et al.** compared the degradation of physically crosslinked ABA and ABA, which was additionally cured by UV light. The degradation time at physiological conditions for irradiated gels was from 10 to 20 days depending on the amount of crosslinks, while the degradation of physically crosslinked gels was within two days **[19]**. This ABA copolymer is quite well examined. Thanks to the ester bonds the material undergoes hydrolysis and is biodegradable **[19]**. The release of different proteins was investigated by changing the concentration of pre-polymer **[64]** and by varying its molecular design different mechanical properties, degradation rates and protein release processes were achieved **[65]**. Material has been already tested *in vivo*. It was subcutaneously implanted into the mice and the response of organism was monitored **[66]**. It was also used to prepare 3D printed constructs for tissue engineering applications **[67]**.

Hybrid networks can be made as well as from modified thermoresponsive PLGA-PEG-PLGA triblock copolymer applicable in biomedicine, especially as the drug carrier under trade names ReGel® and OncoGel® **[68-70]**. **Michlovská et al.** have recently described the synthesis of new triblock copolymer based on PLGA-PEG-PLGA, where OH end groups were modified by itaconic acid, resulting in α,ω-itaconyl-PLGA–PEG–PLGA macromonomer. The whole structure of α,ω-itaconyl-PLGA–PEG–PLGA is shown in the Figure 6. This modification brought into the molecule new functional groups (COOH) and DBs suitable for chemical crosslinking **[11; 12]**.

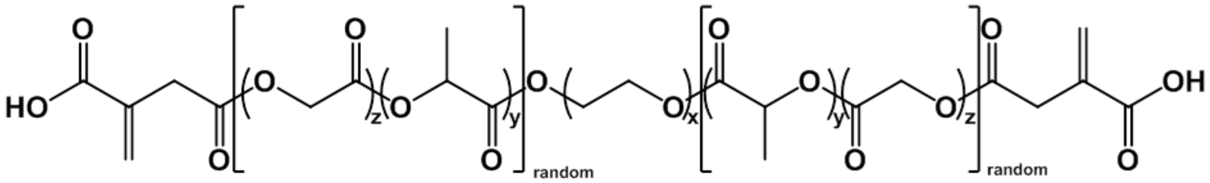

Figure 6: Chemical structure of α,ω-itaconyl-PLGA–PEG–PLGA.

Physical crosslinking of this macromonomer in aqueous solutions rises from hydrophobic interactions between hydrophilic PEG and hydrophobic PLGA blocks, which assemble in micelles. Thermoresponsive properties of this macromonomer can be designed by the change of PLGA/PEG weight ratio and lactide/glycolide (LA/GA) molar ratio. The ratio between PLGA and PEG affects more the critical gel temperature (CGT), whereas critical gel concentration (CGC) is mainly influenced by LA/GA ratio. The higher the PLGA/PEG and LA/GA ratio the lower is the CGT and CGC, respectively **[71]**. This influence shows the Figure 7.

Michlovská et al. used the PI camphorquinone (CQ) and co-initiator 2-(dimethylamino)ethyl methacrylate to chemically crosslink the macromonomer in bulk without supporting physical network. The blue light in the range 430–490 nm was used as the light source. DBs were consumed during the irradiation but material was still soluble in tetrahydrofuran (THF) after the irradiation. However, they improved thermal and mechanical properties of the material and decreased the degradation rate **[12]**.

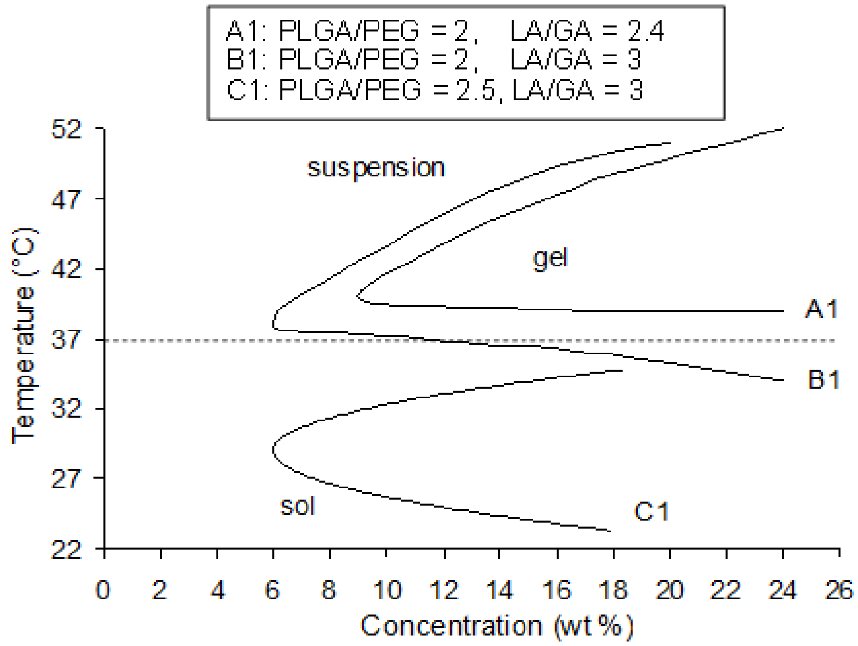

Figure 7: Influence of LA/GA ratio and PLGA/PEG ratio on the critical gel temperature and critical gel concentration ***[71]***.

2.2 Photoinitiators

PIs are chemical compounds, which generates reactive species after the UV or VIS light irradiation **[72]**. They are essential additives of radical photopolymerization **[73]**. Radicals attack DBs of monomers or pre-polymers resulting in the polymerization. The emission spectrum of the light source has to overlap with the absorption spectrum of the PI **[72]**.

There are two types of PIs according to the initiation mechanism. Type I PIs undergo homolytic cleavage to create radicals upon irradiation with light **[72]**. The cleavage can be within bonds C–C or C–X, where X can be oxygen, sulphur or halogen **[23]**. The mechanism of type I PIs is shown in the Figure 8. Type II PIs require co-initiators. After the exposure to the light, the PI is excited and transfers its energy to the co-initiator to produce reactive intermediates **[72]**. The example of this mechanism is shown in the Figure 9.

In situ photopolymerization is a very common used technique in restorative medicine. PI CQ is one of the most frequently used PIs in this field **[74]** and was also used for the chemical crosslinking of α,ω-itaconyl-PLGA–PEG–PLGA in previous studies as already mentioned before **[12]**. It belongs to the group of type II PIs. In the case of CQ usually tertiary amines are used as co-initiators to reach sufficient efficiency. CQ is not suitable for the photopolymerization from aqueous solutions due to its poor water solubility **[75]**.

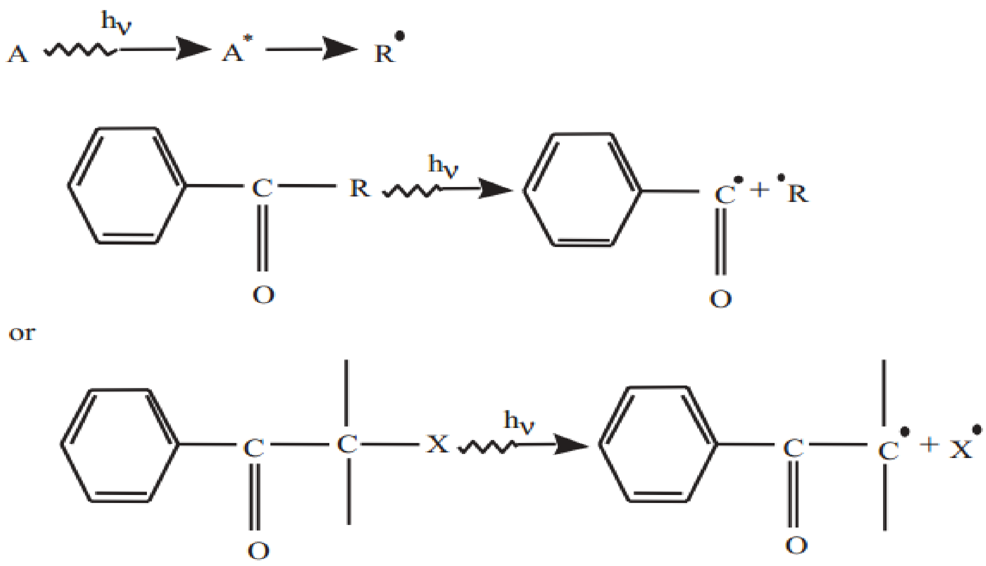

*Figure 8: Examples of the mechanism of type I PIs, where the first reaction is α cleavage and second is β cleavage **[23]**.*

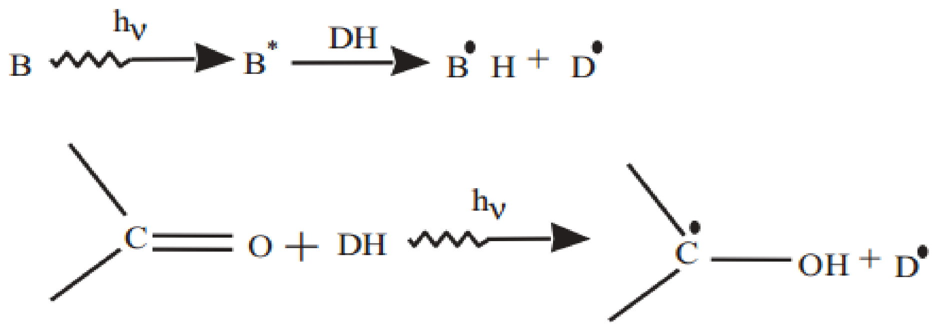

*Figure 9: Example of the mechanism of type II PI – after the light irradiation PI (B) abstracts the hydrogen from the co-initiator (DH) to create radicals **[23]**.*

2.2.1 Water Soluble Photoinitiators

Especially in fields, where the low cytotoxicity and biocompatibility is required, water as a solvent is likely to be used. Water-borne formulations and various applications of hydrogels require water soluble initiators. In spite of that, they are less commercially available than the initiators soluble in organic solvents **[76]**. Insufficient variety of water soluble initiators is also a difficulty in the preparation of 3D hydrogel structures for tissue engineering by two-photon induced polymerization **[77]**.

The most frequently used water-soluble PI is the commercially available I2959 **[76]**. Its structure is shown in the Figure 10. Solubility of I2959 in 100 g of water at 20 °C is about 1 g **[78]**. For some applications higher concentration of PIs is desirable. Therefore, either the modification of I2959 is needed or the use of other PIs is necessary **[76]**.

Stephan Benedikt et al. described highly efficient water soluble PIs suitable also for the VIS light. They tested their solubility, storage stability, reactivity and cytotoxicity. N-acryoylmorpholine was used as the monomer. Monoacylphosphineoxide (MAPO) salt LiTPO showed very good reactivity. The rate of polymerization was 670 $mmol\cdot L^{-1}\cdot s^{-1}$ with the double bond conversion (DBC) of monomer 97.7 % for wavelengths 320–500 nm. Under VIS light irradiation (400–500 nm) the reactivity of LiTPO slightly decreased. The rate of polymerization and DBC was measured as 590 $mmol\cdot L^{-1}\cdot s^{-1}$ and 83.7 %, respectively. It was tested via photo-differential scanning calorimetry. For applications including living cells the use of VIS light irradiation and low cytotoxicity of the initiator is needed. LiTPO showed the best biocompatibility among other PIs examined in the article **[76]**. The chemical structure of the ionic PI LiTPO is shown in the Figure 11.

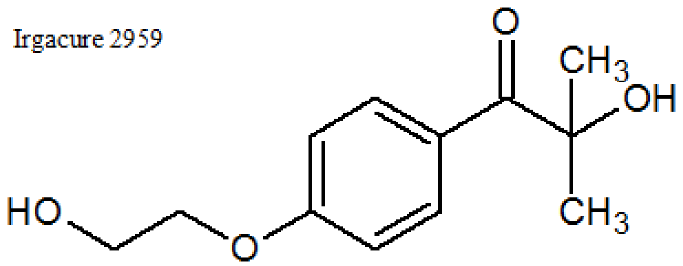

Figure 10: Commercially available, water soluble PI I2959.

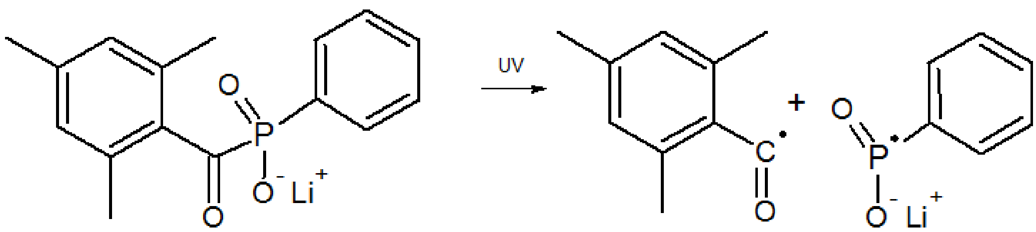

Figure 11: Cleavage of LiTPO initiated by UV irradiation.

2.3 Rheology

Rheology deals with mechanical properties of materials and examines their response to the mechanical force. The term rheology was coined by Eugene C. Bingham in 1920. The word originates from Greek and its meaning includes the definition of rheology, which was also accepted by The Society of Rheology founded in 1929: “Rheology is the study of the deformation and flow of matter” **[79; 80]**.

Rheology has a wide range of applications including both liquids and solids. It plays also important role in the field of polymers **[24]**. Also rheological characterization of hydrogels is of great interest to scientists since they have wide range of applications in tissue engineering as mentioned above. Determination of mechanical properties by the rheology has many advantages. It is a very sensitive technique and requires just a small amount of the sample **[81]**. Liquid-solid transitions significantly influence the mobility of chains, what makes the rheology the proper method for examination of gel point of hydrogels **[24]**.

Regarding the rheology, fluids can have either Newtonian or non-newtonian behaviour. Newtonian fluids are ideal liquids, which obey Newton´s law of viscosity:

$$\tau = \eta \frac{\mathrm{d}x}{\mathrm{d}y\mathrm{d}t} = \eta \cdot \dot{\gamma} \tag{1}$$

where τ is shear stress, η is dynamic viscosity, dx presents the displacement between two virtual layers and dy determines the distance between them. Shear rate $\dot{\gamma}$ determines the speed of the deformation increase. Shear stress can be also defined as the ratio of the shear force and area of the layer, on which the force acts **[82]**. Those relations are schematically shown in the Figure 12.

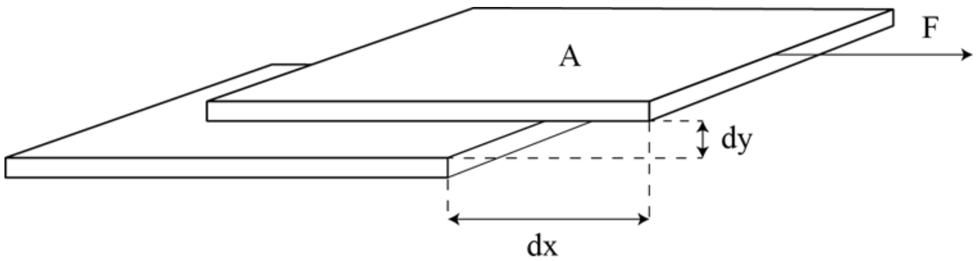

Figure 12: Schematic image of the Newton´s law of viscosity.

According the equation 1, viscosity can be defined as the ratio of shear stress and shear rate. Newtonian liquids have constant viscosity for different shear rates during the rheological measurement. However, there are lots of cases when the viscosity is not the same for different shear rates. This is assigned to the non-newtonian behaviour. This behaviour can be displayed by flow curves. There are 3 possibilities how to show this non-newtonian dependency: η (τ), η ($\dot{\gamma}$) and τ ($\dot{\gamma}$). One can distinguish two basic kinds of non-newtonian behaviour and those are shear thinning and shear thickening. Shear thinning or pseudoplastic behaviour shows materials, when their viscosity decreases with the increasing shear rate. Shear thickening, also called dilatant behaviour, shows materials with the increasing viscosity during the shear rate increase. Some materials have combination of both **[83]**. Different kinds of flow curves are shown in the Figure 13.

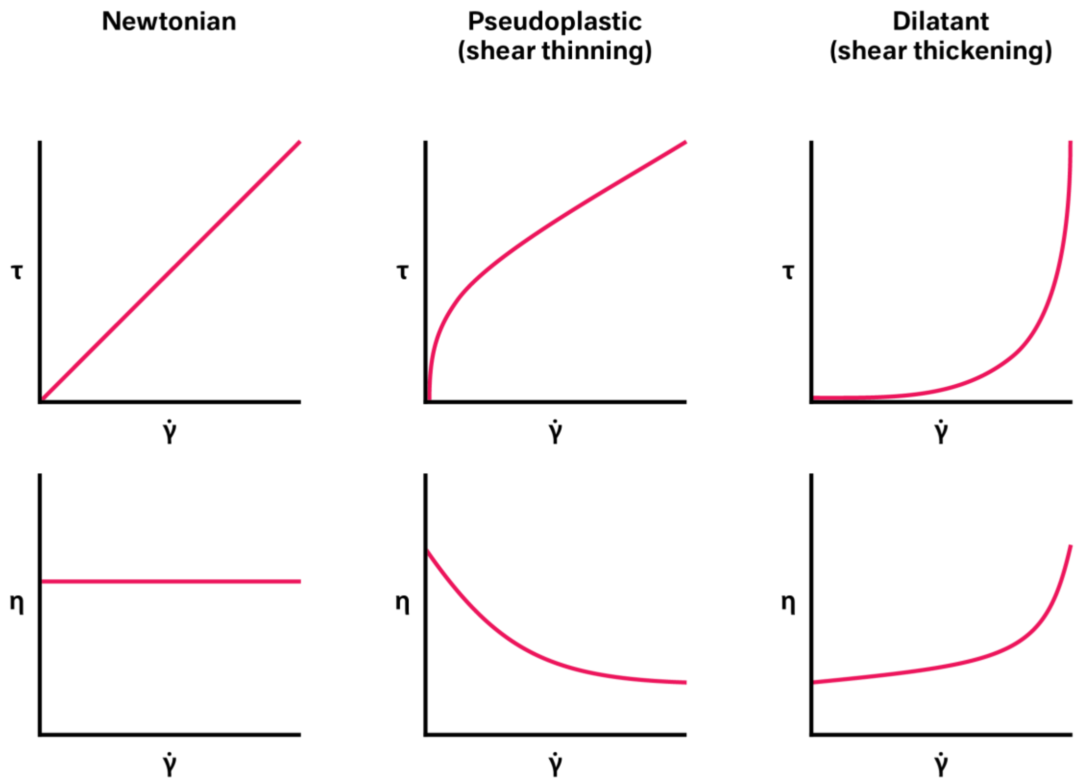

Figure 13: Flow curves of fluids with different rheological behaviour.

Some pseudoplastic materials are also thixotropic, what means that they behaviour is time dependent. The longer time is material sheared, the lower is the viscosity. Thixotropy can be investigated by thixotropic loops. It is shown in the Figure 14. The change of the shear stress during the increasing of the shear rate does not have the same path as it has during the subsequent decreasing of the shear rate. In other words, the viscosity is decreasing at constant shear rate. Time dependent behaviour for the dilatant material is called antithixotropy or rheopexy. Viscosity is increasing at the constant shear rate **[84]**.

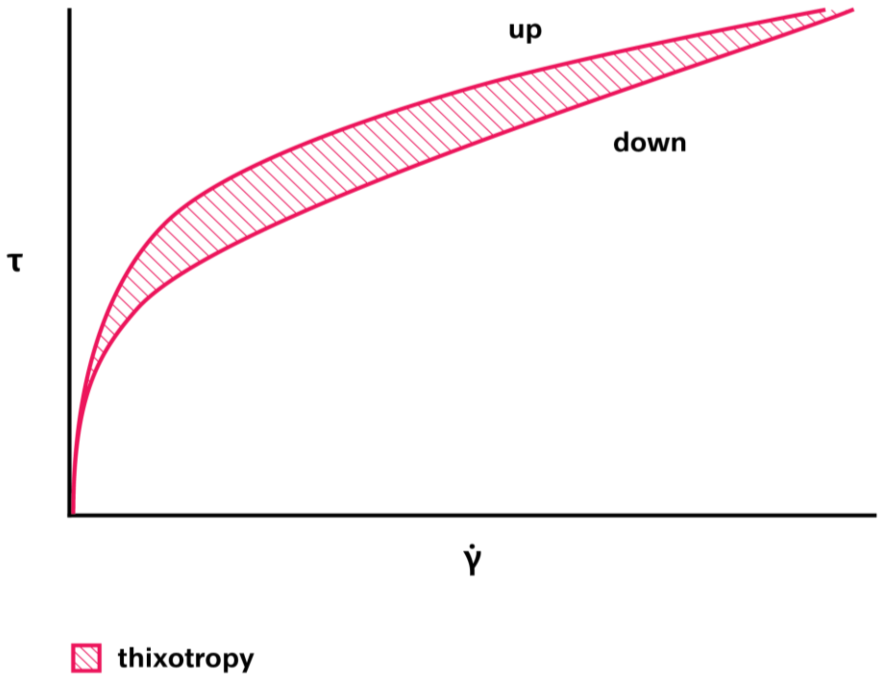

Figure 14: Thixotropic loop showing time dependant behaviour of fluid.

2.3.1 Oscillatory Rheology

Oscillatory rheology also called dynamic mechanical analysis enables the examination of viscoelasticity of materials **[85]**. Sample is located between stationary and oscillating part of measuring system, usually two parallel plates or cone and plate. Sinusoidal strain (γ) deformation is applied on sample while stress (τ) response is measured **[86]**. Elastic solids have sinusoidal stress and sinusoidal strain in phase. Newtonian liquids have sinusoidal stress at same frequency as strain wave, but shifted by phase angle (δ) $\pi/2$. These are two extreme situations. Most of the materials are viscoelastic and has strain wave shifted by δ between $\pi/2$ and 0. This is shown in the Figure 15. Mathematically it can be explained by following equations **[87]**:

$$\gamma = \gamma_0 \sin(\omega t) \tag{2}$$

$$\tau = \tau_0 \sin(\omega t + \delta) \tag{3}$$

Where γ_0 is amplitude of strain, ω is angular frequency, t is time and τ_0 is amplitude of stress. According to Figure 15 one can see that shifted stress wave from viscoelastic response can be broken down in two waves – one in the phase with strain (τ') and one shifted by $\pi/2$ (τ''). Moreover, the wave shifted by $\pi/2$ is in the phase with the maximal rate of strain wave because it is defined as **[87]**:

$$\dot{\gamma} = \frac{d\gamma}{dt} \tag{4}$$

One can write:

$$\tau = \tau' + \tau'' = \tau_0' \sin(\omega t) + \tau_0'' \cos(\omega t) \quad (5)$$

According to trigonometry tan δ can be determined as follows:

$$\tan\delta = \frac{\tau_0''}{\tau_0'} \quad (6)$$

From Hooke´s law it is known that stress is equal to modulus multiplied by strain. Here it leads to two following moduli **[87]**:

$$G' = \frac{\tau_0'}{\gamma_0}, G'' = \frac{\tau_0''}{\gamma_0} \quad (7)$$

Where *G´* is storage modulus and *G´´* is loss modulus. *G´* represents elastic behaviour of material, energy stored in a material during stressing and then consumed for reformation when it is unloaded. *G´´* represents viscous behaviour, and is a measure for the dissipated energy.

By coupling equations 6 and 7 one can write **[87]**:

$$\tan\delta = \frac{G''}{G'} \quad (8)$$

G´ and *G´´* are typical variables which are sought to measure in oscillatory rheology **[85]**.

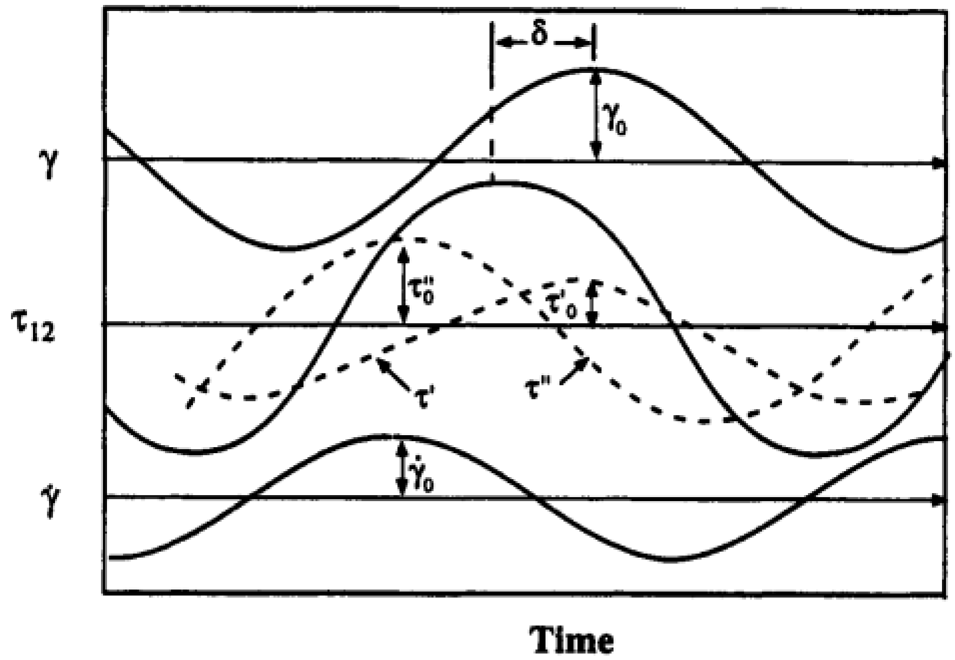

Figure 15: Oscillatory strain deformation and stress response shifted by phase angle δ ***[87]****.*

2.3.2 Photorheology

The irradiation within the rheometer was first time introduced and described in 1992 by Khan and co-workers **[88]**. During the measurement the classical dynamic mechanical analysis is performed and after some time UV or VIS light is triggered on. It enables the real time (RT) monitoring of the material´s mechanical behaviour during the polymerization initiated by light. The time dependency of parameters such as G' and G'' can be determined during the photopolymerization. One can evaluate time to gelation or maximal storage modulus (G'_{max}) after irradiation.

Another possibility, which photorheology offers, is the monitoring of the polymerization shrinkage during the irradiation either by monitoring of the normal force decrease at constant gap **[89]** or gap decrease at constant normal force **[90]**. Shrinkage is a common result of the chemical crosslinking. It occurs due to a replacement of long distance van der Waals bonds by short distance covalent bonds **[91]**. Stress caused by the shrinkage is often the reason of the later mechanical failure. Photopolymerizable materials are widely used in dentistry, where the shrinkage is the most significant downside **[89; 92]**. Shrinkage is highly dependent on the DBC during polymerization. Thanks to the photorheology one can better design parameters of the irradiation and the shrinkage may be minimised. To determine DBC, another analytical technique has to be combined with the photorheology **[89]**.

Sample thickness used in photorheology should be between 50 and 500 μm to achieve reliable rheological values and homogenous photoirradiation **[10]**. Photorheological measurements are also dependent on the intensity of the light source. With the increasing intensity, the number of photons exposed to the sample is higher. When the intensity is lower, the polymerization is delayed. As the result, the time required to reach the gel point or the maximum modulus is longer **[93; 94]**.

2.3.2.1 Hyphenated Photorheology/Fourier Transform Infrared Spectroscopy

Hyphenated photorheology/Fourier transform infrared spectroscopy was first time introduced by **Botella et al. [93]**. Thanks to this coupling one can simultaneously measure viscoelastic properties, polymerization shrinkage and DBC. Subsequently the correlation between them can be determined, because IR spectrum is recorded during the whole measurement. DBC is calculated by the integration of the band area, which represents DBs. This band during the irradiation decreases or even completely disappears. The reactivity of monomers or pre-polymers can be easily determined by this technique. It is of great interest to use this combined technique for UV curable formulations **[10; 89]**.

Due to the IR beam this combination always requires parallel plate-to-plate measuring system. In addition at least one of steel plates has to be replaced by quartz, glass plate, which transmits the IR beam and the UV or VIS light. Example of the setup is shown in the Figure 16.

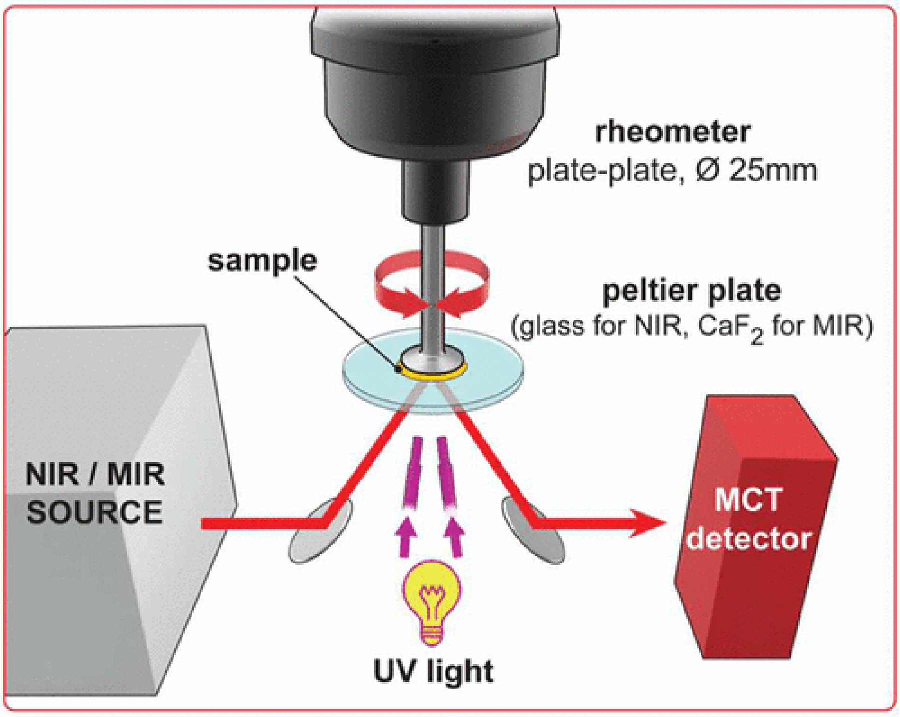

*Figure 16: Schematic example of coupling rheometer, light source and IR measurement **[10]**.*

2.3.2.2 Photorheological Characterization of Hydrogels

Recently photorheology became sought-after method for examination of hydrogels prepared by photoirradiation **[44; 52; 95-99]**. Photoreactivity of prepared precursors and mechanical properties during the whole photopolymerization process can be determined **[44]**.

In the Figure 17 one can see typical photorheological curve and some of parameters, which can be calculated. Time sweep of *G´* is recorded, when at some certain time light is triggered on, what leads to polymerization, increase of modulus. G'_{max} after the polymerization can be determined. **Gorsche et al.** defined G'_{max} as the measure of the crosslinking density. They also defined other two parameters – delay time (τ_D) and slope, which evaluation is shown in the Figure 17. Slope of the modulus increase represents the photoreactivity of sample. τ_D is the cross-point of linear fits from baseline and modulus increase. They suggested to fit curves so, that the correlation coefficient is higher than 0.98 **[10]**. **Aimetti et al.** used photorheology for examination of gel point and determined it as the point, when *G´* overcame *G´´* **[98]**.

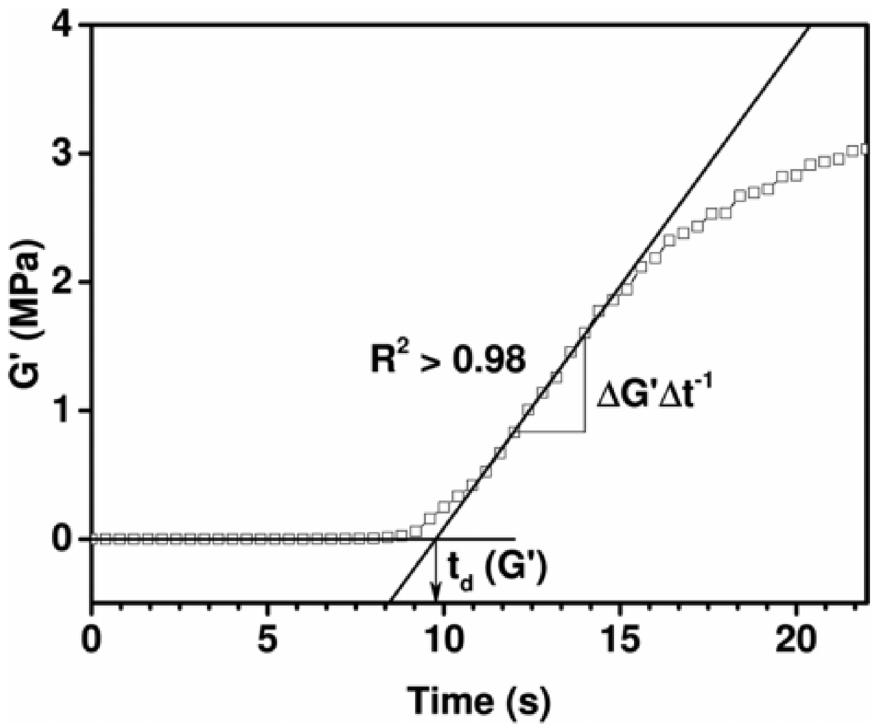

Figure 17: Photorheological curve and determination of τ_D and photoreactivity of hydrogel ***[10]****.*

It was confirmed that higher pre-cursor content increases the photoreactivity **[44; 52; 97]**. Photorheology of hydrogels has been already coupled with near infrared spectroscopy (NIR). It requires the use of deuterium oxide as a solvent. Signal from water would overlap double bond band in NIR **[10; 52]**. **Felix Markus et al.** observed that the start time of DBC after the irradiation in NIR was shorter than the start time of *G´* increase in photorheology **[52]**. As they stated, also others came to the same results **[93; 100]**. This difference can be easily explained. At the beginning of the irradiation chains combine but there is no 3D network. Modulus is increasing later when the elastic network is formed. **[52]**.

Griffin et al. used photorheology even for the determination of rate constants of hydrogel photodegradation from *G´* decrease. Hydrogels had photodegradable ortho-nitrobenzyl groups incorporated in their backbone and light was used to control release of cells **[101]**.

3 MAIN GOALS OF THE WORK

The goal of the proposed work is the examination of the photopolymerization of α,ω-itaconyl-PLGA–PEG–PLGA macromonomer in bulk and its aqueous solutions using the photorheology as a powerful tool for photocurable materials. The aim is to determine proper conditions for the hybrid network formation from aqueous solutions in the presence of highly efficient water soluble photoinitiator, as well as characterise the influence of both physical and chemical parameters on the photopolymerization.

4 EXPERIMENTAL PART

4.1 Chemicals

α,ω-itaconyl-PLGA–PEG–PLGA	M_n = 5 200 g·mol^{-1}, PDI = 1.19 DS = 89 % Macromonomer prepared by L. Michlovská (CEITEC, BUT Brno)
PEGDA poly(ethylene glycol) diacrylate	M_n = 4 600 g·mol^{-1} Macromonomer prepared by Z. Tomášiková (TU Wien)
UPW Ultra-pure water	Solvent for hydrogels
Speedcure TPO-L ethyl (2,4,6-trimethylbenzoyl) phenyl phosphinate	Organosoluble photoinitiator bulk measurements (min 94.5 %, LAMBSON)
LiTPO lithium phenyl-2,4,6-trimethylbenzoylphosphinate	Water soluble photoinitiator (TU Wien)
Irgacure 2959 (I2959) 2-hydroxy-4′-(2-hydroxyethoxy)-2-methyl-propiophenone	Water soluble photoinitiator (Ciba Speciality Chemicals Inc.)
Acetone	Distilled acetone Solvent for bulk measurements, test of chemical crosslinking
THF tetrahydrofuran	Distilled tetrahydrofuran GPC sample preparation, GPC eluent

4.2 Preparation of Samples

α,ω-itaconyl-PLGA–PEG–PLGA polymer was stored in a fridge to avoid the hydrolysis. Before the sample preparation, material was stored a couple of hours at ambient conditions to heat up for the better manipulation. Viscosity of the material is very high and material is very sticky.

4.2.1 Preparation of the Bulk Sample

α,ω-itaconyl-PLGA–PEG–PLGA was dissolved in acetone and 3 wt. % of TPO-L was added. The mixture was vortexed until it was completely dissolved. Later the acetone was evaporated at 40 °C under the vacuum on the Rotavapor R-210.

Samples prepared for ATR-IR were additionally put in to the UV chamber INTELLI RAY 600 Shuttered UV Floodlight for 2400 s and the intensity was set to 50 %.

4.2.2 Preparation of Aqueous Solutions

α,ω-itaconyl-PLGA–PEG–PLGA was weighed into a vial and calculated amount of the ultra-pure water was added by the glass Pasteur pipette. After the addition of water, samples were let to dissolve on magnetic stirrer for 3–5 days at 8 °C. During the day larger pieces of the material were disintegrated with the spatula. The more times it was done, the faster was dissolving of polymer. Solutions were prepared with three different additions of macromonomer – 10 wt. % (100 mg of sample/1 g of UPW), 15 wt. %, 20 wt. %.

Samples were stored at ambient conditions two days and at the third day the photorheological measurements were performed. Before the photorheological measurement PI LiTPO was added relative to the aqueous solution. During the whole experiment four different weight concentrations of LiTPO were used – 0.1 wt. %, 0.5 wt. %, 1 wt. %, 3 wt. %., where 100 % is aqueous solution together with LiTPO. From that time samples had to be protected against the light. They were stored in vials made of the amber glass. All the manipulations with samples either took place in a yellow lab room or samples were additionally protected with an aluminium foil. Before every measurement samples were mixed on Vortex mixer to assure the homogeneity.

One measurement was done with additional crosslinker PEGDA. 5 mol. % of PEGDA per DBs of α,ω-itaconyl-PLGA–PEG–PLGA was added to 20 wt. % solution with 0.5 wt. % of LiTPO.

4.2.3 Preparation of Aqueous Solutions for the Proof of Chemical Network

Aqueous solutions with the content of α,ω-itaconyl-PLGA–PEG–PLGA 15 wt. % and 20 wt. % were mixed with 0.1 wt. %, 0.5 wt. %, 1 wt. % and 3 wt. % of LiTPO. After the addition of the initiator, samples were vortexed for couple of minutes and also mixed with the spatula. Afterwards they were put in to the UV chamber INTELLI RAY 600 Shuttered UV Floodlight for 2400 s and the intensity was set to 50 %. They were covered with a watch glass to avoid the contamination and evaporation. Prepared irradiated samples were stored in the vacuum oven (60 °C) during the night. Dried material was put in to falcons, which were weighed in advance. Falcons with samples were weighed again in order to determine the exact mass of the material. 6 mL of acetone was added to each sample and vortexed. Samples were centrifuged for 15 min at 5000 rpm. Subsequently the supernatant was withdrawn with the syringe. Washing with the acetone was repeated three times. After the washing, samples were stored at ambient conditions during the night. The other day, when the weight of residual material was constant, falcons were weighed again.

4.3 Methods

4.3.1 Photorheology and Real Time Near Infrared Spectroscopy

Photorheological measurements were carried out with Anton Paar Modular Rheometer MCR 302 WESP. Plate-to-plate measuring system was used. Upper steel plate with the diameter 25 mm is the mobile plate. Bottom glass plate enables light irradiation and IR beam pass through the sample. The bottom plate is immobile. As the light source Omnicure type S2000-XLA with the range of wavelengths 400–500 nm was used. Later also the Omnicure type S2001 with the filter 320–500 nm was used as the light source since the PI I2959 does not work in the VIS light range. Omnicure was calibrated by EXFO R2000 Radiometer. It contains the detector which responds to wavelengths between 250–1000 nm. The intensity 4 $W \cdot cm^{-2}$ was used for aqueous solutions and 4.3 $W \cdot cm^{-2}$ for the bulk. The intensity of the light was higher for the bulk because the tape was used during the bulk measurement. Tape was applied to the lower glass plate. It was used to prevent the measuring system damage. Since the light comes from the lower plate, its intensity decreased when the tape is used.

Samples were applied in the middle of the glass plate with the spatula. Afterwards the steel stamp was lowered to the measuring position. Excess of sample was wiped off by paper tissue. Whenever it was possible, liquid samples were applied on the glass plate by micropipette (75 μL) directly into the measuring gap. Subsequently, the paraffin oil was applied on edges of the steel stamp before every measurement of aqueous solution to avoid the evaporation. There was no need to avoid the evaporation in bulk sample. Measurements were performed in the mode of constant gap 150 μm between measuring plates. Amplitude of the strain was for all measurements 1 % and frequency was 1 Hz. G' and G'' were measured every second during the experiment. Every measurement contains different time and temperature intervals. This will be specified for every measurement in the result part.

During the measurement of bulk also RT-NIR was performed. It was done on the FTIR-Spectrometer Bruker Vertex 80. This device is coupled with the photorheometer. External mirrors guide the IR beam to the sample on the glass plate and it allows RT monitoring of the DBC during the irradiation. The signal from the IR is detected on the external Mercury-Cadmium-Telluride (MCT) detector, which is cooled down by liquid nitrogen. Background was measured before every measurement at zero gap (16 scans). NIR measurement was always switched on by trigger 5 seconds before the irradiation started. Data were recorded from 4 000 cm^{-1} to 7 000 cm^{-1} with the resolution 4 cm^{-1} during the whole irradiation. Between two recorded spectra there was 1 s waiting time due to a huge amount of recorded data. The whole set-up of photorheometer coupled with IR spectrometer is shown in the Figure 18.

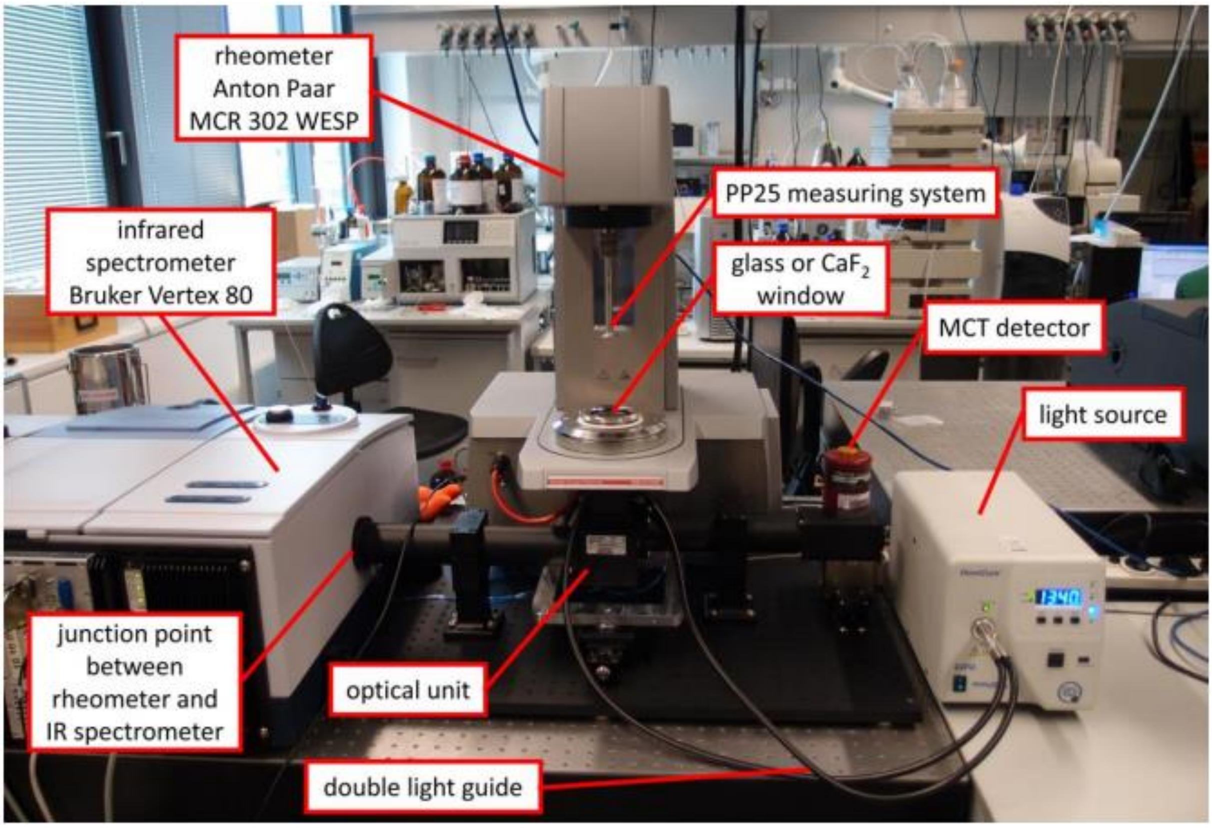

Figure 18: RT-IR-photorheology set-up ***[10]***.

4.3.2 Rheology

Modular Compact Rheometer Anton Paar Physica MCR 300 was used for the measuring of shear rate sweeps, temperature sweeps and time sweeps. Bottom plate contains the Peltier temperature control. Shear rate sweeps were done with the measuring system plate to plate with the constant gap 0.15 mm. Upper mobile steel plate had the diameter 25 mm. Measuring system cone-plate was used to measure temperature and time sweeps. Upper cone plate CP25 with the diameter 25 mm and cone angle 0.979° and band gap 48 μm was used.

Shear rate sweeps measurements were carried out at 25 °C for aqueous solutions. Shear rate was linearly increasing from 1 s^{-1} to 1000 s^{-1} in 500 s. Then 10 s it stayed at 1000 s^{-1} and subsequently the shear rate was decreasing back to 1 s^{-1} in 500 s. This was performed for all three concentration of aqueous solution without the PI and with the content of PI 0.1 wt. %, 0.5 wt. %, 1 wt. % and 3 wt. %.

Temperature sweeps of 10 wt. %, 15 wt. % and 20 wt. % solutions from 8 °C to 60 °C were performed. Before the measurement samples were stored in the fridge approximately one day from the time they were taken out from the magnetic stirrer. Samples were transferred in an ice bath and directly pipetted to the plate cooled down to 8 °C. Parameters of the measurement were adopted from the dissertation work of **Chamradová [102]**. It was performed at shear stress 0.4 Pa and angular frequency was set to 1 rad·s^{-1}. The rate of heating was 0.5 °C per minute. 150 μL of the sample was applied on the plate by micropipette. Plate was already cooled down to 8 °C. If some bubbles occurred they were burst with the syringe needle. At the trim position excess of the formulation was wiped off with a paper tissue. Afterwards the paraffin oil was applied on edges of the steel stamp at the measuring position to avoid the evaporation.

4.3.3 Gel Permeation Chromatography (GPC)

Number-average molecular weight (M_n) and polydispersity index (PDI = M_w/M_n) of the α,ω-itaconyl-PLGA–PEG–PLGA bulk were determined using gel permeation chromathography with multi-angle light scattering method (GPC-MALS). An instrumental setup included Agilent HPLC 1 100 Series instrument with degasser, pump, autosampler, set of two PLgel 5 mm Mixed-C 300 × 7.5 mm columns (Agilent, USA) thermostated to 25 °C and UV-VIS diode array detector in connection with a DAWN HELEOS II multi-angle laser light scattering detector, ViscoStar-II differential viscometer and Optilab T-rEX refractive index detectors (Wyatt Technology, Germany). Both MALS and RI detectors operated at 658 nm. THF was used as the mobile phase at a flow rate of 1 mL·min^{-1}. Astra 6.1 software was used for data collection and analysis and Agilent software was used to control the HPLC. The measurement was done by dr. L. Michlovská (CEITEC).

Change in the molecular weight of 15 wt. % aqueous solution at certain time was determined by GPC. 50 µL of the sample dissolved in THF was injected into a chromatography system Using Waters 717plus Autosampler. THF with the flow rate 1 mL·min^{-1} was used as an eluent. Columns were heated up to 40 °C. Molecular weight was determined via Refractive Index Detector Waters 2 410 according the calibration curve. Calibration was done for polystyrene standards of the wide range of molecular weights. For this reason, results from these GPC measurements can only be used for a relative comparison of the values as no absolute molecular weight are obtained. Run time of one measurement was 40 min. Samples for GPC were prepared always in the concentration 5 mg of 15 wt. % aqueous solution per 3 mL of THF. Before the measurement samples were filtered through the 0.22 µm PTFE syringe filter. Data were evaluated by OmniSec software from Malvern.

4.3.4 Proton Nuclear Magnetic Resonance (^{1}H NMR)

Molecular weight and polymer characterization results were confirmed using proton nuclear magnetic resonance ^{1}H NMR spectroscopy on 700 MHz Bruker AVANCE III HD instrument using 128 scans in deuterated chloroform ($CDCl_3$) solvent at 25 °C. Chemical shifts were reported in ppm relative to tetramethylsilane (TMS). ^{1}H NMR spectra were evaluated using ACD/1D NMR Processor. Measurement was provided by dr. O. Humpa from Masaryk University in Brno and evaluated by dr. L. Michlovská.

4.3.5 Attenuated total reflectance - Fourier Transformed Infrared Spectroscopy (ATR-FTIR)

ATR-FTIR measurements of bulk before and after the irradiation in UV chamber were performed on the spectrometer Perkin Elmer Spectrum 65. Spectra were recorded from 4000 cm^{-1} to 600 cm^{-1} at resolution 4 cm^{-1}.

5 RESULTS AND DISCUSSION

5.1 Well-defined α,ω-itaconyl-PLGA–PEG–PLGA Macromonomer

Material was prepared by dr. L. Michlovská (CEITEC, BUT BRNO). Synthesis is described elsewhere **[12]**. The degree of modification was determined by ^{1}H NMR spectroscopy. Batch prepared for this diploma thesis contains the highest amount of end-bonded ITA, which has been achieved till now. The degree of modification was 89 mol. %. Ratios between PLGA/PEG and LA/GA determined by NMR spectroscopy are in a very good agreement with theoretical values. Number average molecular weight (M_n) was determined by both NMR and GPC. M_n determined by GPC differs 6 % from the theoretical and NMR value. However, this difference is still acceptable. PDI is very low (1.19) and it shows high uniformity. Results from NMR and GPC are shown in the Table 1.

Table 1: Characterization of α,ω-itaconyl-PLGA–PEG–PLGA.

	M_n [g·mol^{-1}]	PLGA/PEG	LA/GA	ITA [mol. %]	PDI
theoretical	5 250	2.50	3.00	-	-
NMR	5 280	2.52	2.96	89	-
GPC	5 580	-	-	-	1.19

5.2 Photocrosslinking "Proof of Concept"

ATR-IR study was done as initial experiment to proof the concept of photocrosslinking. Using this method one can relatively easy and fast determine the DBC. Spectrum of the bulk sample was measured before and after the exposure to UV light in UV chamber in the presence of 3 wt. % of PI TPO-L. The light in UV chamber has high intensity and is composed of wide range of UV light. If the DBC would not occur in this experiment, it would not make sense to continue with the concept.

Spectral analysis of α,ω-itaconyl-PLGA–PEG–PLGA with ATR-IR is described elsewhere **[12]**. Spectra were more or less same at the first sight. However, after the zooming, double bond band was found at 1640 cm^{-1} for non-irradiated material. Band disappeared after the irradiation. Band corresponds to DBs from itaconic acid. DBs were consumed during the irradiation. The zoomed difference in spectra is shown in the Figure 19. Non-irradiated material was measured both with and without the PI. Spectra were completely same because the amount of added PI (3 wt. %) is probably negligible for ATR-IR.

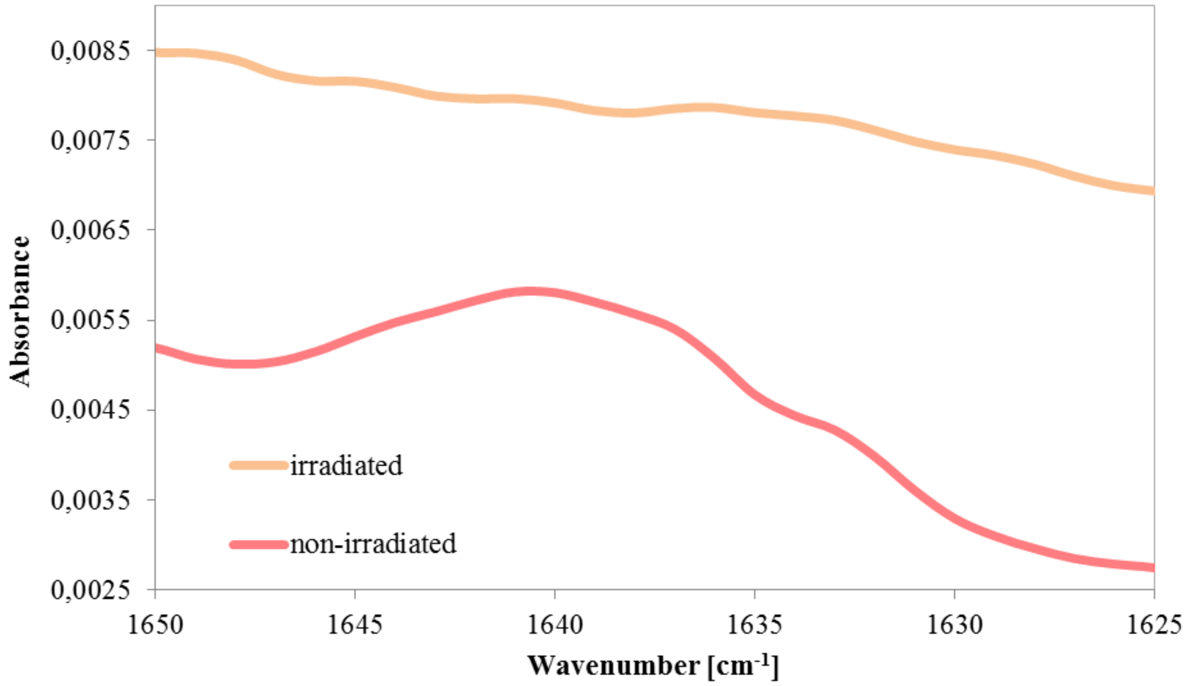

Figure 19: Part of the spectra from ATR-IR: double bond band of non-irradiated α,ω-itaconyl-PLGA–PEG–PLGA disappears after the exposure to the UV light.

5.3 Photocrosslinking in Bulk

As described in the experimental part, the intensity of the light was set on the Omnicure to 4.3 W·cm^{-2} for bulk measurements. However, the proper way how to set the intensity is to measure the exact intensity of the light above the lower glass plate. This is done in order to determine the intensity of the light on the surface of the sample. At the very beginning USB2000+ Fiber Optic Spectrometer was used to do so. Unfortunately, the device got broken so the above mentioned value on the calibrated Omnicure was set. This approach still allows the comparison of measurements between each other.

Firstly, the bulk sample was prepared without acetone. However, the viscosity of the material is so high that it was not possible to properly mix and homogenize the mixture of polymer and PI. The sample with the TPO-L was stored in the oven at 60 °C and afterwards mixed with the spatula. Even when this process was repeated couple of times the measurement was not successful. Therefore, we decided to use acetone for the preparation in order to ensure homogeneity.

In the photorheology it is very difficult to obtain reproducible results for systems with a low reactivity. Even though that this batch of α,ω-itaconyl-PLGA–PEG–PLGA has the highest DS (89 mol. %), the amount of DBs is still very low regarding the length of the macromonomer. Material is also very viscous and sticky. Therefore, it was very difficult to always use the same amount of the sample for all measurements. This was probably the reason why especially the initial modulus differed considerably. The graph shown in the Figure 20 is the average from 6 measurements. It shows the dependence of *G´´* and *G´* on the irradiation, which was started after 305 s. First 900 s of the irradiation is performed at 60 °C. Afterwards, the temperature decreases to 25 °C, which causes the second build-up of the moduli.

Cross point of G´ and G´´ was not observed during the irradiation at 60 °C. It means that the network does not create upon the irradiation. In spite of that the irradiation immediately leads to the increase of the *G´´* and the *G´*. We assume that molecular weight of polymer is increasing, when the material is irradiated. Chains terminated by itaconic acid recombine and create longer chains. Difference between the modulus before the irradiation at 60 °C and after was calculated to be (5 600 ± 1 400) Pa. In some measurements G´ and G´´ crossed after the sample was cooled down to 25 °C. This may be assigned to physical crosslinking of the material. During the polymerization normal force should decrease as the result of the shrinkage, when the constant gap between two plates is set. However, normal force was increasing in this case. It should mean that the material expands during the polymerization. However, it was found that this misleading information is due to the tape, which was used during the measurement. Unfortunately, shrinkage may not be determined, when the tape is used at the temperature higher than ≈ 40 °C. When it was cooled down the normal force started to decrease.

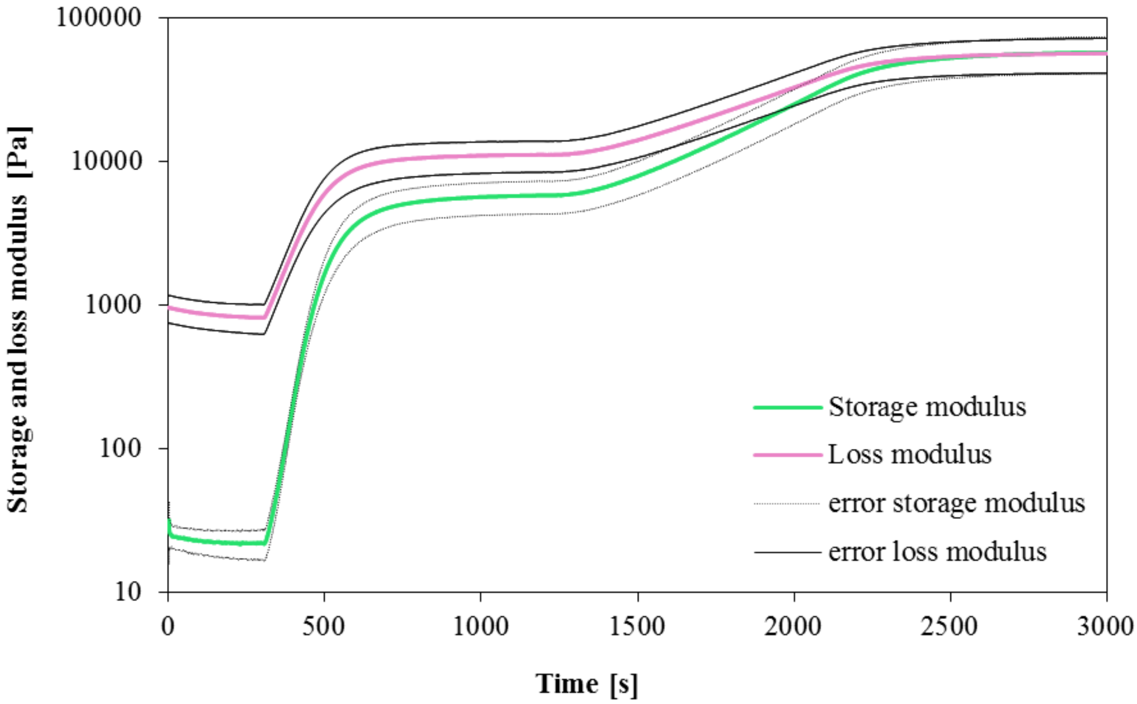

Figure 20: Development of the G´ and G´´ during the whole photorheological measurement of the bulk.

The reactivity of the formulation may be determined from the slope of the *G´* increase. It is shown in the Figure 21. Linear fit was performed. It has been agreed that the value of correlation coefficient R^2 must be higher than 0.98. The slope was calculated to be (21 ± 6) $Pa \cdot s^{-1}$. Another variable, which may be determined from the photorheological measurement is the τ_D, which is the time between the start of the irradiation and the cross point of the linear fittings of the *G′* baseline and *G′* increase. This evaluation is also shown in the Figure 21. The τ_D in the case of the bulk polymerization is (115 ± 4) s.

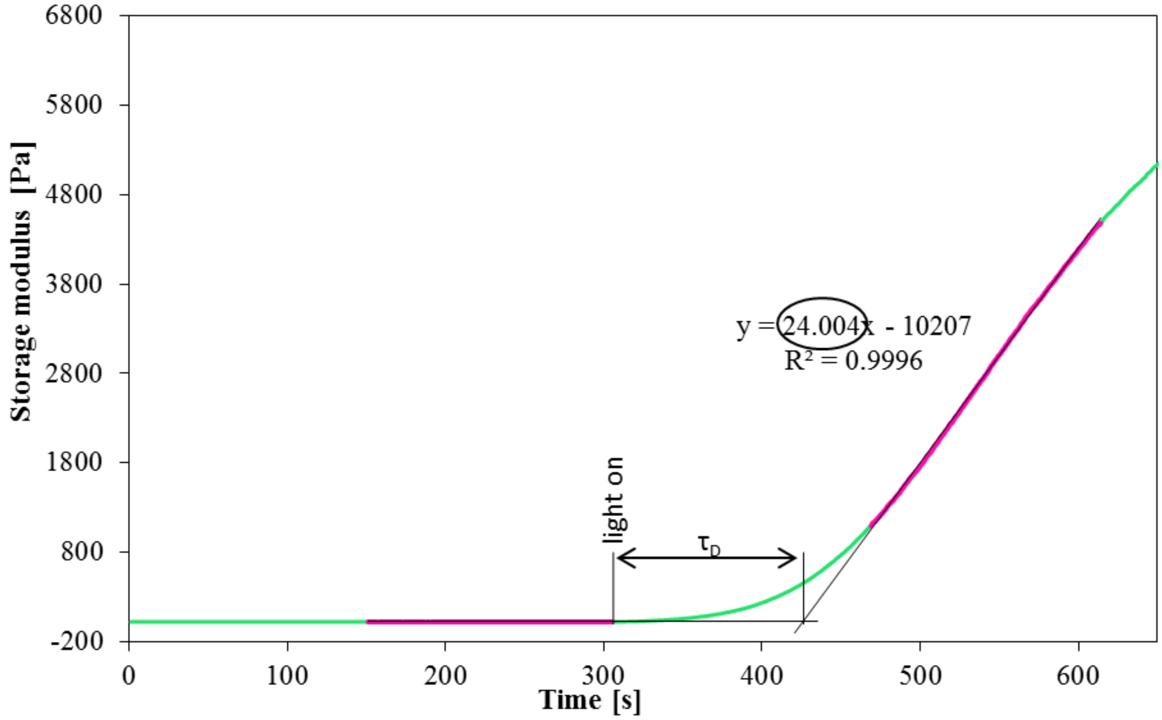

Figure 21: Determination of the τ_D and the slope of the G′ modulus increase after the irradiation.

Simultaneously with the photorheological measurement RT-IR measurement was performed. The whole NIR spectrum before the irradiation is shown in the Figure 22. The part of the NIR spectra, which was measured simultaneously with the rheology, may be divided in to 2 parts. Bands with the wavenumber less than 5000 cm^{-1} are combination bands and bands above 5000 cm^{-1} are assigned to 1st overtone region. The region in the spectra approximately from 4000 cm^{-1} to 4600 cm^{-1} is called first combination region CH. Those wide bands arise from the combination of CH stretching and CH bending. The band with the maximum at 4721 cm^{-1} represents OH group vibrations and COO polymeric vibrations. The band with the maximum at 5246 cm^{-1} is assigned to C=O stretching and COOH vibrations. Bands between 5600 cm^{-1} and 6100 cm^{-1} belong to the 1st overtone CH region. **[103]**

The band with a very small absorption, in order 10^{-4}, which has the maximum approximately at 6 175 cm^{-1} originates from the vibration of CH_2=. It means that this band indicates the presence of DBs from itaconic acid. The RT 3D image of the band is shown on the Figure 23. During the irradiation of the bulk the peak is diminishing, DBs are consumed. The DBC was calculated by the equation 1. Area of DB band was determined by the integration of the band. Integration was done in the software OPUS 7.0 for all spectra recorded during the measurement. The absorbance was very small regarding the background. It just gives the evidence, that the amount of DBs is very low per molecular weight of the pre-polymer. DBC graph is shown in the Figure 24. It shows only first 500 s of the irradiation, because later there is no obvious difference in the DBC. Due to a low signal-noise ratio DBC cannot be precisely determined. From values above 500 s the average and error were obtained for every single curve to approximately determine the percentage of the DBC. Subsequently the average of average and the average of error were calculated. The conversion after the rounding was (74 ± 14) %.

$$DBC[\%] = 100 \cdot \left(1 - \frac{\text{DB band area in time}}{\text{DB band area at the beginning}}\right) \tag{9}$$

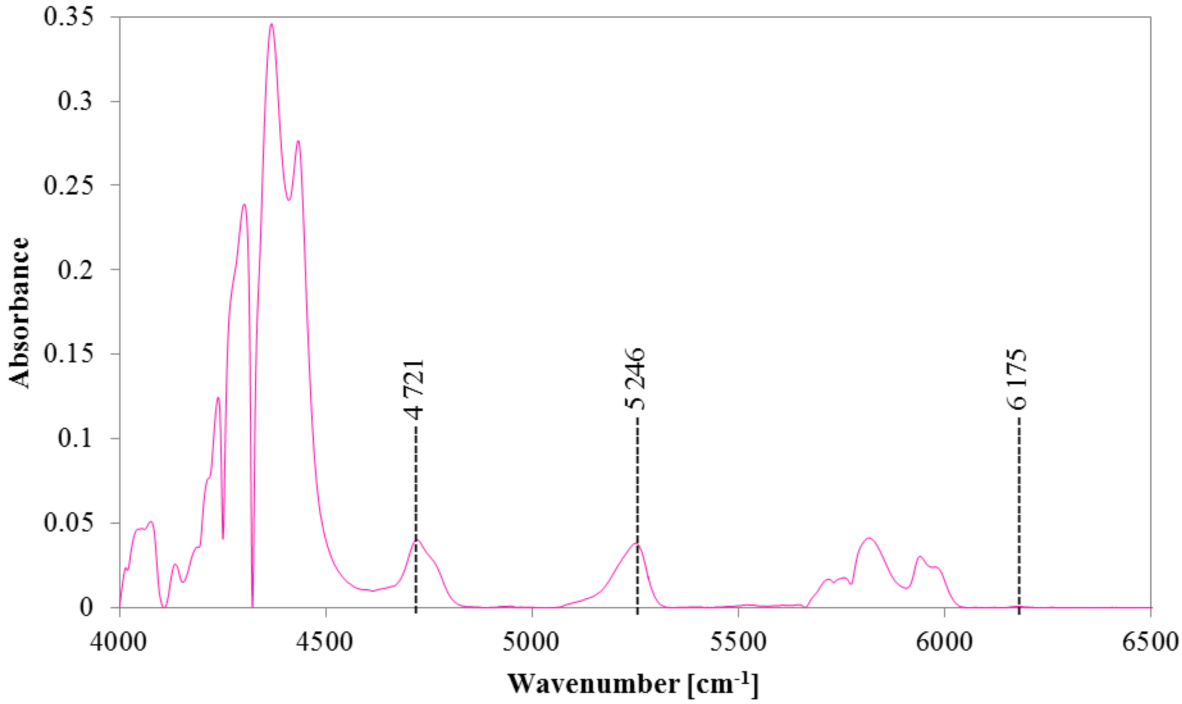

Figure 22: The NIR spectrum of α,ω-itaconyl-PLGA–PEG–PLGA.

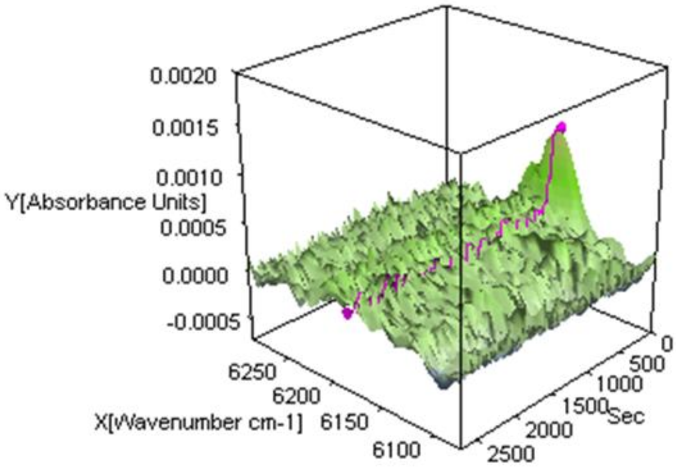

Figure 23: 3D image of the diminishing of DBs in time during the irradiation of the bulk α,ω-itaconyl-PLGA–PEG–PLGA.

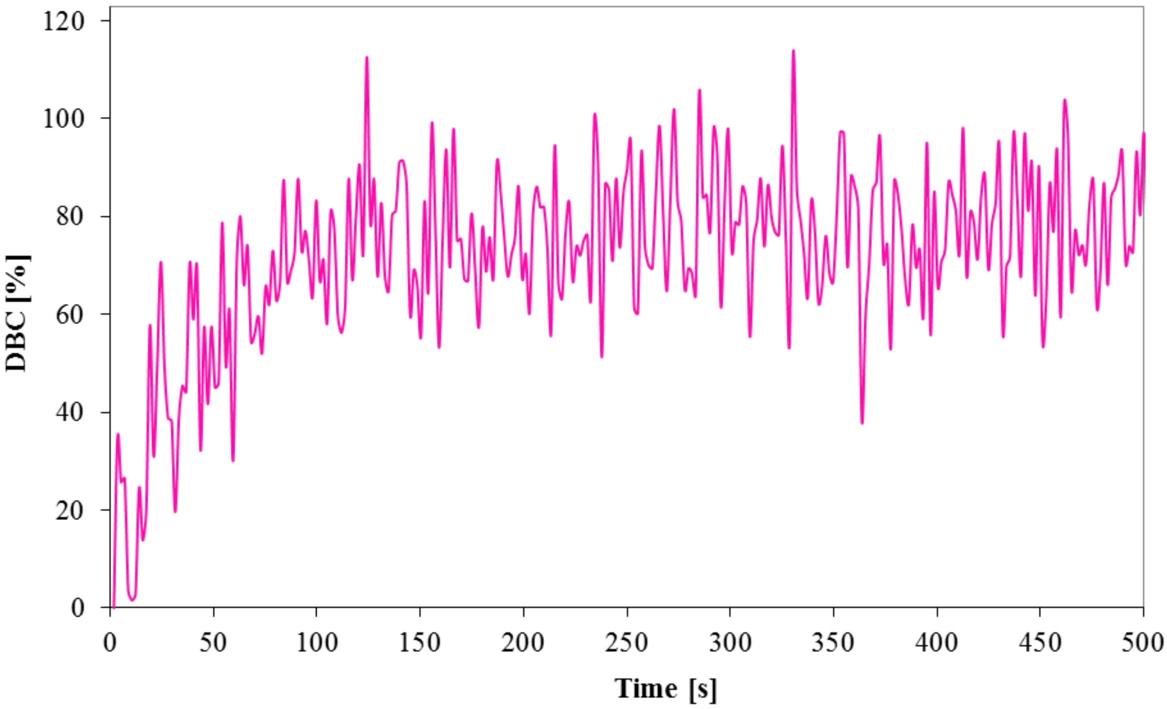

Figure 24: DBC during the irradiation of the bulk α,ω-itaconyl-PLGA–PEG–PLGA.

5.4 Behaviour of α,ω-itaconyl-PLGA–PEG–PLGA Aqueous Solutions

5.4.1 Sol-gel Phase Transition

According to previous studies **[104]**, when the CGT was determined, we expected that the aqueous solutions will stay in the liquid state at the laboratory temperature. However, photorheological measurements and visual observations showed that after some time material undergoes gelation also already at the laboratory temperature. This time differs for different concentrations. The higher the concentration, the earlier the gel has been created, corresponding to the general sol-gel phase transition diagram. In the Figure 25 aqueous solutions are shown immediately after they were withdrawn from the magnetic stirrer (A) and after 24 h (B) and also in 48 h (C) at ambient conditions. One can see that in first 24 h 20 wt. % and 15 wt. % solutions have already created a gel while the 10 wt. % was still in a liquid state, but its viscosity also increased. In 48 h also 10 wt. % solution underwent gelation. We assumed that this may be caused by higher amount of end-bonded ITA. It was previously proved that the ITA decreases the critical gel temperature **[105]**. Introducing of DBs often decreases the solubility of polymers in water **[38]**. Based on this we decided to determine the critical gel temperature of this particular batch by rheology.

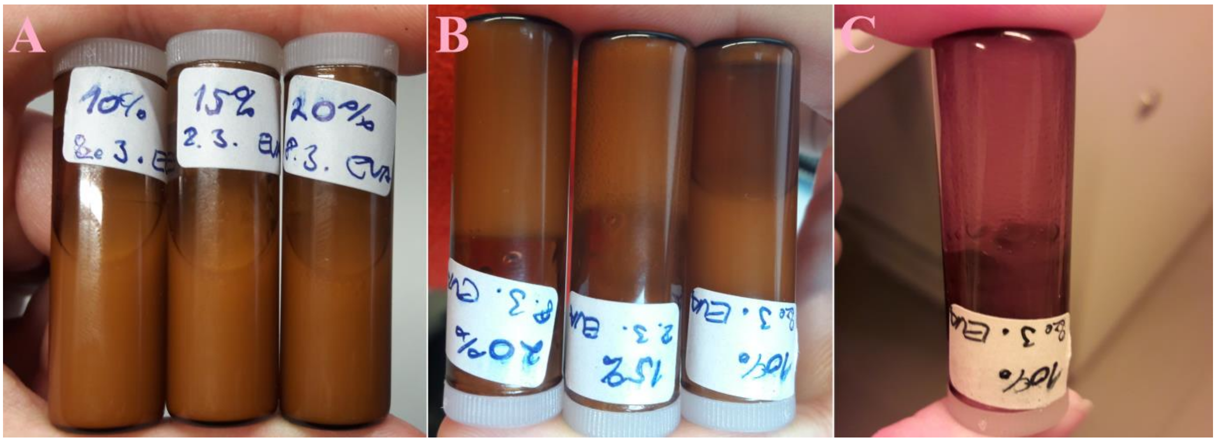

Figure 25: Aqueous solutions A - immediately after they were taken from the magnetic stirrer, B – after 24 h, C – after 48 h.

Temperature sweeps were performed and obtained curves were smoothed in OriginPro 7.5. Curves are shown in the Figure 26. Always one representative curve was chosen. It was not possible to make average curves because temperature for one measured point was not exactly the same among three measurements. One can see that modulus increases with the higher concentration of the solution. In comparison with previous studies **[104]** modulus is higher, what is probably the result of higher DS for itaconic acid. Physical gel is supported by both hydrophobic interactions and hydrogen bonds between H from carboxylic groups and O in backbone of esters. Surprisingly all three concentrations showed the sol-gel temperature (T_{SG}) higher than the laboratory temperature. It was approximately 30 °C for 15 wt. % and 20 wt. % solutions and 31 °C for 10 wt. % solution. Second cross point of G' and G′′ is defined as the gel-suspension transition. Gel-suspension temperature (T_{GS}) was for all three concentrations approximately 36 °C. Transition temperatures and temperatures, when the maximal modulus was achieved together with corresponding *G´* are shown in the Table 2. Even though that temperature sweeps of 10 wt. % solution were performed couple of times, only two times cross points were achieved. For this reason two values are shown instead of average and error.

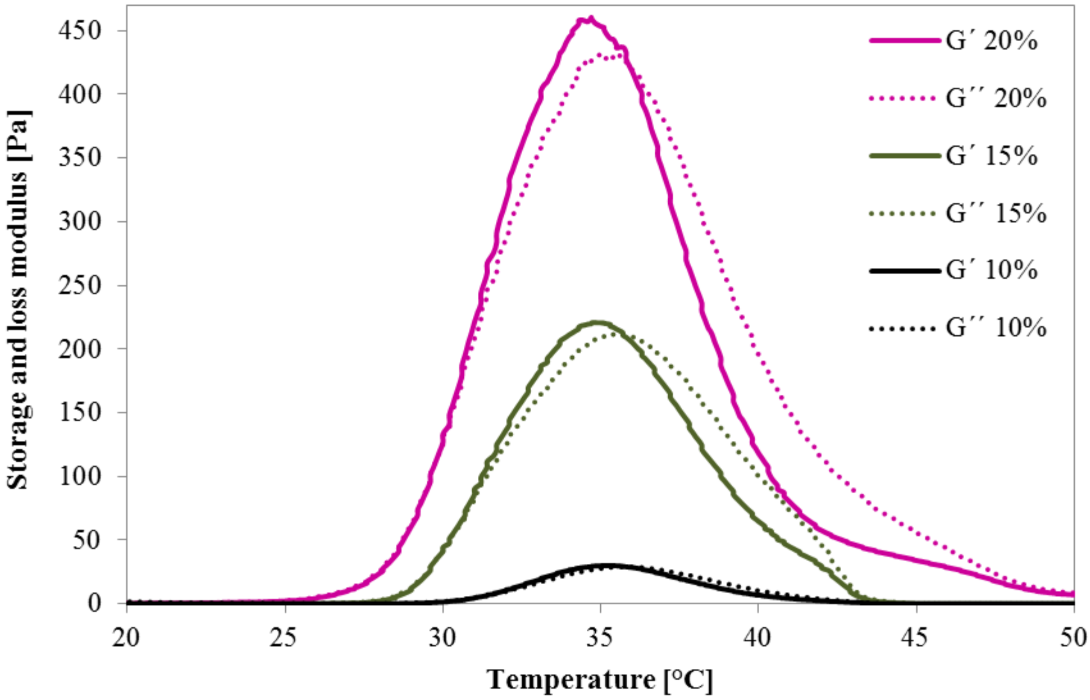

Figure 26: Temperature sweeps of 10 wt. %, 15 wt. %, 20 wt. % solutions.

Table 2: Temperature and G´ values obtained from temperature sweeps.

Sample concentration	T_{SG} [°C]	$G´_{SG}$ [Pa]	T_{max} [°C]	$G´_{max}$ [Pa]	T_{GS} [°C]	$G´_{GS}$ [Pa]
10%	30.8 ± 0.1	6; 4	35.1; 35.2	25; 30	35.9; 35,9	24; 29
15%	29.9 ± 0.1	36 ± 5	34.8 ± 0.1	213 ± 25	35.7 ± 0.1	205 ± 21
20%	29.8 ± 0.2	109 ± 40	34.8 ± 0.1	505 ± 94	36.1 ± 0.1	450 ± 83

It was assumed that either even the small oscillation may increase the gel temperature or the rate of heating 0.5 °C per minute is still too fast. According this we decided to measure time sweep of 15 wt. % aqueous solution at 25 °C. It is shown in the Figure 27. After 6 460 s at 25 °C gel was really created. Due to the lack of time the measurement was stopped despite the fact that the modulus was still increasing. This was performed twice, second time even shorter time just to verify time, when the gel is created (6 420 s). Resulting gel after 13 140 s of time sweep is shown in the Figure 28. Polymer chains probably need longer time to assemble in to micelle structure at 25 °C. At higher temperature diffusion is faster and gel may be created without delay.

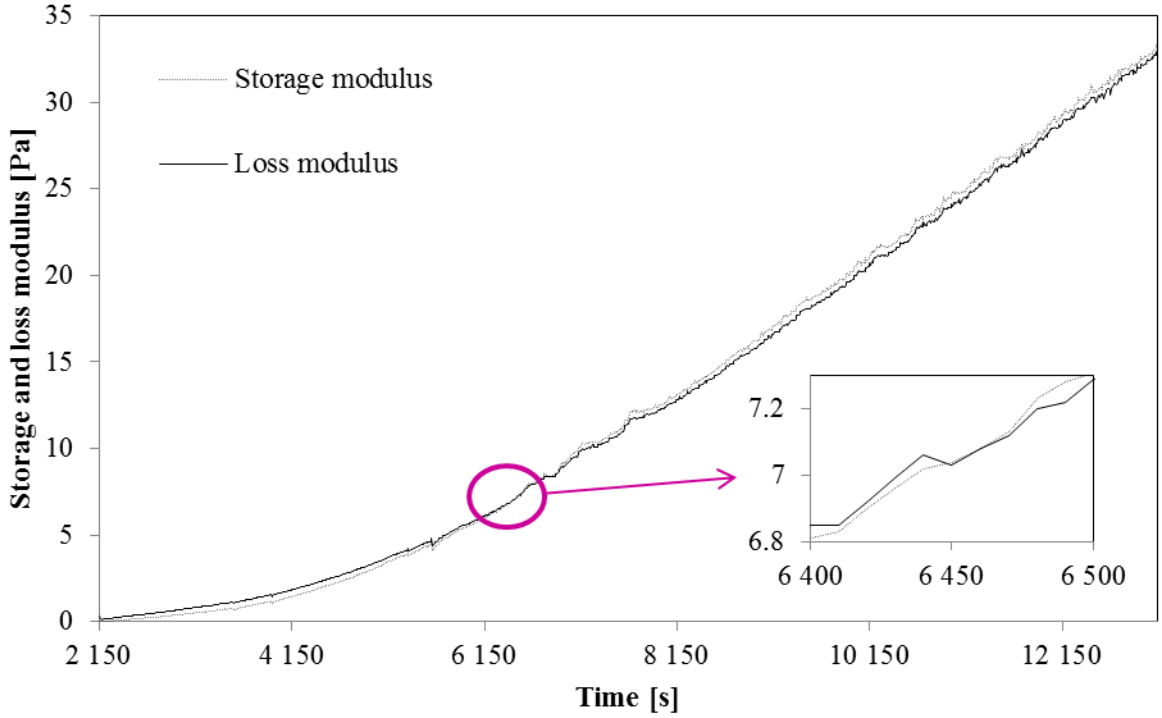

Figure 27: Time sweep of 15 wt. % solution of α,ω-itaconyl-PLGA–PEG–PLGA carried out at 25 °C.

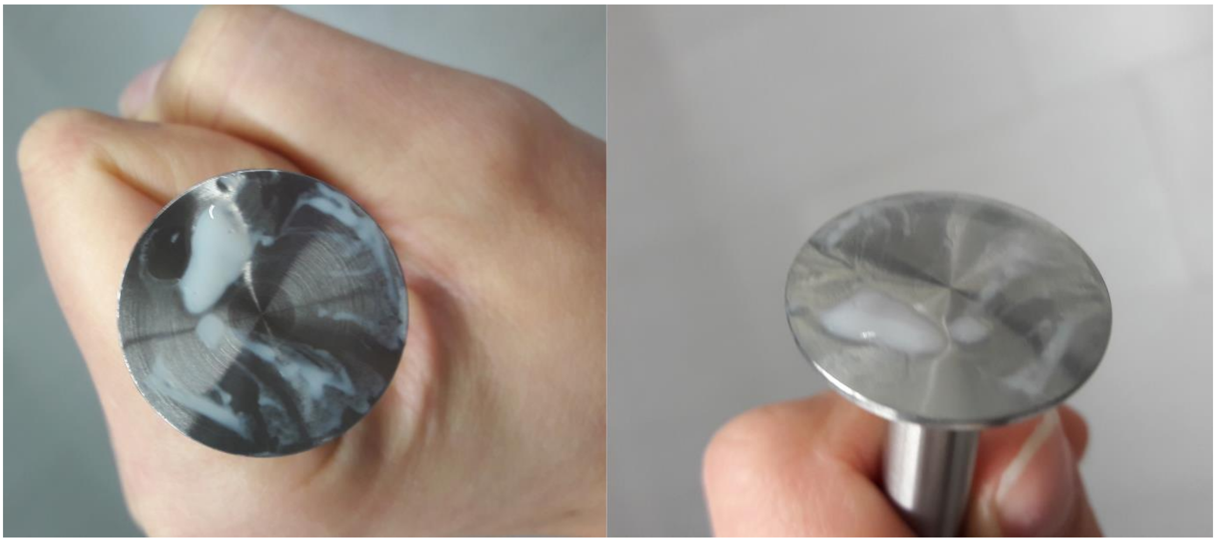

Figure 28: The physical gel created during the time sweep of 15 wt. % solution carried out at 25 °C.

5.4.2 Thixotropic Behavior

As it was mentioned above after some time at ambient conditions all three aqueous solutions showed the gelation and did not flow anymore. We noticed that after samples were shaken on the vortex mixer their viscosity again decreased. Later when the photorheological measurements were performed, it was critical to achieve the same initial *G*′. Couple of times in a row the measurement was stopped and turned on again, when it was observed that the initial modulus increased steadily. Samples were vortexed before every measurement and it took some time until they again achieved steady modulus. Regarding these facts shear rate sweeps were measured to confirm the thixotropic behaviour of formulations. Figure 29, Figure 30 and Figure 31 show the thixotropic behaviour of solutions. Shear stress is not constant when the shear rate changes and paths of curves differ for the increasing and decreasing shear rate. Even at the constant shear rate 1000 s^{-1} shear stress decreases. Thixotropic behaviour was observed and measured also for solutions with LiTPO. This will be discussed in the next chapter.

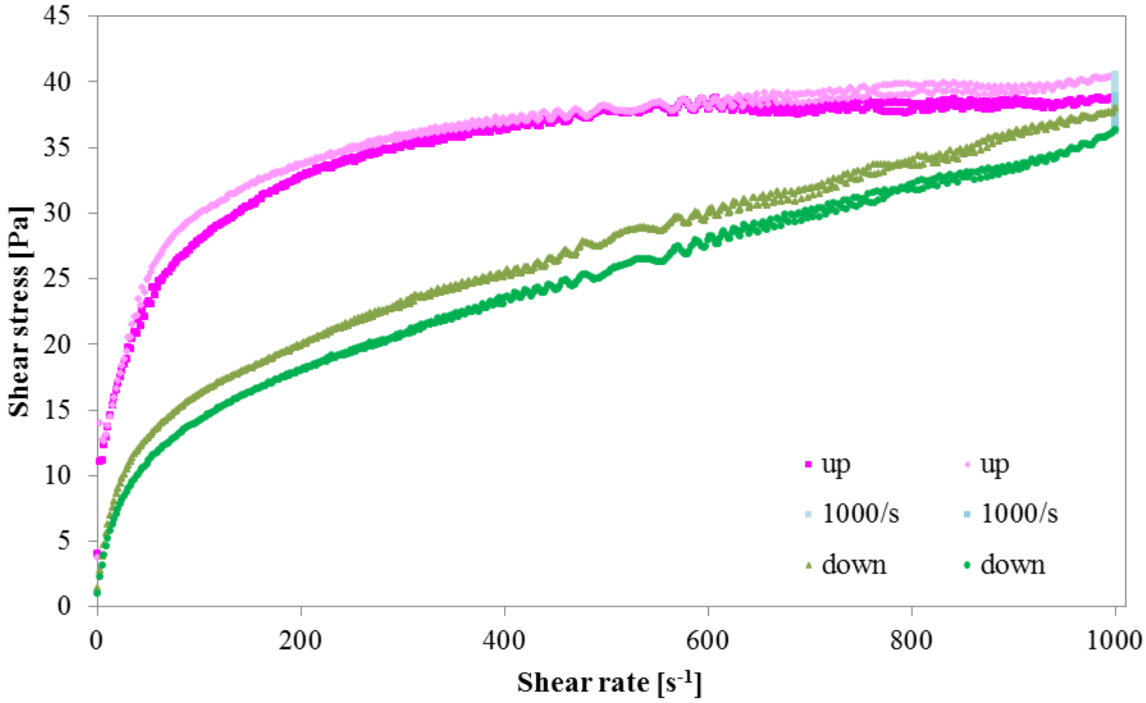

Figure 29: Thixotropy of 10 wt. % physical hydrogel.

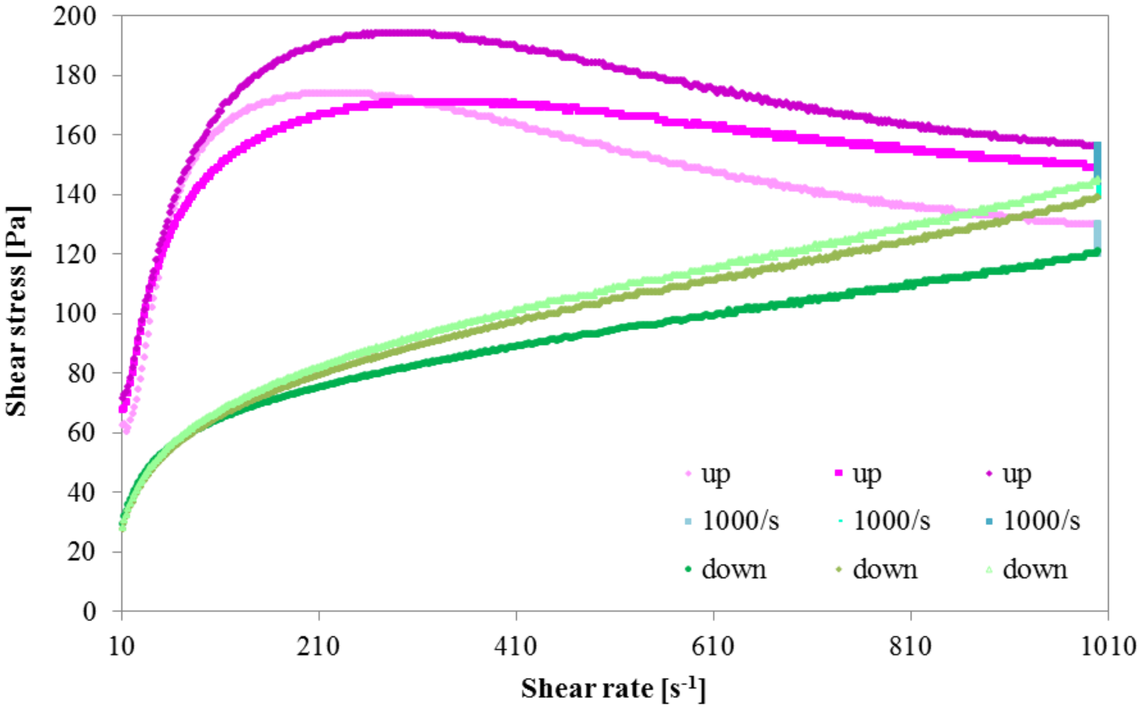

Figure 30: Thixotropy of 15 wt. % physical hydrogel.

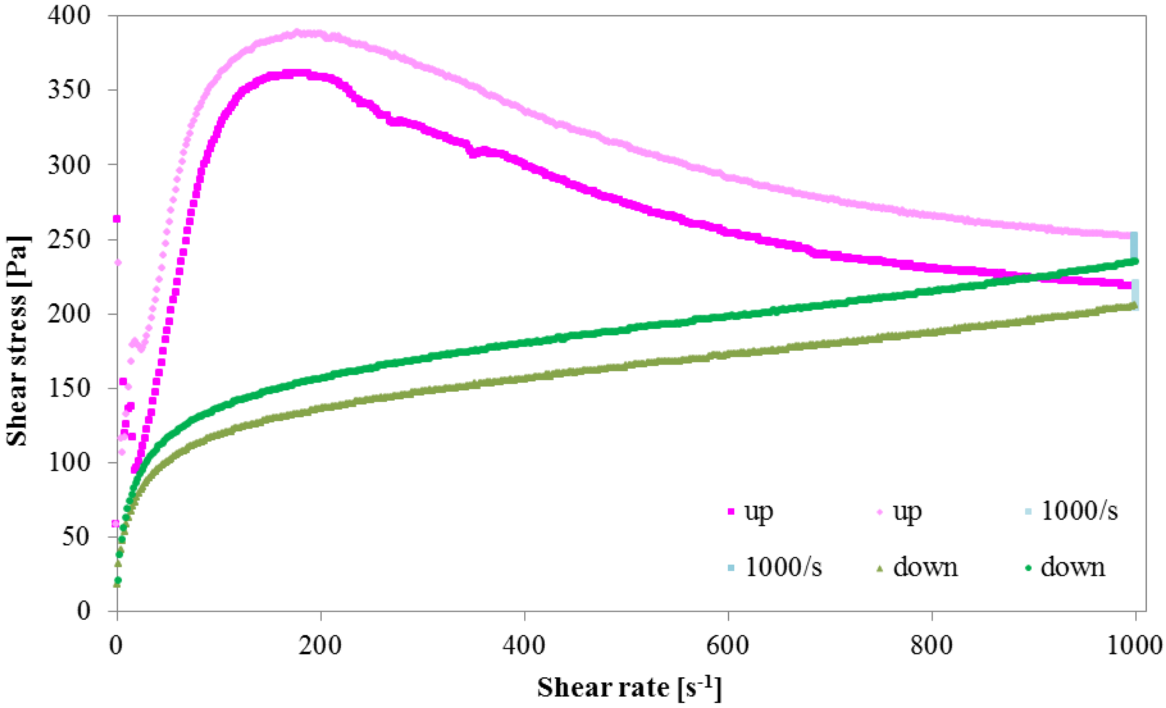

Figure 31: Thixotropy of 20 wt. % physical hydrogel.

5.4.3 Influence of LiTPO on the Physical Gelation

The solubility of the PI LiTPO in water is 47 g·L^{-1} **[76]**. Therefore, concentration of 3 wt. % was chosen as the highest concentration for the photorheology measurements. It was expected that the higher the concentration of the PI will be used, the better chemical crosslinking and the higher modulus will be achieved. Based on this, first measurements were done with the concentration of the PI of 3 wt. %. At the beginning the PI was always added immediately after the solutions were taken from the magnetic stirrer (8 °C). Solutions were in a liquid state so it was not observed immediately that the initiator destructs the micelle structure. Later on we decided to perform all measurements after the solution had been 2 days at ambient conditions. For solutions of all three concentrations gelation was observed after some time at ambient conditions as mentioned above. Afterwards the PI was added and solutions were homogenized by vortexing. Physical gel, which was created by hydrophobic interactions completely, disappeared after the addition of 3 wt. % of PI and the formulation changed to liquid. It was assumed that PI influences the pH of solutions, that leads to higher dissociation of carboxylic groups from itaconic acid. Carboxylic groups are associated in micelles. When the degree of dissociation is high, repulsive force from negative charges may lead to the breakdown of micelle structure. We decided to measure pH of solutions after the addition of different PI concentrations. According the Figure 32 one can see that the addition of the PI causes the increase of pH. The increase is more or less linear. Naturally, the lower the concentration of macromonomer, the higher is the pH. This is pronounced between 10 wt. % and 15 wt. % concentration. Difference between 15 wt. % and 20 wt. % is very low.

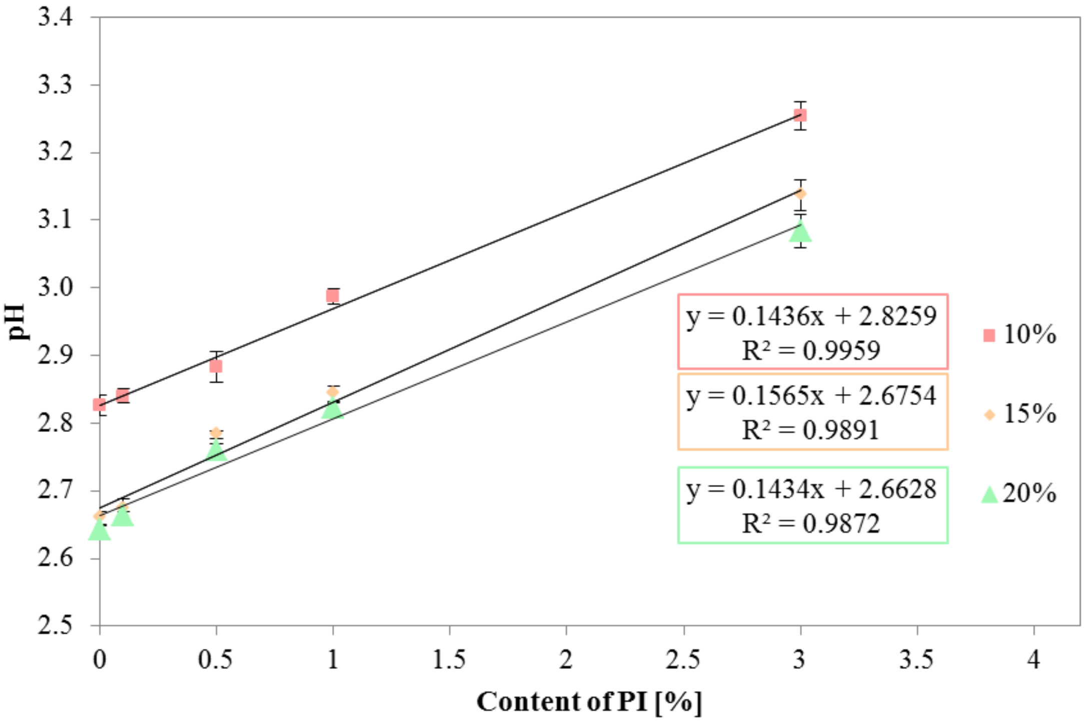

Figure 32: Influence of the LiTPO on the pH of macromonomer aqueous solutions.

Itaconic acid contains two carboxyl groups with different pK_a (3.85; 5.45). In α,ω-itaconyl-PLGA–PEG–PLGA there is only one carboxyl group. The other mediates connection with the copolymer. Carboxyl group in the macromonomer is the one with pKa 3.85. pH, which solutions had after the addition of 3 wt. % of PI, is still lower than pK_a. It means that the amount of protonated acid is still higher than deprotonated. We assume that even the deprotonation less than pK_a produces repulsive force sufficient to disrupt the micelle structure. This strong influence of just a slight decrease of pH on the viscosity may be caused by the closeness of DBs in micelle structure.

Up and down shear rate sweeps were performed to show the influence of the LiTPO on viscosity of aqueous solutions and show the thixotropy. Measurements were performed 3 times, but only one representative curve is shown in graphs. Average could have not been calculated because shear rates were not the same for one measuring point among three measurements.

As it was mentioned before, solutions are thixotropic even after the addition of PI. Only solutions with 3 wt. % of PI and also 10 wt. % solution with 1 wt. % of PI do not show thixotropy (Figure 34, Figure 36, Figure 38). Viscosity of solution decreases so much that solutions show more or less Newtonian behaviour in the set range of shear rates. Only at very low shear rates the viscosity is not constant but this can be caused by error at the beginning of measurement. Unfortunately, measurements started from the shear rate $1\,s^{-1}$ so we cannot observe the behaviour for smaller shear rates. 1 wt. % of PI decreases viscosity but solution still shows quite a strong thixotropy (Figure 34, Figure 36, Figure 38).

Additions of PI 0.1 wt. % and 0.5 wt. % do not influence the micelle structure and viscosity so significantly (Figure 33, Figure 35, Figure 37). 0.1 wt. % of PI slightly increases the viscosity for all concentrations of macromonomer. 0.5 wt. % of PI causes the decrease of the viscosity of 15 wt. % and 20 wt. % hydrogels but only for the very low shear rates. For higher shear rates the viscosity with 0.5 wt. % of PI and without PI is approximately the same.

During the down sweep the viscosity of solutions without PI and with 0.1 wt. % of PI is approximately the same. 0.5 wt. % addition of PI causes slight decrease. It is difficult to find the exact trend of influence because it can vary for different sheer rates.

The most important finding is that the addition of PI 1 wt. % and 3 wt. % destroys micelle structure at 25 °C while additions 0.1 wt. % and 0.5 wt. % maintain hydrophobic interactions

.

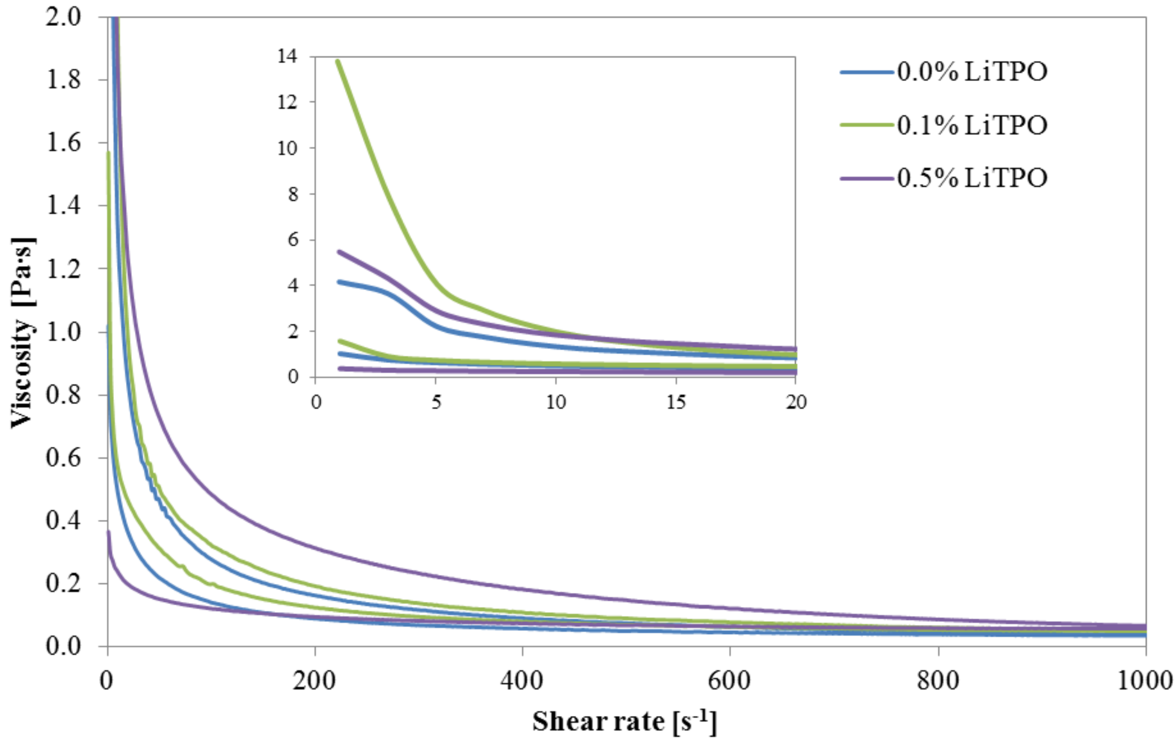

Figure 33: Up and down shear rate sweeps of 10 wt. % solution of α,ω-itaconyl-PLGA–PEG–PLGA with different concentrations of LiTPO – thixotropic behaviour.

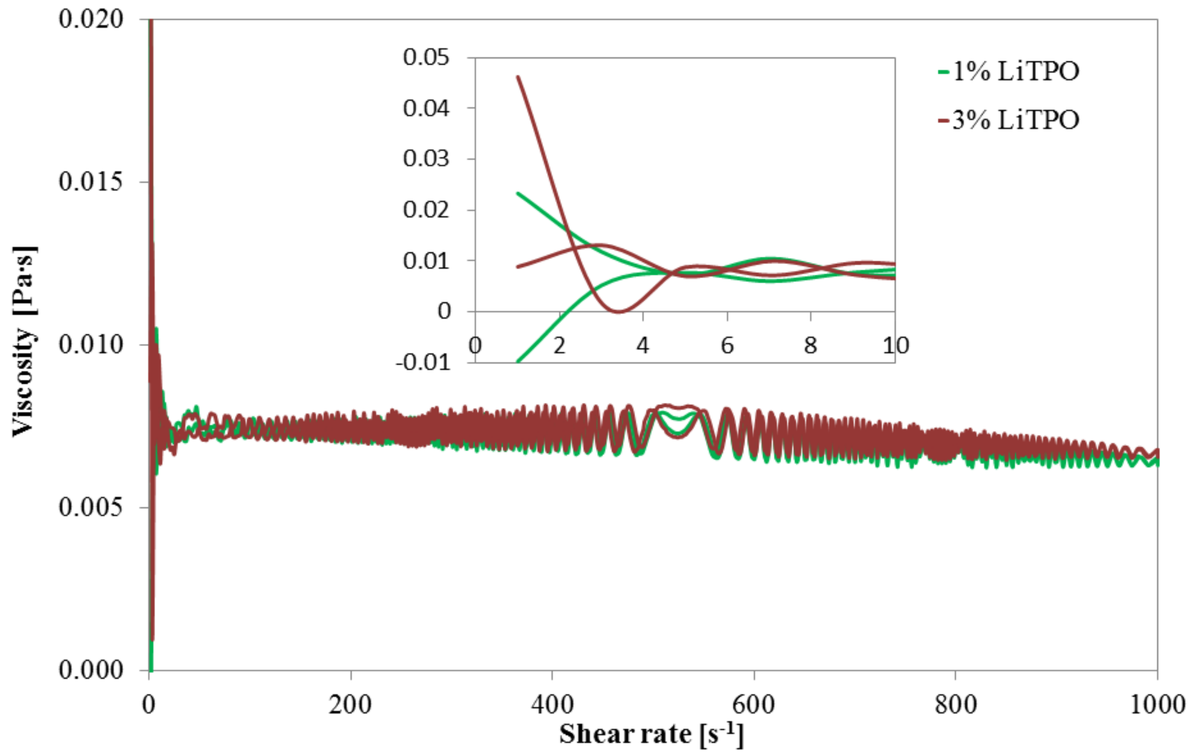

Figure 34: Up and down shear rate sweeps of 10 wt. % solution of α,ω-itaconyl-PLGA–PEG–PLGA.

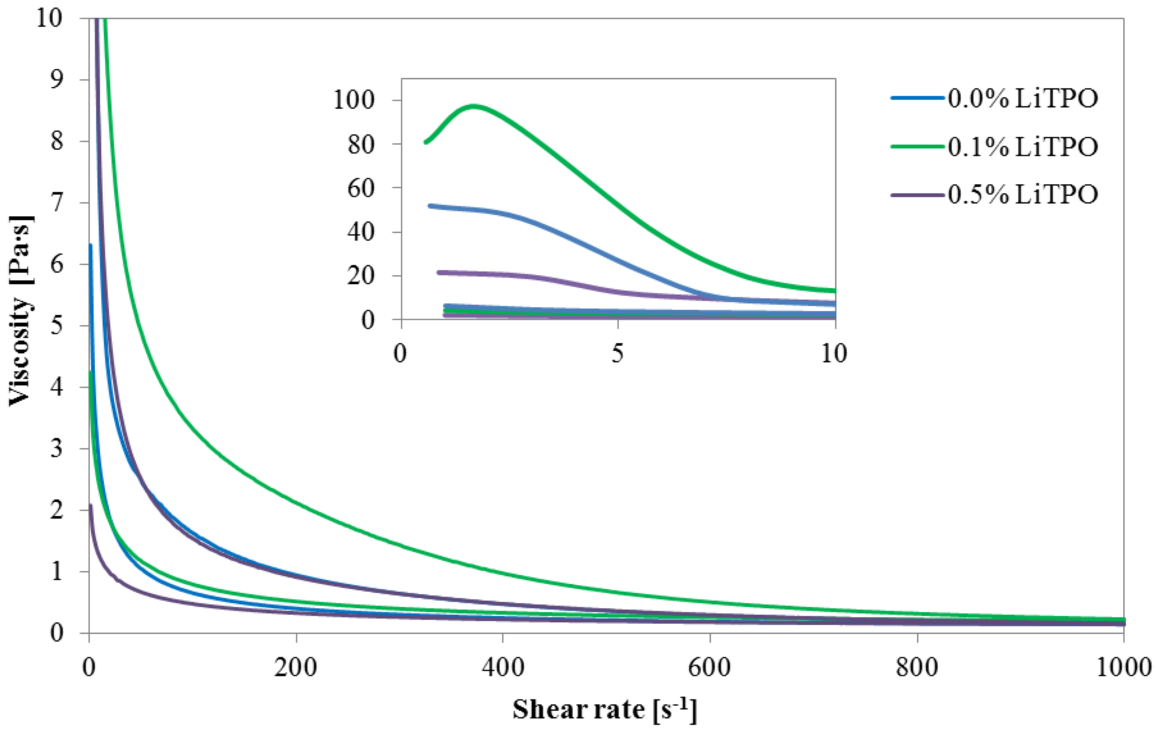

Figure 35: Up and down shear rate sweeps of 15 wt. % solution of α,ω-itaconyl-PLGA–PEG–PLGA with different concentrations of LiTPO – thixotropic behaviour.

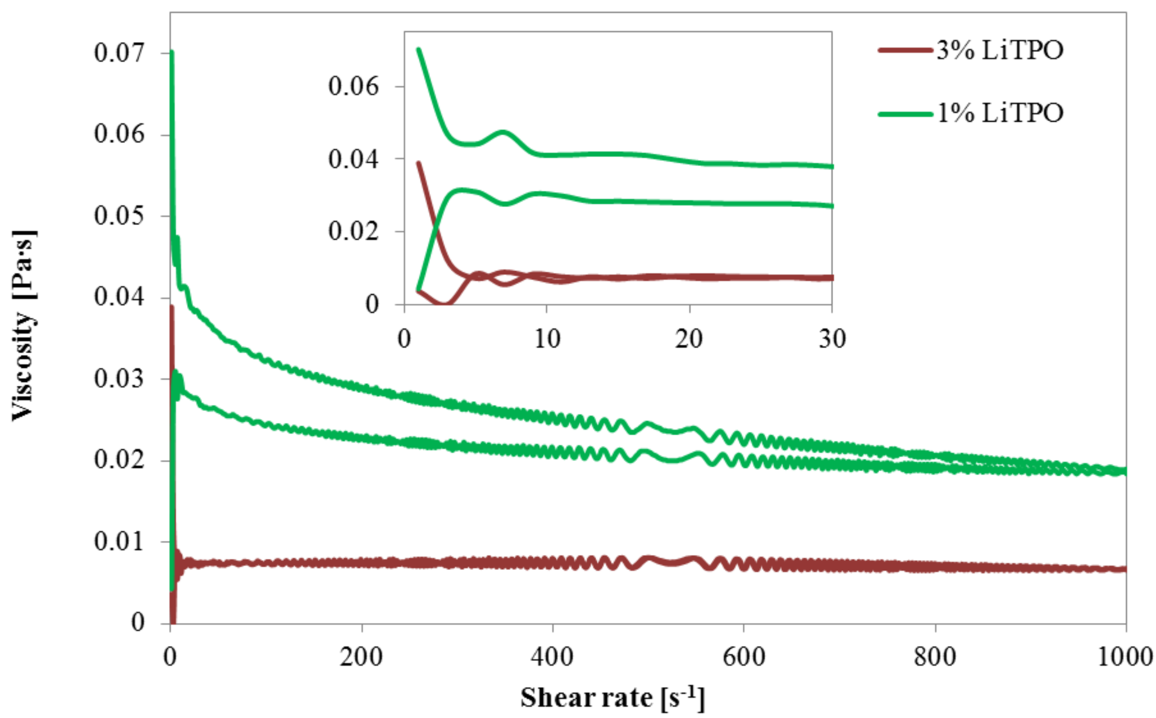

Figure 36: Up and down shear rate sweeps of 15 wt. % solution of α,ω-itaconyl-PLGA–PEG–PLGA with different concentrations of LiTPO – the one with 1 wt. % of LiTPO shows thixotropic behaviour.

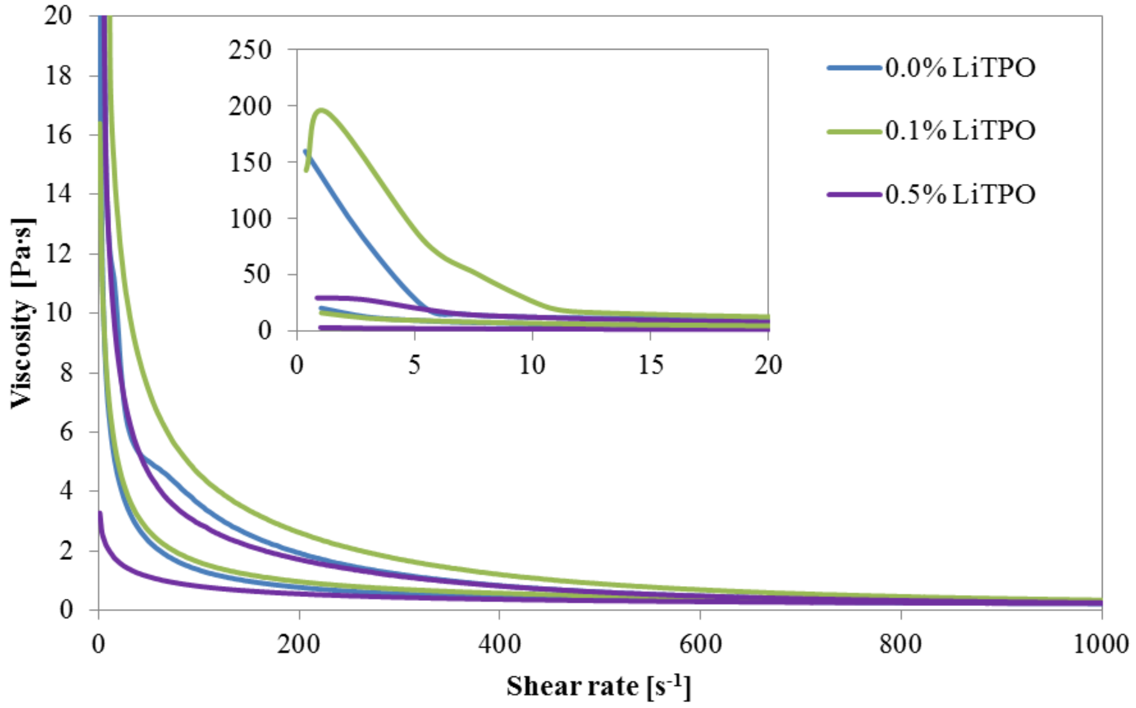

Figure 37: Up and down shear rate sweeps of 20 wt. % solution of α,ω-itaconyl-PLGA–PEG–PLGA with different concentrations of LiTPO – thixotropic behaviour.

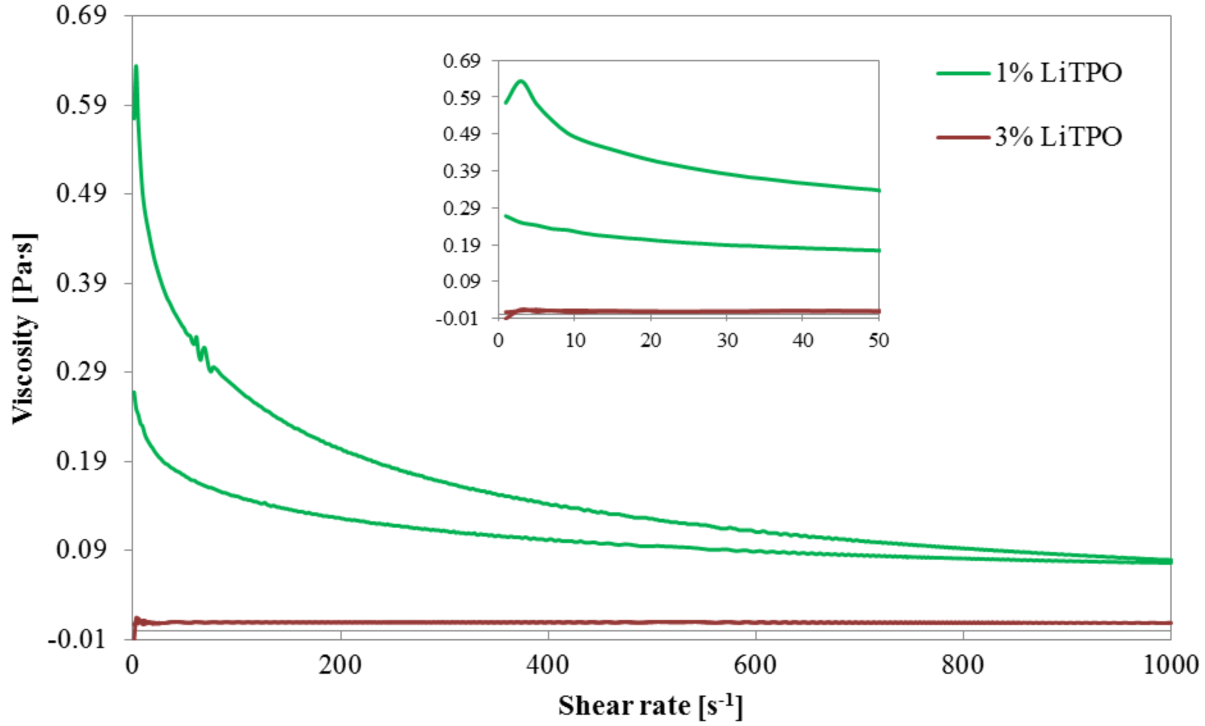

Figure 38: Up and down shear rate sweeps of 20 wt. % solution of α,ω-itaconyl-PLGA–PEG–PLGA with different concentrations of LiTPO – the one with 1 wt. % of LiTPO shows thixotropic behaviour.

5.4.4 Proof of Chemical Network after the Irradiation

In previous studies α,ω-itaconyl-PLGA–PEG–PLGA macromonomer was photocrosslinked using the PI CQ and co-initiator 2-(dimethylamino)ethyl methacrylate (DMAEM). Mechanical properties of bulk were improved; however, it was still soluble in THF **[12]**. At the beginning of experimental work, always when the bulk or hydrogel were photopolymerized, they were submersed in THF or acetone. It looked like material completely dissolved because solution was transparent. It was assumed that also after the photopolymerization with LiTPO no chemical network is created. During GPC measurements of aqueous solutions, which were performed before and after irradiation, it was found that the signal from the GPC measurements after the irradiation is lower, even though the same concentrations were used. A closer look revealed that material dispersed in small particles and settles after some time but was removed by syringe filtration. For this reason the real concentration was lower than expected from the sample mass.

We decided to prove the chemical network creation by simple weighing. Water solutions (10 wt. %, 15 wt. %) were crosslinked in UV chamber dried in a vacuum oven and subsequently dissolved in distilled acetone. The weight of residual non-dissolved material was determined as the percentage of created chemical network in comparison with the initial weight of dried gel. This measurement was done just once due to a high demand for the amount of sample. Therefore absolute values are not very reliable. However it was confirmed that chemical network creates upon the light irradiation when the LiTPO PI is used. For both 10 wt. % and 15 wt. % hydrogel the amount of chemical network increases with the amount of PI. It is shown in the Figure 39. The highest chemical crosslinking was achieved for 20 wt. % gel with 3 wt. % of PI. 416 mg of photocrosslinked 15 wt. % hydrogel (3 wt. % LiTPO) submersed in 20 mL of distilled acetone is shown in the Figure 40.

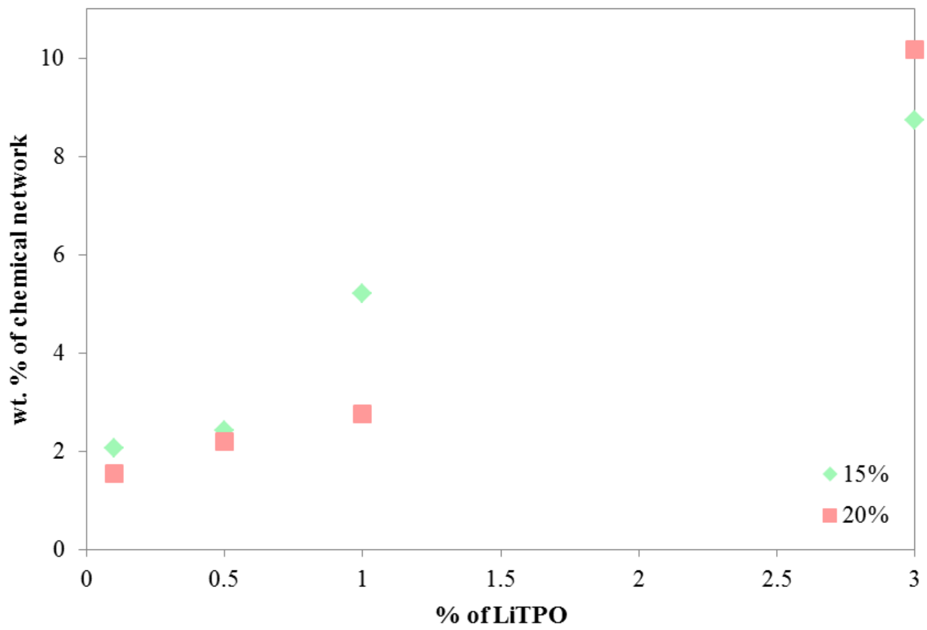

Figure 39: Graph shows the percentage of created chemical network for different contents of PIs.

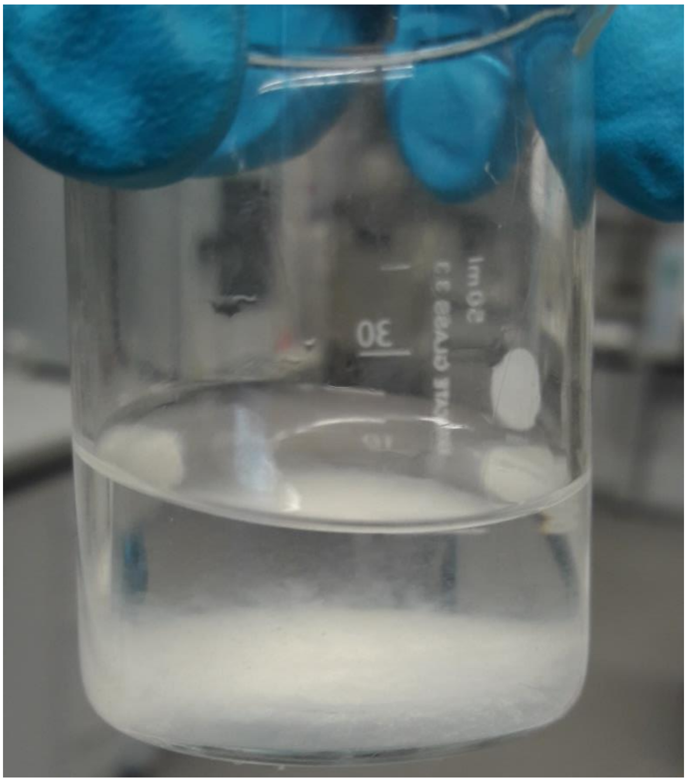

Figure 40: 15 wt. % photocrosslinked gel in distilled acetone.

5.4.5 Storage Stability of Aqueous Solutions

After few days at the magnetic stirrer at 8 °C the solution was white and milky without any visible particles. It was assumed that there are still aggregates in the size above 500 nm **[106]**. It was found, that when the solutions were stored for a couple of days at ambient conditions milky liquid state changed to transparent viscous state. GPC measurement was done to determine the molecular weight during dissolution. It was investigated whether the dissolution is accompanied by degradation or not. Measurements were always performed twice to show that also values within one day can differ. Generally, M_w, compared to M_n, is not as sensitive to variations in setting the integration limits during evaluation. Therefore, we chose M_w as the main factor to compare molecular weights for different storage times. The values for weight average molecular weight (M_w) for different storage times are shown in the Figure 41. M_w decreased less than 6 % on the 2nd and 3rd day of measurements. 4th day it was more than 12 %. Therefore we decided to perform photorheological measurements on the 3rd day. All other values obtained from GPC (M_n, PDI) are shown in the Table 3. PDI of the bulk was determined to be 1.19 as it was stated before. Already the first day at ambient conditions the PDI of 15 wt. % solution was 1.51, meaning that some hydrolysis occurred during dissolution.

Table 3: Table of values from GPC measurements in time.

Time	M_w [g·mol^{-1}]		M_n [g·mol^{-1}]		PDI	
1. day	8990	8770	5800	5810	1.55	1.51
2. day	8410	8320	4360	4480	1.93	1.86
3. day	8430	8440	4360	4480	1.92	1.88
4. day	7940	7650	4410	4070	1.80	1.90
5. day	8040	8170	4570	4510	1.76	1.81
6. day	8160	8070	4890	4370	1.67	1.85
7. day	7330	7140	4130	3590	1.78	1.99

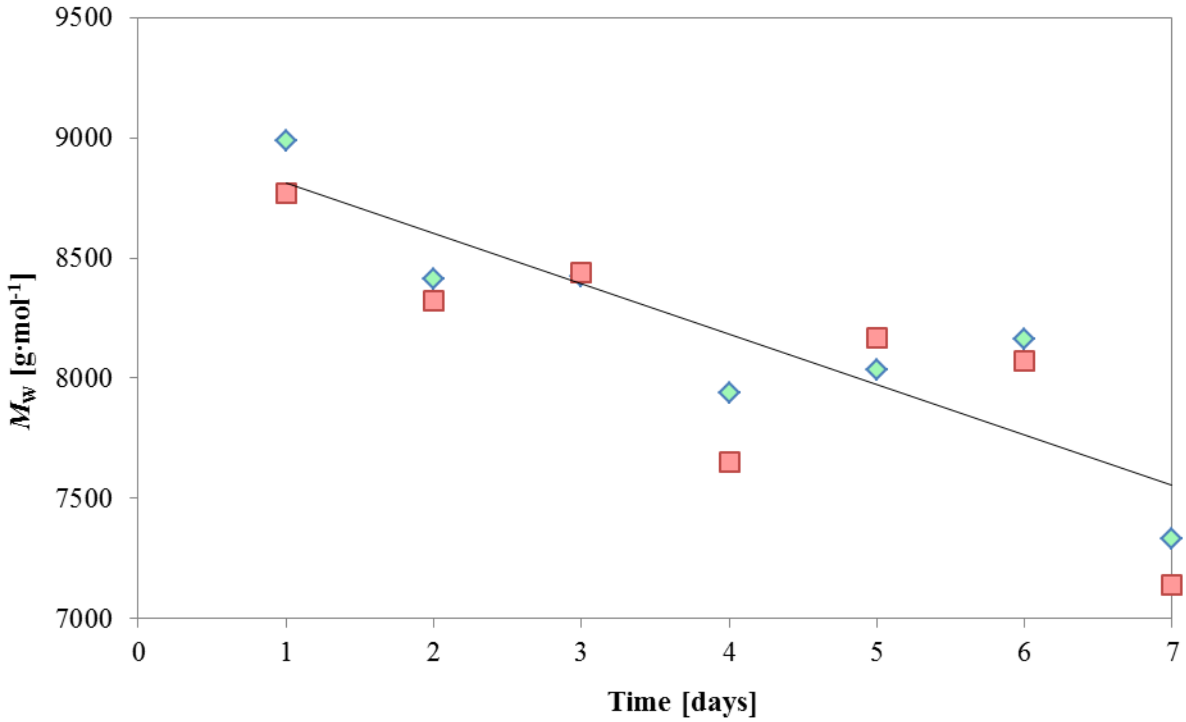

Figure 41: Change of M_w of 15 wt. % solution at ambient conditions in time.

5.4.6 Photocrosslinking in Water

5.4.6.1 Photocrosslinking at 25 °C

In comparison with bulk, photorheology of aqueous solutions was not monitored by RT monitoring to determine DBC. It would not be possible to observe the DB band since the concentration of DBs is even lower here. If the sample would contain sufficient amount of DBs, solutions would have to be prepared in D_2O. Otherwise the signal from H_2O would overlap with the double bond peak.

It was a problem to obtain reproducible initial *G´*. One reason for that was the aforementioned thixotropic behaviour of the material. In order to avoid this time dependant behaviour the samples were exposed to high shear rates at the beginning of measurement. The concept was to stress the sample at such a shear rate, which reset the samples and thereby increase the reproducibility of the measurements. The shear rate 8 s^{-1} was chosen. This was done before the shear rate sweeps, which showed that it was not sufficient at all. According the shear rates sweeps at least the shear rate 20 s^{-1} would be necessary.

Measurements at 25 °C had four intervals. First 300 s of rotation was performed at the shear rate 8 s^{-1}, as mentioned above. Than the shear rate was decreased from 8 s^{-1} to 0 s^{-1} in 300 s. Afterwards, the oscillation started. After 300 s of oscillation the light was triggered on for next 300 s. Data in diagrams are shown from 605 s or 610 s due to a high error at the beginning of oscillation.

In the case of 10 wt. % and 15 wt. % solution the addition of the 0.1 wt. % of PI even increase the initial modulus (Figure 43, Figure 44). This may be due to the decrease of solubility of macromonomer in the presence of the low amount of PI. Higher concentrations of PI decrease the initial modulus for all solutions. For the concentration 0.5 wt. % of PI the decrease is not so significant and solutions still did not flow (Figure 42). On the other hand 1 wt. % of LiTPO led to very low viscous liquid state. This happens, when certain critical concentration of PI is exceeded. At this concentration of PI, deprotonated carboxylic groups are in such an amount, which is sufficient to cause the destruction of micelle structure due to the repulsive force between negative charges.

It was assumed that physical crosslinking is essential for the later chemical crosslinking. In micelles DBs are hold together in proximity due to hydrophobic interactions between PLGA and PEG part. This was expected to facilitate the polymerization. This idea was proved by photorheological measurements. One can see that the highest modulus after the photopolymerization was achieved with the 0.1 wt. % of LiTPO while 1 wt. % addition led to the modulus approximately the same as solution had without the irradiation, making this concentration obsolete. 0.5 wt. % addition of PI led to the increase of modulus but not as much as it was for 0.1 wt. %.

In order to compare the influence of chemical crosslinking on mechanical properties of physical gel also the measurement of the solution without LiTPO was performed. It was not expected that the modulus started to slightly decrease upon the irradiation. This effect was more pronounced for concentrations 15 wt. % and 20 wt. % (Figure 43, Figure 44). It is assumed that this effect is caused by a local temperature inhomogeneity owing the irradiation.

At the very beginning of practical work 3 wt. % of LiTPO was used. This did not lead to any significant increase of modulus. But in comparison with the material without the PI there was not decrease because light interacted mainly with LiTPO.

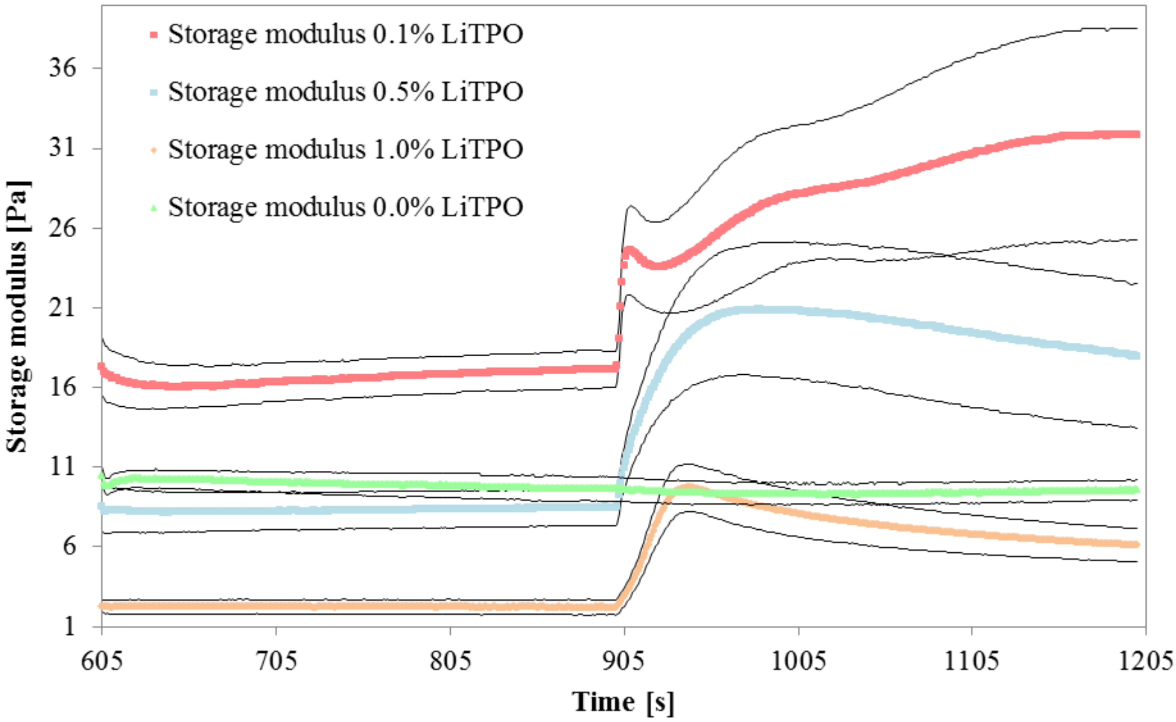

Figure 42: Average curves of the G´ of the 10 wt. % hydrogel during the chemical crosslinking at 25 °C. Black lines show the error of the measurement.

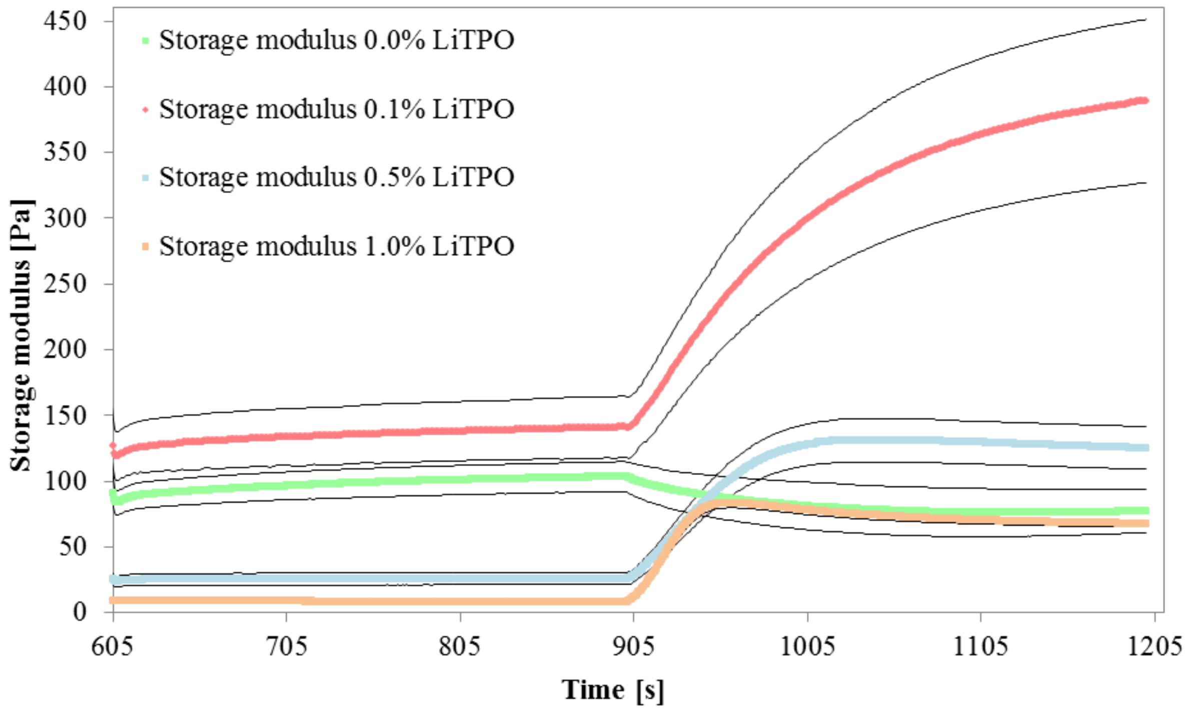

Figure 43: Average curves of the G´ of the 15 wt. % hydrogel during the chemical crosslinking at 25 °C. Black lines show the error of the measurement.

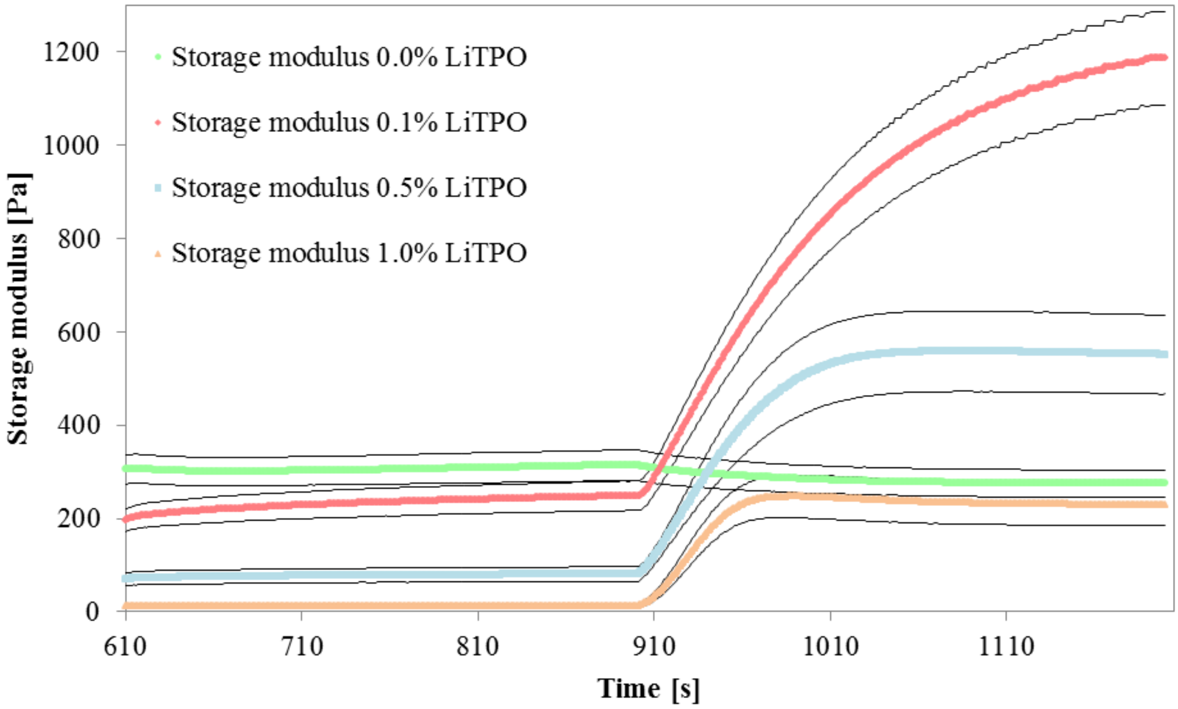

Figure 44: Average curves of the G´ of the 20 wt. % hydrogel during the chemical crosslinking at 25 °C. Black lines show the error of the measurement.

In Figure 45 a comparison of G'_{max} for different concentrations of macromonomer and different concentrations of LiTPO is shown. The higher the concentration of macromonomer, the higher the G'_{max} achieved after the irradiation is. Influence of the macromonomer content is most significant when 0.1 wt. % of PI is used. Besides the macromonomer content also the amount of PI influences G'_{max} as it was mentioned above. The influence has the same trend for all concentrations. The highest G' is achieved for the 0.1 wt. % of PI. 0.5 wt. % and 1 wt. % lead to the decrease of G'_{max}. The addition of PI 0.5 wt. % still leads to the higher G' in comparison with the modulus without any PI. However, after the photopolymerization of the aqueous solution with 1 wt. % of PI the modulus reached about the same level as the modulus without PI.

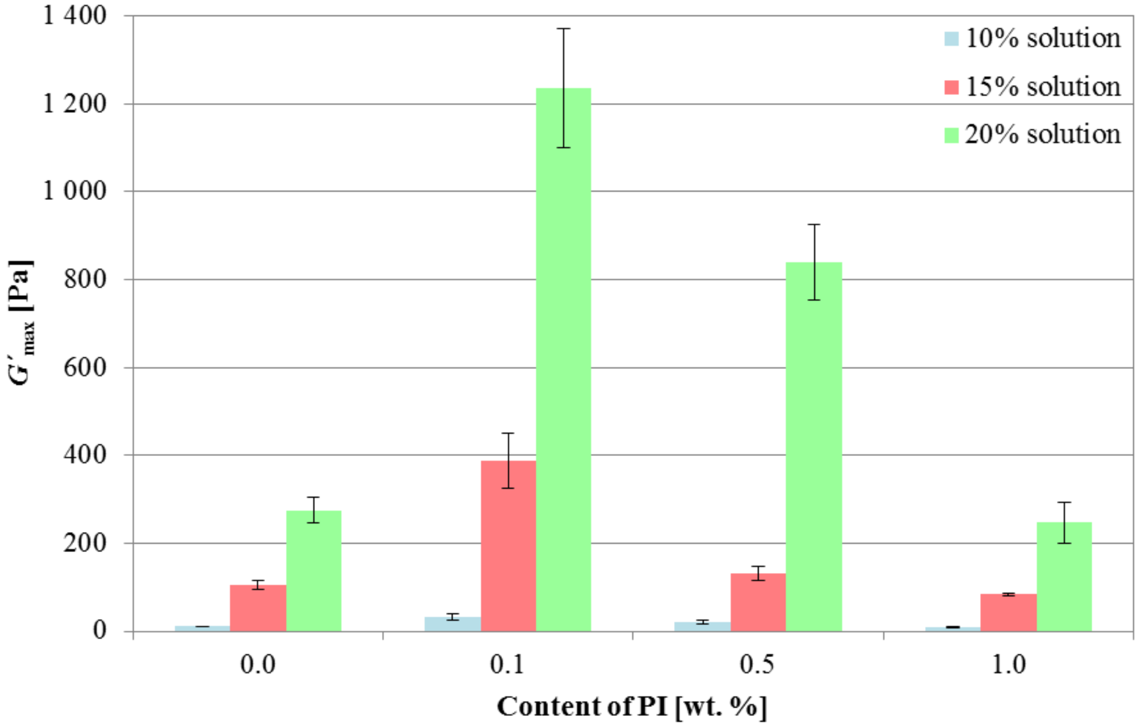

Figure 45: Dependency of the G'_{max} on macromonomer content and PI content.

As before, the slope, a measure of the photoreactivity, and τ_D were determined. It is shown in the Figure 46 and Figure 47. One can see that the higher the macromonomer content the higher the slope and the longer the delay time. In solutions with higher macromonomer content there are more DBs, which are essential for this photopolymerisation. On the other hand the higher content of macromonomer, the more chains and entanglements and it is more difficult for radicals to attack DBs. For the same reason the slope and τ_D are higher for the bulk sample. This statement does not apply for the 20 wt. % solution with the content of PI 0.5 wt. %, when τ_D is shorter than in the case of 15 wt. % solution. No trend was observed for the influence of PI on the slope and τ_D.

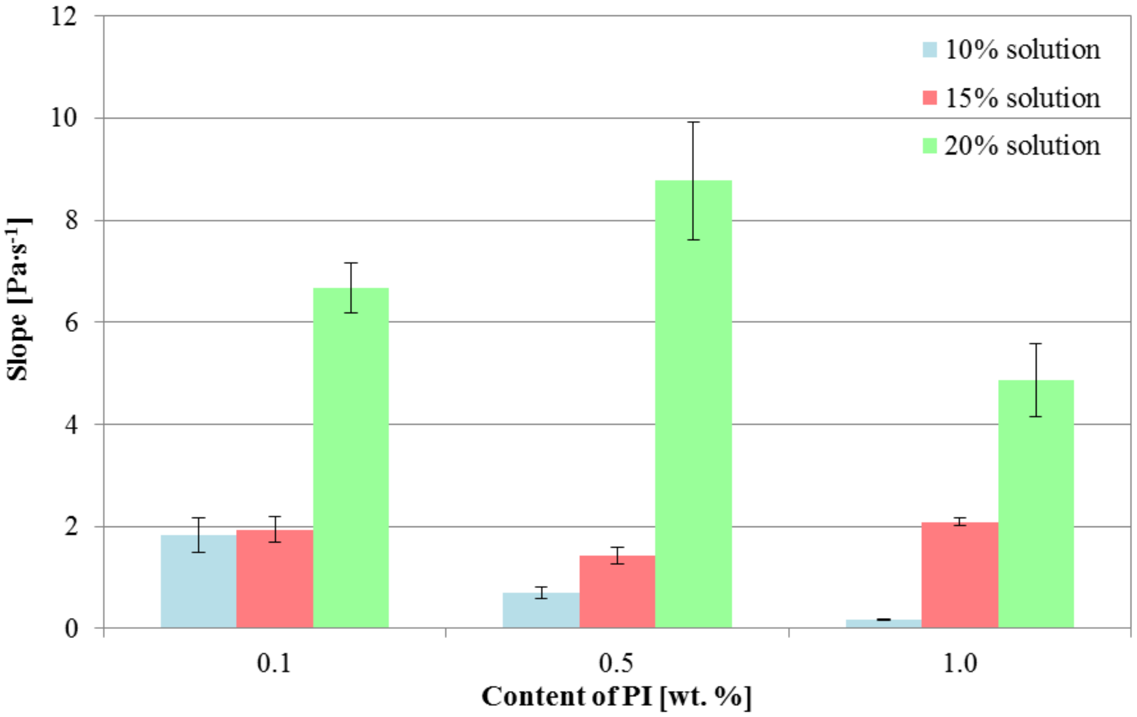

Figure 46: Dependency of the slope as the index of the photoreactivity on the macromonomer and LiTPO content.

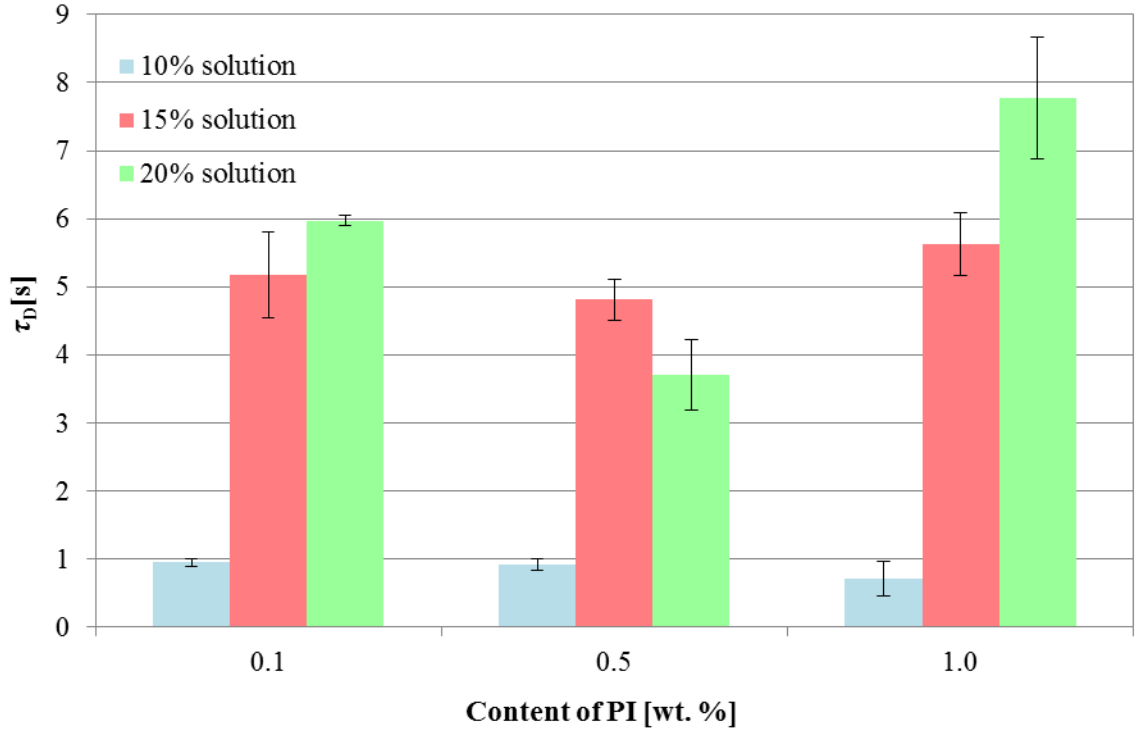

Figure 47: Dependency of τ_D on the macromonomer and LiTPO content.

Photocrosslinking at 25 °C with crosslinker PEGDA

To obtain better mechanical properties, 20 wt. % α,ω-itaconyl-PLGA–PEG–PLGA solution was crosslinked with the addition of 5 mol. % PEGDA per DBs in the presence of 0.5 wt. % of LiTPO. It was homogenised in ultrasonic bath for 1 hour. Acrylates react very fast and high G′ can be achieved. However, they are quite brittle after photocrosslinking. In this experiment the highest G'_{max} was achieved among the all measurements of aqueous solutions in this work (Figure 48). Created gel is shown in the Figure 49. However, it was too brittle to be transferred from the plate.

The slope of storage modulus increase was equal to (30 ± 7) $Pa \cdot s^{-1}$. This high photoreactivity in comparison with other solutions is due DBs from acrylates. τ_D was determined to (6.4 ± 0.5) s. It is higher than τ_D of 20 wt. % solution with 0.5 wt. % of LiTPO without PEGDA. The viscosity after the addition of PEGDA increased, what impedes diffusion. Moreover DBs from ITA are hidden in micelles on hydrophobic ends and PEGDA is hydrophilic. This all can prolong $\tau_{D.}$

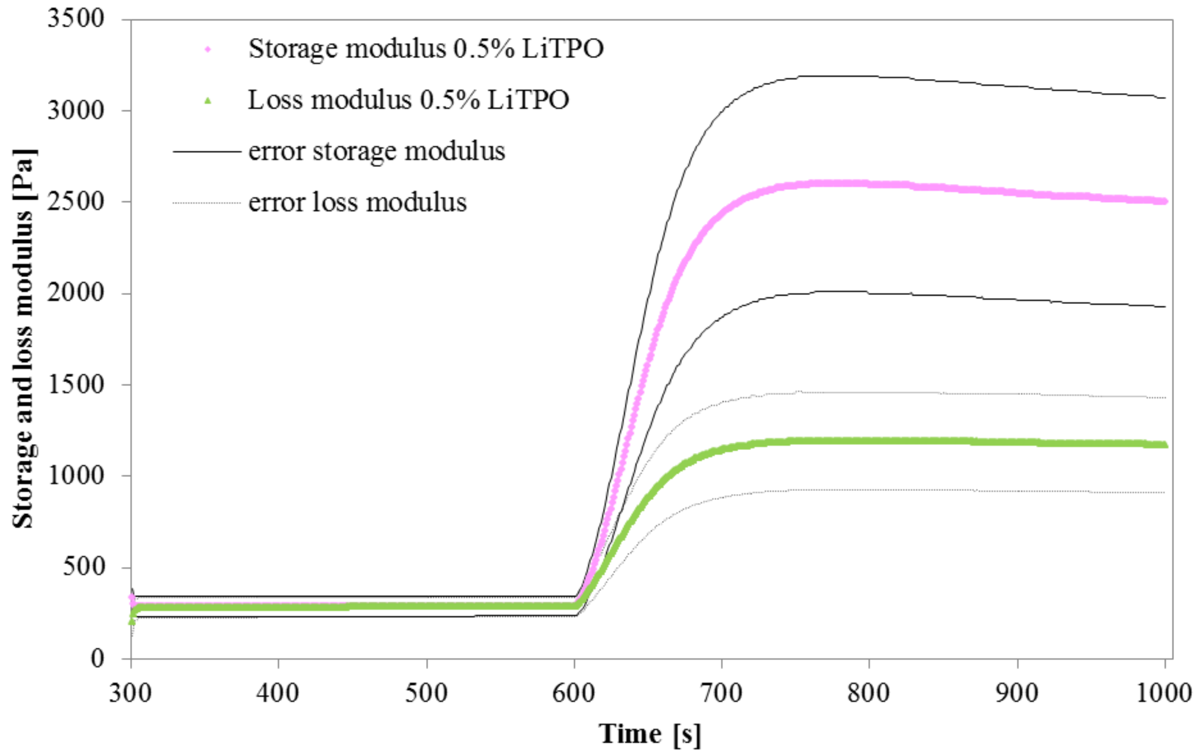

Figure 48: Photopolymerization of α,ω-itaconyl-PLGA–PEG–PLGA with crosslinker PEGDA.

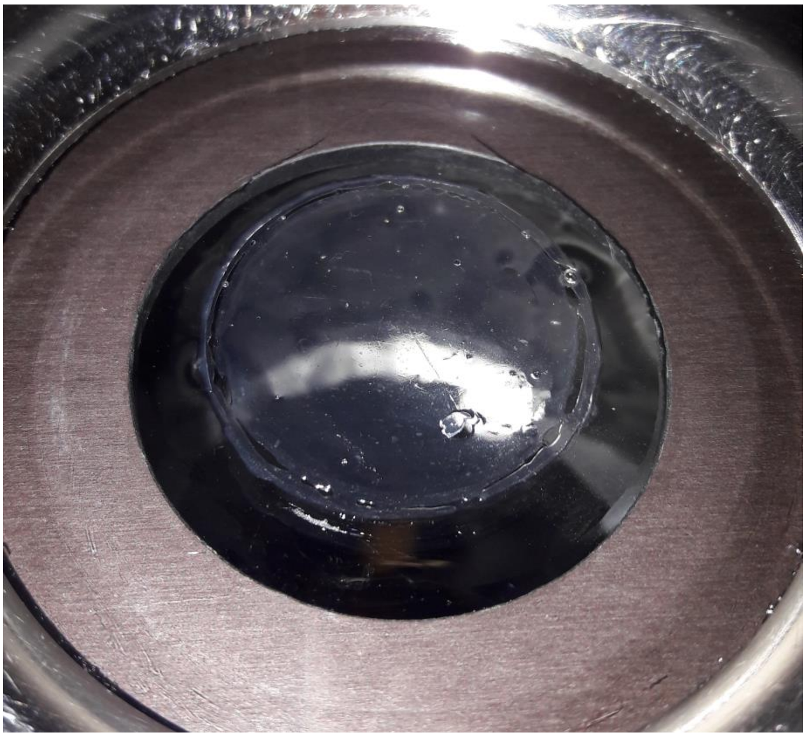

Figure 49: Gel created after the irradiation of 20 wt. % solution α,ω-itaconyl-PLGA–PEG–PLGA in the presence of crosslinker PEGDA and 0.5 wt. % of LiTPO.

5.4.6.2 Photocrosslinking at 37 °C

Part of our concept was, that hydrogels based on α,ω-itaconyl-PLGA–PEG–PLGA can be prepared *in situ* e.g. for the treatment of wounds. This requires performing of photocrosslinking at 37 °C.

Samples were applied on the glass plate at 25 °C. Afterwards steel stamp went to measuring position and linear temperature increase from 25 to 37 °C was done at rate 2 °C min^{-1}. Then next 20 min samples were let to rest at 37 °C. Then the oscillation started. All samples were already in a gel state, either samples, which did not create gel before the irradiation at 25 °C. G' was above G''. After 300 s the light was triggered on for different time, dependant on the length of modulus increase.

0.1 wt. % of PI in the case of 10 wt. % solution has not led to the increase of modulus (Figure 50). Immediately after the irradiation there was a small increase but subsequently modulus drop down. After the measurement was finished, there was not a gel but suspension created. Macromonomer precipitated. It is a bit strange because G' was still above G''. According the temperature sweeps, macromonomer should already precipitate at this temperature. However, macromonomers with concentrations of PI 0.5 wt. % and 1 wt. % did not. This is probably due to the fact, that PI influences the micelle structure as it was already mentioned. It was assumed that LiTPO moves the CGT and therefore also the curve shown in the Figure 7. The higher the concentration of PI, the higher was the CGT. 0.5 wt. % and 1 wt. % moved the zone of gel stability to higher temperatures while the addition of 0.1 wt. % was not sufficient to do so in such a manner.

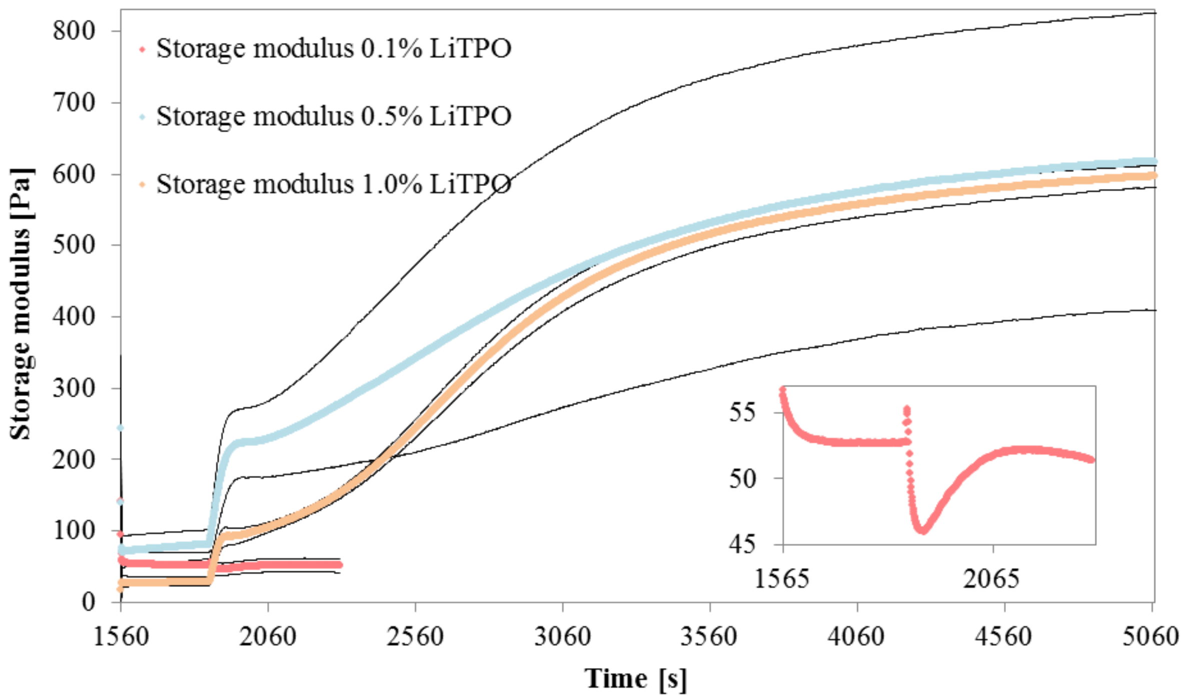

Figure 50: Average curves of the G′ modulus of the 10 wt. % hydrogel during the chemical crosslinking at 37 °C. Black lines show the error of measurements.

On the other hand in the case of 15 wt. % and 20 wt. % solutions, 0.1 wt. % of LiTPO was sufficient amount to move the zone of gel stability to 37 °C. It is because the higher is the content of macromonomer, the broader is the zone of modulus increase as it is shown in the Figure 26. The increase of modulus in the presence of 0.1 wt. % of LiTPO is much higher in the case of 20 wt. % solution (Figure 52) than for the 15 wt. % solution (Figure 51).

For all three concentrations the addition of 0.5 wt. % and 1 wt. % lead approximately to the same modulus after the irradiation when the error is included. The increase of the modulus took very long time for 0.5 wt. % and 1 wt. % of PI at 37 °C in comparison with 25 °C. It was assumed that at this temperature physical gel before the irradiation was stronger, micelles were more connected between each other and therefore the time till the LiTPO attacks some of DBs in the middle of micelles was longer. This long slight increase can also be caused by small drop of the modulus after initial increase. This is caused by delamination between created gel and plate. Delamination, which occurred for 0.5 wt. % and 1 wt. %, is very slight. However, in the case of 20 wt. % solution strong delamination occurred for 0.1 wt. % of LiTPO reproducibly (Figure 52). Delamination does not influence the quality of the gel but spoils the reproducibility. Delamination usually occurs when the amount of PI is exceeded. Therefore, photorheological measurement of 20 wt. % solution was performed with 0.05 wt. % of LiTPO. However, after the light was triggered on, modulus decreased. After the measurement was finished, it was found out that precipitation of macromonomer occurred. 0.05 wt. % did not move the zone of gel stability to 37 °C. Interestingly *G′* was still above *G′′*.

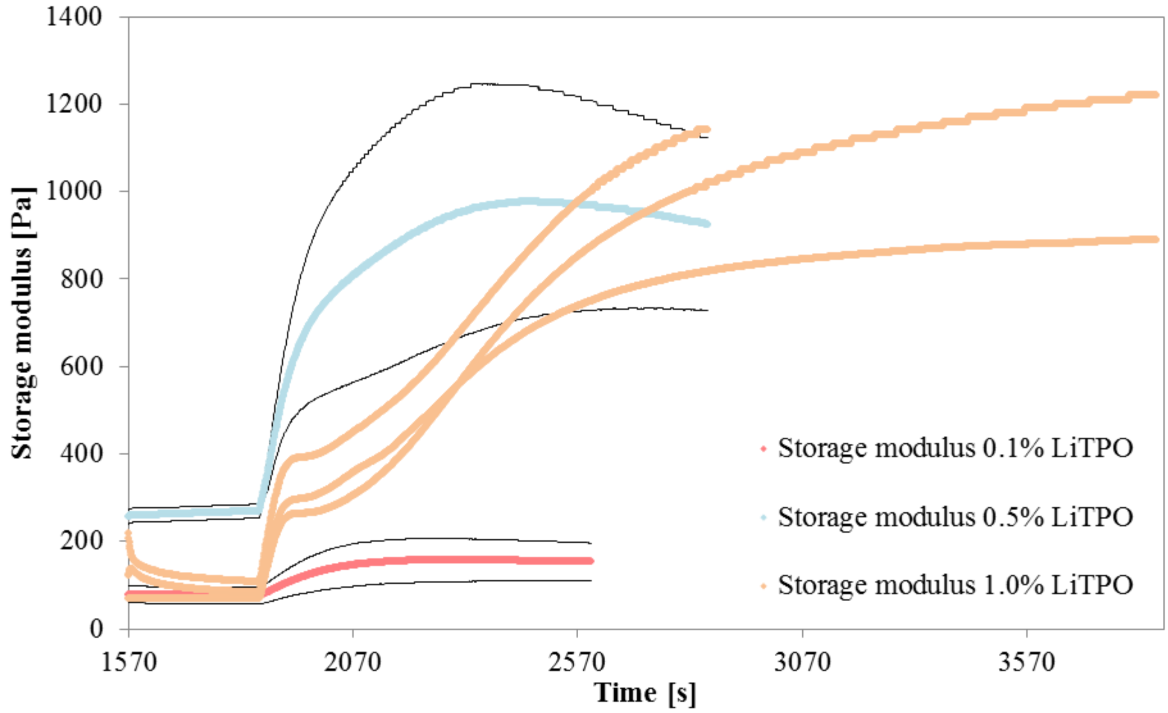

Figure 51: Curves showing the G′ modulus of the 15 wt. % hydrogel during the chemical crosslinking at 37 °C. Black lines show the error of measurements.

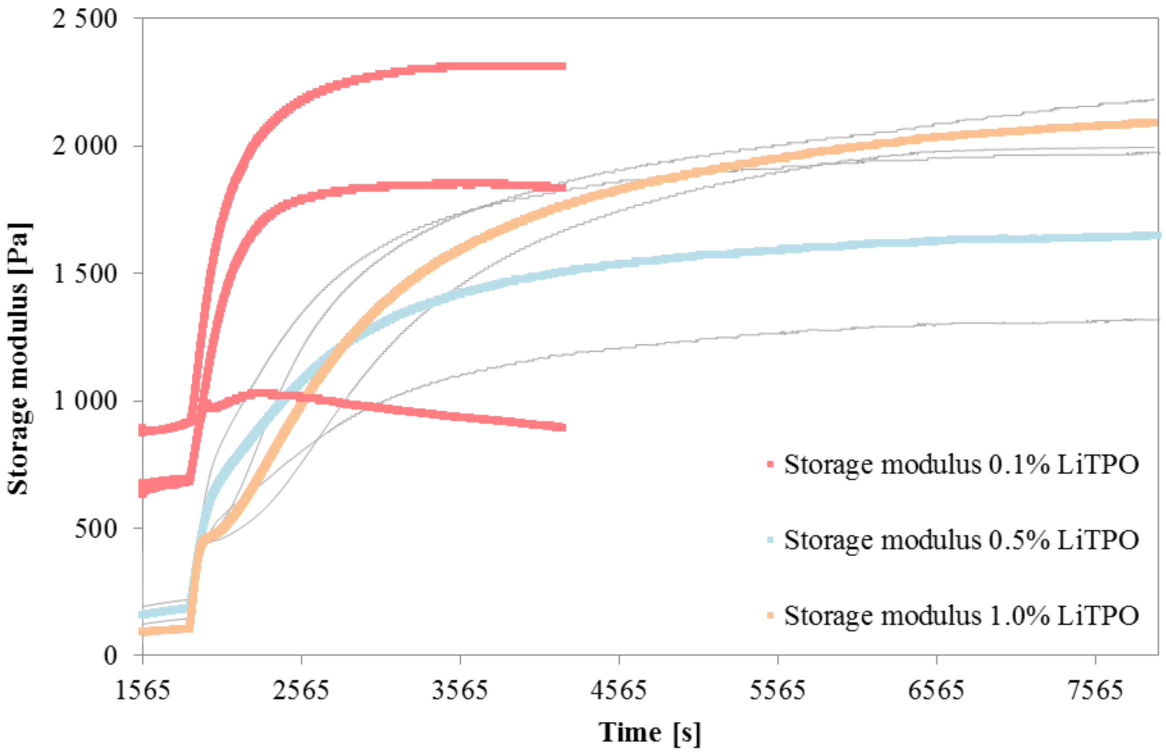

Figure 52: Curves showing the G′ modulus of the 20 wt. % hydrogel during the chemical crosslinking at 37 °C.

Highest modulus and best mechanical properties were achieved for 20 wt. % solutions photocrosslinked at 37 °C. The gel created from 20 wt. % solution with the content of PI

1 wt. % is shown in the Figure 53. Gel was submersed in UPW and even after 22 days it has not dissolved yet.

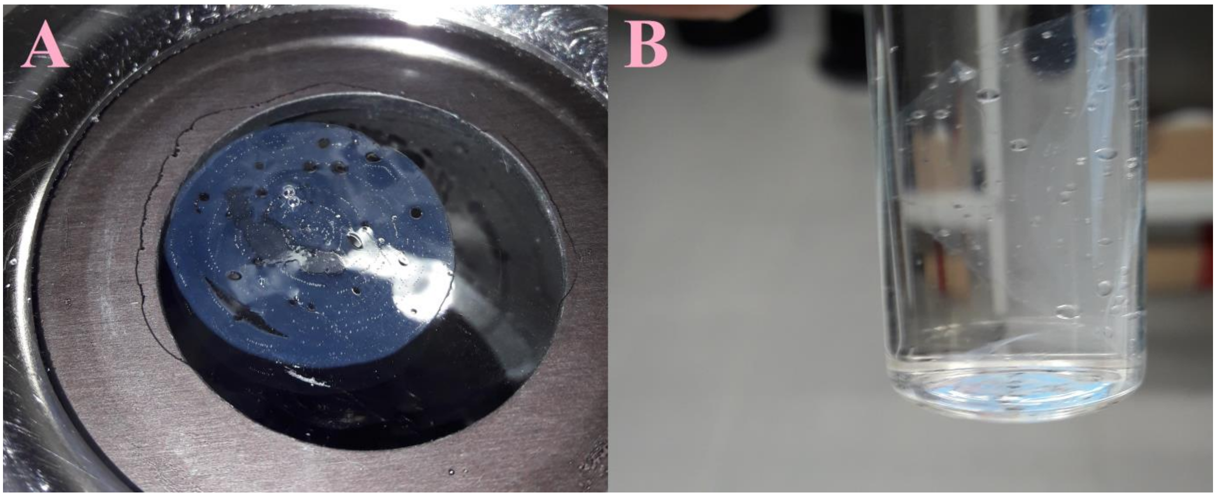

Figure 53: Gel from 20 wt. % solution with 1 wt. % of LiTPO photocrosslinked at 37 °C, B: stable in water, oil drops from the measurement.

In Figure 54 one can see the comparison of G'_{max} for all measurements at 37 °C. The higher the macromonomer content the higher was G'_{max}. G'_{max} for the 10 wt. % solution with 0.1 wt. % of LiTPO was excluded due to the precipitation. The amount of PI did not have a significant influence on G'_{max} except for the 15 wt. % solution with 0.1 wt. % of LiTPO, where the G'_{max} is considerably lower. Columns in Figure 54, which are bounded with dark line, are average only from 2 measurements. Therefore, error in those two cases represents two measured values of G'_{max}. In the case of 20 wt. % solution, it is due to the delamination in one measurement and in the case of 15 wt. % one, it is due to the fact, that one measurement is shorter than other two. It was not expected that modulus increase will take such a long time.

Hydrogels with better mechanical properties were obtained in general by photocrosslinking at 37 °C. Exceptions were only 10 wt. % and 15 wt. % solutions with 0.1 wt. % of LiTPO.

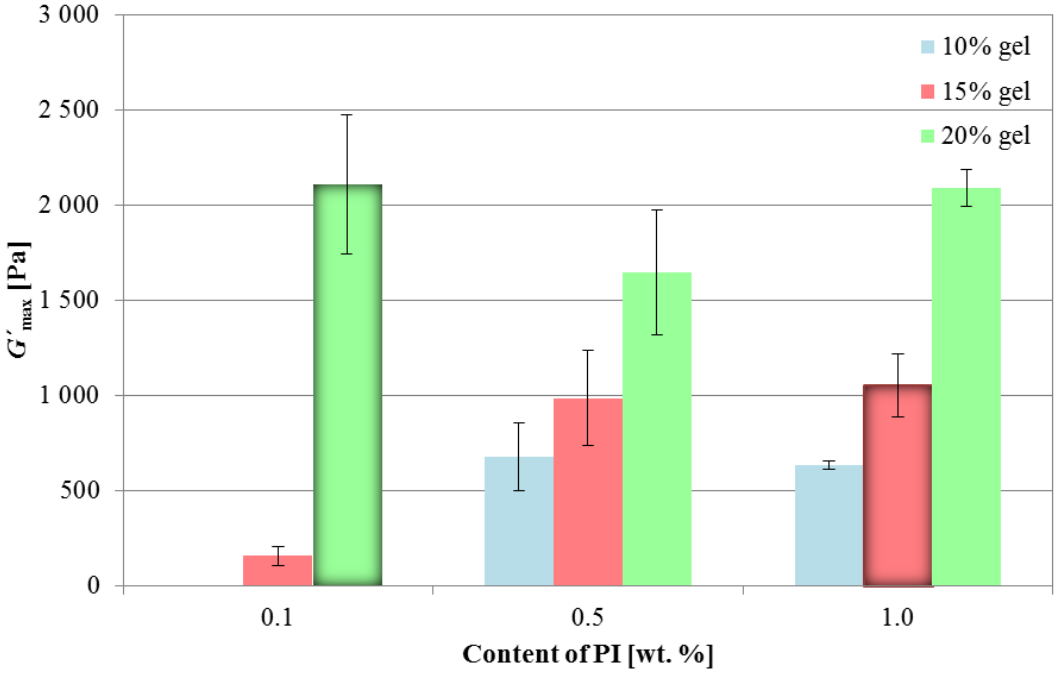

Figure 54: $G'_{\max}$ obtained from photorheological measurements at 37 °C.

The slope of the modulus increase (Figure 55) and τ_D (Figure 56) were determined. Nevertheless, errors among measurements are so high that it was difficult to characterise the relation between photoreactivity, content of macromonomer and content of PI. The lowest photoreactivity was found for 10 wt. % solution. When the error is included, there is no difference in τ_D among measurements.

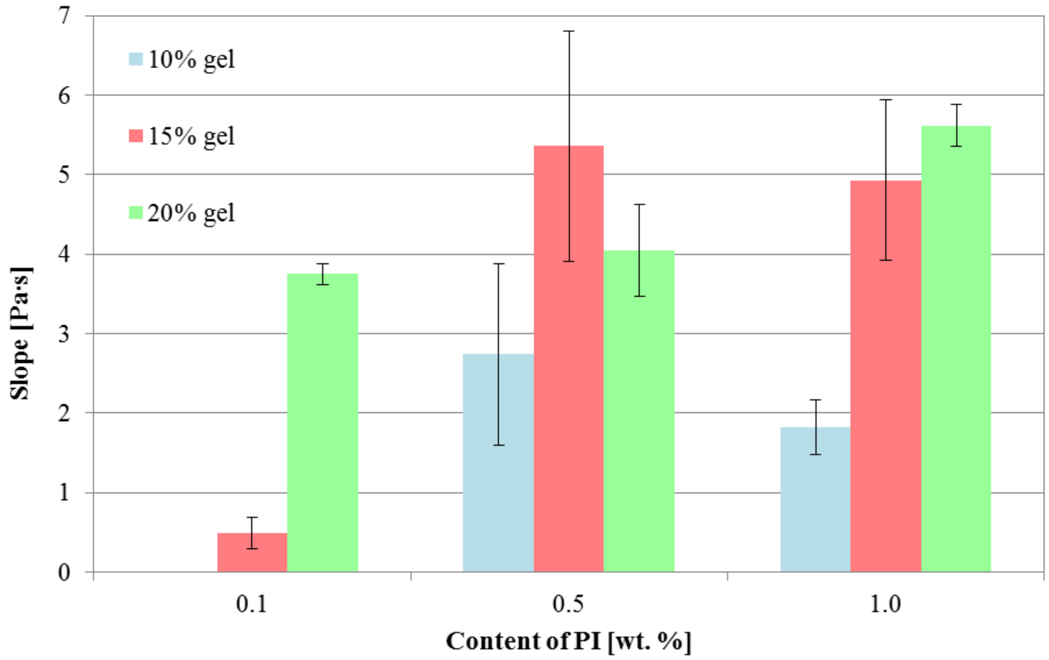

Figure 55: Slope obtained from photorheological measurements at 37 °C.

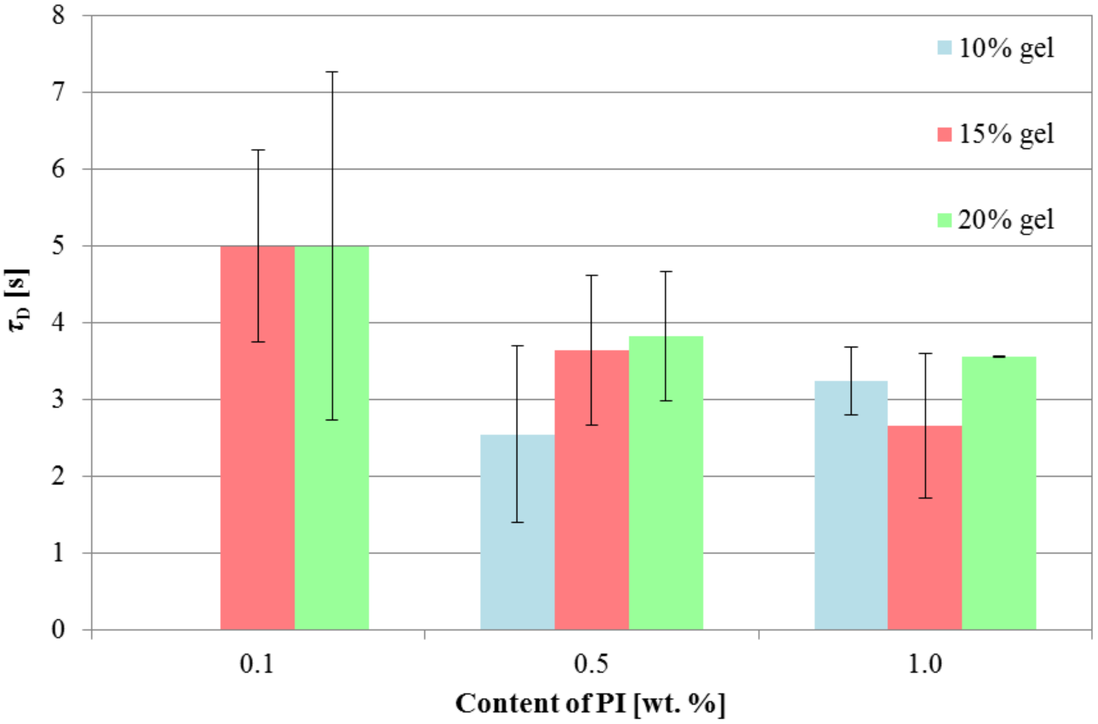

Figure 56: τ_D obtained from photorheological measurements at 37 °C.

5.4.6.3 Comparison of LiTPO and I2959

When it was found out that LiTPO influences the initial modulus and micelle structure, also the commercial I2959 was used for comparison. The concentration 0.5 wt. % was chosen to add in 20 wt. % solution due to a low solubility of I2959 in water. The light source with the filter 320–500 nm was used for this experiment. I2959 would not react in the range of VIS light. Measurements had four intervals. First 300 s of oscillation was performed at 25 °C. Then temperature increased from 25 °C to 37 °C at the rate 0.5 $°C \cdot min^{-1}$. Afterwards 30 min of oscillation was performed at 37 °C and then the irradiation started for 15 min.

I2959 increases the initial G´, because either it participates within hydrophobic interactions or just decreases the solubility of macromonomer. On the other hand LiTPO decreases initial *G´*. Nevertheless its high photoreactivity compensates lower initial *G´*. As it was mentioned in theory part, LiTPO has higher reactivity under UV light. This is the reason why the increase here is steeper and reaction is faster in comparison with measurements under VIS light. Slope of the modulus increase with LiTPO was 41 and 35 $Pa \cdot s^{-1}$. This is the clear evidence that photoreactivity of LiTPO increases under UV light. It could not have been determined for the third measurement due to the small drop after the irradiation started. For all other measurements at 37 °C the slope was less than 10 $Pa \cdot s^{-1}$.

In two from three measurements with I2959 delamination occurred even during the physical gelation. Maybe lower frequency of oscillation would help to avoid delamination. There is also another possibility to start the oscillation later already at 37 °C as it was done for other measurements at 37 °C. Exact values of τ_D, slope and G'_{max} are not determined in this case due to high error. Though it is obvious that G'_{max} results in higher values, when UV light source is used.

In spite of the fact that LiTPO decreases modulus and viscosity of solution, its use is in this case still more efficient than the use of commercial I2959.

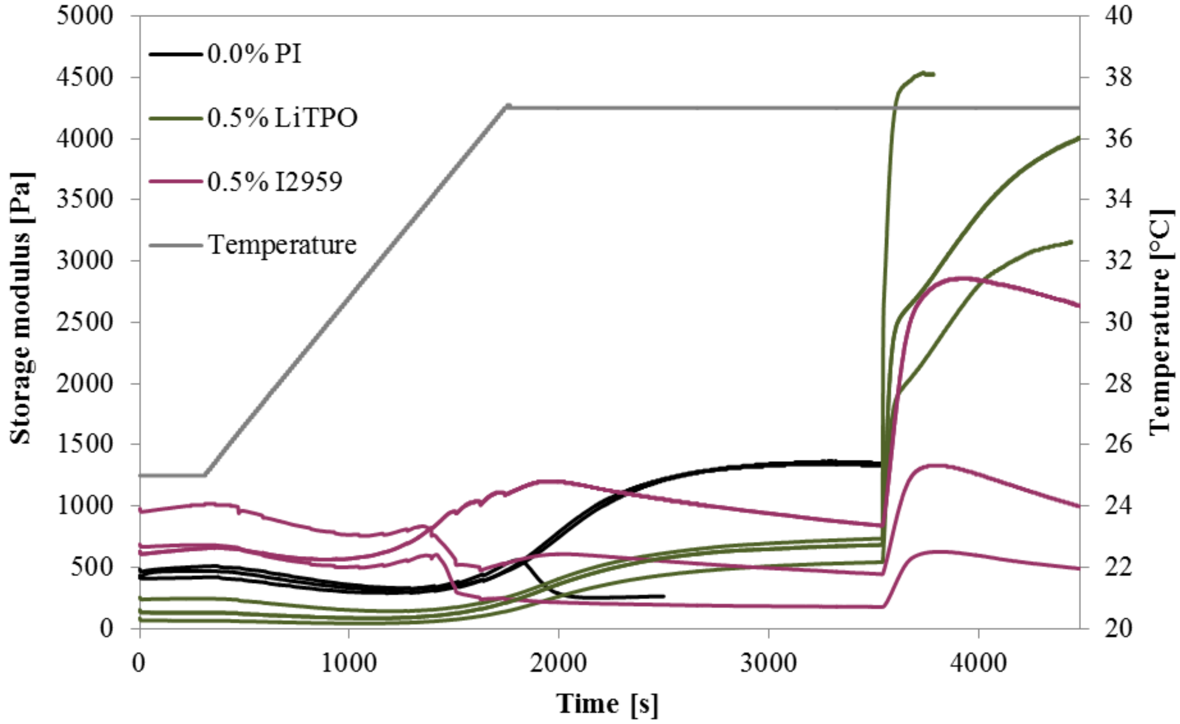

Figure 57: Comparison of LiTPO and I2959 influence on physical crosslinking and subsequent photoirradiation.

5.4.6.4 Photocrosslinking with 3 wt. % of LiTPO

As it was mentioned before, gel was not created at 25 °C with the content of LiTPO 3 wt. %. 10 wt. % solution with 3 wt. % of LiTPO also did not create physical gel at 37 °C, neither the chemical. Temperature sweep from 37 °C to 60 °C was performed to see if the physical gel will create at higher temperatures. At 46 °C sol-gel cross point occurred and at 59.2 °C there was gel-suspension cross point. This finding again confirms the theory that PI LiTPO moves CGT to higher temperatures. According previous experiments it is assumed that temperatures of transitions depend on previous temperature and time history. The temperature 52 °C was chosen to perform the photoirradiation of 10 wt. % solution with content of LiTPO 3 wt. %. This experiment was done at the beginning of practical work and therefore 10 wt. % solution was not measured on the third day from the time it was taken from magnetic stirrer, but the same day as it was taken out. The measurement was performed three times, however, one curve was considered as outlier and is not shown in the Figure 58.

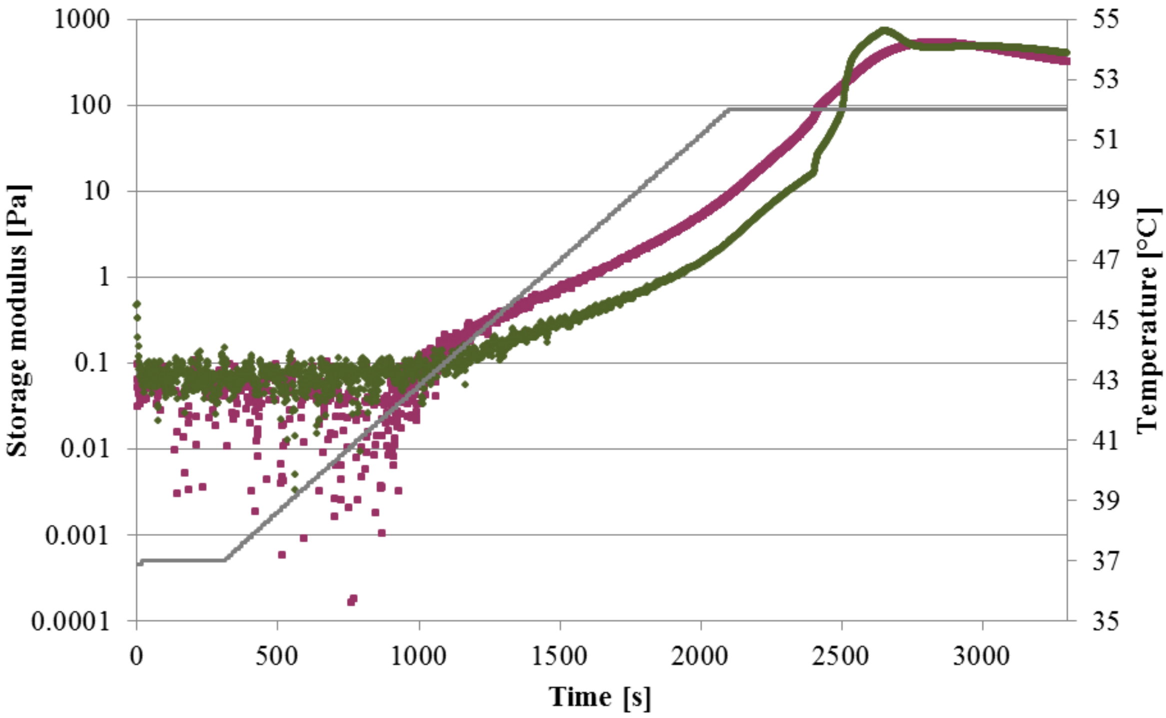

Figure 58: Physical and chemical crosslinking of 10 wt. % solution with 3 wt. % addition of PI.

At the time 2 400 s one can see steeper increase of storage modulus. This is the point, where the light was triggered on. One can see that modulus was still increasing even without the irradiation. It is assumed that even better final modulus would be achieved if the irradiation would start later, when the modulus increase from physical crosslinking would be stabilized. G'_{max} was determined to be 537 Pa and 722 Pa, respectively, which is quite high for such a low concentration of macromonomer and high temperature. After the hydrogel was taken out it had yellowish colour and did not transfer back to liquid state, remained solid. This confirms that chemical network stabilized the material.

6 CONCLUSION

Photocrosslinking of α,ω-itaconyl-PLGA–PEG–PLGA macromonomer was performed under the visible light in the range between 400 and 500 nm. Photorheology was used to examine mechanical properties of material during the photopolymerization. Firstly, photocrosslinking of bulk in the presence of organosoluble photoinitiator TPO-L was performed at 60 °C. It led to the increase of moduli and molecular weight, however, storage and loss moduli did not cross, and therefore the chemical network has not been formed. Consumption of double bonds from itaconic acid was proved by both RT-NIR and ATR-IR resulting only in prolonging the polymer chains without the hydrogel formation.

Aqueous solutions of α,ω-itaconyl-PLGA–PEG–PLGA are thermoresponsive. According to temperature sweeps sol-gel transition should occur at temperature higher than 29 °C for all three prepared concentrations (10 wt. %, 15 wt. %, 20 wt. %). However, it was found that after some time they gel either at ambient conditions. Immediate crosslinking at higher temperature is caused by faster diffusion and therefore, polymers can assembly in micelles without delay.

There was an issue to obtain reproducible photorheological curves due to the high thixotropy of the measured material. Thixotropy was proved by shear rate sweeps. Photopolymerization of aqueous solutions was performed in the presence of water soluble photoinitiator LiTPO. It was investigated, that micelles are essential for further chemical crosslinking, whereas photoinitiator LiTPO influences the micelle creation. While optimal concentration of LiTPO at 25 °C was very low (0.1 wt. %), at 37 °C the highest modulus exhibited 0.5 and 1 wt. % of LiTPO addition. However, when the addition of LiTPO was too high (3 wt. % at 25 °C), increased pH has led to higher deprotonation of carboxylic groups resulting in repulsive force and micelle destruction. This has caused decreasing the polymer solution viscosity with changing thixotropic behaviour to Newtonian ones. Therefore, the light irradiation has not increased moduli. Nevertheless, after the temperature has been increased to 60 °C the physical gel was recovered resulting in the conclusion that LiTPO moves the zone of gel stability to higher temperatures. This effect may be an advantage for injectable hydrogels. Critical gel temperature may be influenced not only by the ratios of PLGA/PEG and PLA/PGA during the synthesis but also by adding additional initiator, which later provides chemical crosslinking. Formation of chemical network was proved by submersion of photocrosslinked material in distilled acetone where the chemical network has not dissolved.

Photopolymerization of α,ω-itaconyl-PLGA–PEG–PLGA was also performed in the presence of 5 mol. % of PEGDA per double bonds of copolymer. It resulted in higher photoreactivity and storage modulus. However, double bonds from acrylates also brought fragility into the material.

As a conclusion, the ability to photocrosslink α,ω-itaconyl-PLGA–PEG–PLGA water solution has been proved in this thesis. Photopolymerization increased mechanical stability of material. If the later cytotoxicity tests are successful, proposed polymeric material could be applicable in biomedical applications such as tissue adhesive and drug delivery hydrogels.

7 REFERENCES

[1] RUEL-GARIÉPY, E. AND J.-C. LEROUX In situ-forming hydrogels—review of temperature-sensitive systems. European Journal of Pharmaceutics and Biopharmaceutics, 9// 2004, 58(2), 409-426.

[2] JEONG, B., Y. H. BAE, D. S. LEE AND S. W. KIM Biodegradable block copolymers as injectable drug-delivery systems. Nature, 08/28/print 1997, 388(6645), 860-862.

[3] ZENTNER, G. M., R. RATHI, C. SHIH, J. C. MCREA, et al. Biodegradable block copolymers for delivery of proteins and water-insoluble drugs. Journal of Controlled Release, 5/14/ 2001, 72(1–3), 203-215.

[4] KIM, Y. J., S. CHOI, J. J. KOH, M. LEE, et al. Controlled release of insulin from injectable biodegradable triblock copolymer. Pharm Res, Apr 2001, 18(4), 548-550.

[5] HILL-WEST, J. L., S. M. CHOWDHURY, A. S. SAWHNEY, C. P. PATHAK, et al. Prevention of postoperative adhesions in the rat by in situ photopolymerization of bioresorbable hydrogel barriers. Obstet Gynecol, Jan 1994, 83(1), 59-64.

[6] WEST, J. L. AND J. A. HUBBELL Photopolymerized hydrogel materials for drug delivery applications. Reactive Polymers, 1995/06/01 1995, 25(2), 139-147.

[7] CRUISE, G. M., O. D. HEGRE, F. V. LAMBERTI, S. R. HAGER, et al. In vitro and in vivo performance of porcine islets encapsulated in interfacially photopolymerized poly(ethylene glycol) diacrylate membranes. Cell Transplant, May-Jun 1999, 8(3), 293-306.

[8] SUN, G., X. ZHANG, Y. I. SHEN, R. SEBASTIAN, et al. Dextran hydrogel scaffolds enhance angiogenic responses and promote complete skin regeneration during burn wound healing. Proc Natl Acad Sci USA, 2011, 108.

[9] OUYANG, L., C. B. HIGHLEY, C. B. RODELL, W. SUN, et al. 3D Printing of Shear-Thinning Hyaluronic Acid Hydrogels with Secondary Cross-Linking. ACS Biomaterials Science & Engineering, 2016/10/10 2016, 2(10), 1743-1751.

[10] GORSCHE, C., R. HARIKRISHNA, S. BAUDIS, P. KNAACK, et al. Real Time-NIR/MIR-Photorheology: A Versatile Tool for the in Situ Characterization of Photopolymerization Reactions. Anal Chem, Apr 19 2017.

[11] MICHLOVSKÁ, L., L. VOJTOVÁ, L. MRAVCOVÁ, S. HERMANOVÁ, et al. Functionalization Conditions of PLGA-PEG-PLGA Copolymer with Itaconic Anhydride. Macromolecular Symposia, 2010, 295(1), 119-124.

[12] MICHLOVSKA, L., L. VOJTOVA, O. HUMPA, J. KUCERIK, et al. Hydrolytic stability of end-linked hydrogels from PLGA-PEG-PLGA macromonomers terminated by [small alpha],[small omega]-itaconyl groups. RSC Advances, 2016, 6(20), 16808-16816.

[13] HENNINK, W. E. AND C. F. VAN NOSTRUM Novel crosslinking methods to design hydrogels. Advanced Drug Delivery Reviews, 1/17/ 2002, 54(1), 13-36.

[14] PAL, K., A. K. BANTHIA AND D. K. MAJUMDAR Polymeric Hydrogels: Characterization and Biomedical Applications. Designed Monomers and Polymers, 2009/01/01 2009, 12(3), 197-220.

[15] AHMED, E. M. Hydrogel: Preparation, characterization, and applications: A review. Journal of Advanced Research, 3// 2015, 6(2), 105-121.

[16] SHIGA, T. Deformation and Viscoelastic Behavior of Polymer Gels in Electric Fields. In *Neutron Spin Echo Spectroscopy Viscoelasticity Rheology*. Berlin, Heidelberg: Springer Berlin Heidelberg, 1997, p. 131-163.

[17] MADAGHIELE, M., C. DEMITRI, A. SANNINO AND L. AMBROSIO Polymeric hydrogels for burn wound care: Advanced skin wound dressings and regenerative templates. Burns & Trauma, 2014, 2(4), 153-161.

[18] FINOSH, G. T. AND M. JAYABALAN Reactive oxygen species¡ªControl and management using amphiphilic biosynthetic hydrogels for cardiac applications. Advances in Bioscience and Biotechnology, 2013, Vol.04No.12, 13.

[19] VERMONDEN, T., N. E. FEDOROVICH, D. VAN GEEMEN, J. ALBLAS, et al. Photopolymerized thermosensitive hydrogels: synthesis, degradation, and cytocompatibility. Biomacromolecules, Mar 2008, 9(3), 919-926.

[20] PARK, H., K. PARK AND W. S. W. SHALABY *Biodegradable Hydrogels for Drug Delivery*. Edtion ed.: Taylor & Francis, 1993. ISBN 9781566760041.

[21] ELISSEEFF, J., K. ANSETH, R. LANGER AND J. S. HRKACH Synthesis and Characterization of Photo-Cross-Linked Polymers Based on Poly(l-lactic acid-co-l-aspartic acid). Macromolecules, 1997/04/01 1997, 30(7), 2182-2184.

[22] SCHMEDLEN, R. H., K. S. MASTERS AND J. L. WEST Photocrosslinkable polyvinyl alcohol hydrogels that can be modified with cell adhesion peptides for use in tissue engineering. Biomaterials, 11// 2002, 23(22), 4325-4332.

[23] NGUYEN, K. T. AND J. L. WEST Photopolymerizable hydrogels for tissue engineering applications. Biomaterials, 2002, 23.

[24] WINTER, H. H. AND M. MOURS. Rheology of Polymers Near Liquid-Solid Transitions. In *Neutron Spin Echo Spectroscopy Viscoelasticity Rheology*. Berlin, Heidelberg: Springer Berlin Heidelberg, 1997, p. 165-234.

[25] GHOBRIL, C. AND M. W. GRINSTAFF The chemistry and engineering of polymeric hydrogel adhesives for wound closure: a tutorial. Chemical Society Reviews, 2015, 44(7), 1820-1835.

[26] MICHLOVSKA, L. SYNTHESIS AND CHARACTERIZATION OF MULTIFUNCTIONALIZED BIODEGRADABLE COPOLYMERS. Brno University of Technology, 2014.

[27] DUMITRIU, S. *Polysaccharides: Structural Diversity and Functional Versatility, Second Edition*. Edtion ed.: CRC Press, 2004. ISBN 9781420030822.

[28] PRADAS, M. M. AND M. J. VICENT *Polymers in Regenerative Medicine: Biomedical Applications from Nano- to Macro-Structures*. Edtion ed.: Wiley, 2015. ISBN 9781118356685.

[29] WEST, J. L. AND J. A. HUBBELL Separation of the arterial wall from blood contact using hydrogel barriers reduces intimal thickening after balloon injury in the rat: The roles of medial and luminal factors in arterial healing. Proceedings of the National Academy of Sciences, November 12, 1996 1996, 93(23), 13188-13193.

[30] HILL-WEST, J. L., S. M. CHOWDHURY, M. J. SLEPIAN AND J. A. HUBBELL Inhibition of thrombosis and intimal thickening by in situ photopolymerization of thin hydrogel barriers. Proceedings of the National Academy of Sciences of the United States of America, 1994, 91(13), 5967-5971.

[31] ELISSEEFF, J., K. ANSETH, D. SIMS, W. MCINTOSH, et al. Transdermal photopolymerization for minimally invasive implantation. Proceedings of the National Academy of Sciences, March 16, 1999 1999, 96(6), 3104-3107.

[32] ELISSEEFF, J., K. ANSETH, D. SIMS, W. MCINTOSH, et al. Transdermal Photopolymerization of Poly (Ethylene Oxide)-Based Injectable Hydrogels for Tissue-Engineered Cartilage. Plastic and Reconstructive Surgery, 1999, 104(4), 1014-1022.

[33] PUBLISHING, P. S. *Handbook of Intelligent Scaffold for Tissue Engineering and Regenerative Medicine*. Edtion ed.: Pan Stanford Publishing, 2012. ISBN 9789814267861.

[34] QUINN, C. P., C. P. PATHAK, A. HELLER AND J. A. HUBBELL Photo-crosslinked copolymers of 2-hydroxyethyl methacrylate, poly(ethylene glycol) tetra-acrylate and ethylene dimethacrylate for improving biocompatibility of biosensors. Biomaterials, 1995/01/01 1995, 16(5), 389-396.

[35] KIM, B. S., J. S. HRKACH AND R. LANGER Biodegradable photo-crosslinked poly(ether-ester) networks for lubricious coatings. Biomaterials, 2// 2000, 21(3), 259-265.

[36] BRYANT, S. AND K. ANSETH. Photopolymerization of Hydrogel Scaffolds. In *Scaffolding In Tissue Engineering.* CRC Press, 2005, p. 71-90.

[37] KÜHTREIBER, W. M., R. P. LANZA AND W. L. CHICK *Cell Encapsulation Technology and Therapeutics*. Edtion ed.: Birkhauser, 1999. ISBN 9780817640101.

[38] KIM, S.-H., C.-Y. WON AND C.-C. CHU Synthesis and characterization of dextran-maleic acid based hydrogel. Journal of Biomedical Materials Research, 1999, 46(2), 160-170.

[39] BABO, P. S., R. L. PIRES, L. SANTOS, A. FRANCO, et al. Platelet Lysate-Loaded Photocrosslinkable Hyaluronic Acid Hydrogels for Periodontal Endogenous Regenerative Technology. ACS Biomaterials Science & Engineering, 2016/12/20 2016.

[40] GIANNUZZO, M., F. CORRENTE, M. FEENEY, L. PAOLETTI, et al. pH-Sensitive hydrogels of dextran: Synthesis, characterization and in vivo studies. Journal of Drug Targeting, 2008, 16(9), 649-659.

[41] KIM, S.-H. AND C.-C. CHU In Vitro Release Behavior of Dextran-Methacrylate Hydrogels Using Doxorubicin and other Model Compounds. Journal of Biomaterials Applications, 2000, 15(1), 23-46.

[42] SUN, G., Y.-I. SHEN, C. C. HO, S. KUSUMA, et al. Functional groups affect physical and biological properties of dextran-based hydrogels. Journal of Biomedical Materials Research Part A, 2010, 93A(3), 1080-1090.

[43] ZHANG, J.-Z., C.-S. XIAO, J.-C. WANG, X.-L. ZHUANG, et al. Photo cross-linked biodegradable hydrogels for enhanced vancomycin loading and sustained release. Chinese Journal of Polymer Science, 2013, 31(12), 1697-1705.

[44] BAUDIS, S., D. BOMZE, M. MARKOVIC, P. GRUBER, et al. Modular material system for the microfabrication of biocompatible hydrogels based on thiol–ene-modified poly(vinyl alcohol). Journal of Polymer Science Part A: Polymer Chemistry, 2016, 54(13), 2060-2070.

[45] MARTENS, P. AND K. S. ANSETH Characterization of hydrogels formed from acrylate modified poly(vinyl alcohol) macromers. Polymer, 10// 2000, 41(21), 7715-7722.

[46] MARTENS, P., T. HOLLAND AND K. S. ANSETH Synthesis and characterization of degradable hydrogels formed from acrylate modified poly(vinyl alcohol) macromers. Polymer, // 2002, 43(23), 6093-6100.

[47] MARTENS, P. J., C. N. BOWMAN AND K. S. ANSETH Degradable networks formed from multi-functional poly(vinyl alcohol) macromers: comparison of results from a generalized bulk-degradation model for polymer networks and experimental data. Polymer, 5// 2004, 45(10), 3377-3387.

[48] MÜHLEBACH, A., B. MÜLLER, C. PHARISA, M. HOFMANN, et al. New water-soluble photo crosslinkable polymers based on modified poly(vinyl alcohol). Journal of Polymer Science Part A: Polymer Chemistry, 1997, 35(16), 3603-3611.

[49] NUTTELMAN, C. R., S. M. HENRY AND K. S. ANSETH Synthesis and characterization of photocrosslinkable, degradable poly(vinyl alcohol)-based tissue engineering scaffolds. Biomaterials, 9// 2002, 23(17), 3617-3626.

[50] DUMITRIU, S. AND V. POPA *Polymeric Biomaterials: Structure and Function*. Edtion ed.: CRC Press, 2013. ISBN 9781420094718.

[51] MING KUO, S., S. JEN CHANG AND Y. JIIN WANG Properties of PVA-AA cross-linked HEMA-based hydrogels. Journal of Polymer Research, 1999, 6(3), 191-196.

[52] MARKUS, F., F. DREHER, S. LASCHAT, S. BAUDIS, et al. Physically and chemically gelling hydrogel formulations based on poly(ethylene glycol) diacrylate and Poloxamer 407. Polymer, 1/13/ 2017, 108, 21-28.

[53] NALAMPANG, K., R. PANJAKHA, R. MOLLOY AND B. J. TIGHE Structural effects in photopolymerized sodium AMPS hydrogels cross-linked with poly(ethylene glycol) diacrylate for use as burn dressings. J Biomater Sci Polym Ed, 2013, 24.

[54] NGUYEN, Q. T., Y. HWANG, A. C. CHEN, S. VARGHESE, et al. Cartilage-like mechanical properties of poly (ethylene glycol)-diacrylate hydrogels. Biomaterials, 2012, 33.

[55] SAWHNEY, A. S., C. P. PATHAK AND J. A. HUBBELL Bioerodible hydrogels based on photopolymerized poly(ethylene glycol)-co-poly(.alpha.-hydroxy acid) diacrylate macromers. Macromolecules, 1993/02/01 1993, 26(4), 581-587.

[56] SCOTT, R. A. AND N. A. PEPPAS Highly crosslinked, PEG-containing copolymers for sustained solute delivery. Biomaterials, Aug 1999, 20(15), 1371-1380.

[57] CRUISE, G. M., D. S. SCHARP AND J. A. HUBBELL Characterization of permeability and network structure of interfacially photopolymerized poly(ethylene glycol) diacrylate hydrogels. Biomaterials, 1998/07/01 1998, 19(14), 1287-1294.

[58] FAIRBANKS, B. D., M. P. SCHWARTZ, C. N. BOWMAN AND K. S. ANSETH Photoinitiated polymerization of PEG-diacrylate with lithium phenyl-2,4,6-trimethylbenzoylphosphinate: polymerization rate and cytocompatibility. Biomaterials, 12// 2009, 30(35), 6702-6707.

[59] BEAMISH, J. A., J. ZHU, K. KOTTKE-MARCHANT AND R. E. MARCHANT The Effects of Monoacrylated Poly(Ethylene Glycol) on the Properties of Poly(Ethylene Glycol) Diacrylate Hydrogels Used for Tissue Engineering. Journal of biomedical materials research. Part A, 2010, 92(2), 441-450.

[60] TAN, G., Y. WANG, J. LI AND S. ZHANG Synthesis and Characterization of Injectable Photocrosslinking Poly (ethylene glycol) Diacrylate based Hydrogels. Polymer Bulletin, 2008, 61(1), 91-98.

[61] HERN, D. L. AND J. A. HUBBELL Incorporation of adhesion peptides into nonadhesive hydrogels useful for tissue resurfacing. J Biomed Mater Res, Feb 1998, 39(2), 266-276.

[62] RAMAN, R., N. E. CLAY, S. SEN, M. MELHEM, et al. 3D printing enables separation of orthogonal functions within a hydrogel particle. Biomedical Microdevices, 2016, 18(3), 49.

[63] SUN, G. AND C.-C. CHU Synthesis, characterization of biodegradable dextran–allyl isocyanate–ethylamine/polyethylene glycol–diacrylate hydrogels and their in vitro release of albumin. Carbohydrate Polymers, 8/15/ 2006, 65(3), 273-287.

[64] CENSI, R., T. VERMONDEN, M. J. VAN STEENBERGEN, H. DESCHOUT, et al. Photopolymerized thermosensitive hydrogels for tailorable diffusion-controlled protein delivery. Journal of Controlled Release, 12/16/ 2009, 140(3), 230-236.

[65] CENSI, R., T. VERMONDEN, H. DESCHOUT, K. BRAECKMANS, et al. Photopolymerized thermosensitive poly(HPMAlactate)-PEG-based hydrogels: effect of network design on mechanical properties, degradation, and release behavior. Biomacromolecules, Aug 09 2010, 11(8), 2143-2151.

[66] CENSI, R., S. VAN PUTTEN, T. VERMONDEN, P. DI MARTINO, et al. The tissue response to photopolymerized PEG-p(HPMAm-lactate)-based hydrogels. J Biomed Mater Res A, Jun 01 2011, 97(3), 219-229.

[67] CENSI, R., W. SCHUURMAN, J. MALDA, G. DI DATO, et al. A Printable Photopolymerizable Thermosensitive p(HPMAm-lactate)-PEG Hydrogel for Tissue Engineering. Advanced Functional Materials, 2011, 21(10), 1833-1842.

[68] ZENTNER, G. M., R. RATHI, C. SHIH, J. C. MCREA, et al. Biodegradable block copolymers for delivery of proteins and water-insoluble drugs. J Control Release, May 14 2001, 72(1-3), 203-215.

[69] GAO, Y., Y. SUN, F. REN AND S. GAO PLGA–PEG–PLGA hydrogel for ocular drug delivery of dexamethasone acetate. Drug development and industrial pharmacy, 2010, 36(10), 1131-1138.

[70] MAKADIA, H. K. AND S. J. SIEGEL Poly lactic-co-glycolic acid (PLGA) as biodegradable controlled drug delivery carrier. Polymers, 2011, 3(3), 1377-1397.

[71] MICHLOVSKÁ, L., L. VOJTOVÁ, L. MRAVCOVÁ AND J. JANČÁR Thermogelling water solutions of multifunctional macromonomers based on PLGA-PEG-PLGA triblock copolymers. Challenges of Modern Technology, 2011, Vol. 2, no. 1, 12-15.

[72] SIGMA-ALDRICH. Photoinitiators: Classification. 2016.

[73] HAGEMAN, H. J. Photoinitiators and Photoinitiation Mechanisms of Free-Radical Polymerisation Processes. In N.S. ALLEN ed. *Photopolymerisation and Photoimaging Science and Technology.* Springer Netherlands, p. pp 1-53.

[74] SANTINI, A., I. T. GALLEGOS AND C. M. FELIX Photoinitiators in dentistry: a review. Prim Dent J, Oct 2013, 2(4), 30-33.

[75] KAMOUN, E. A., A. WINKEL, M. EISENBURGER AND H. MENZEL Carboxylated camphorquinone as visible-light photoinitiator for biomedical application: Synthesis, characterization, and application. Arabian Journal of Chemistry, 9// 2016, 9(5), 745-754.

[76] BENEDIKT, S., J. WANG, M. MARKOVIC, N. MOSZNER, et al. Highly efficient water-soluble visible light photoinitiators. Journal of Polymer Science Part A: Polymer Chemistry, 2016, 54(4), 473-479.

[77] LI, Z., J. TORGERSEN, A. AJAMI, S. MUHLEDER, et al. Initiation efficiency and cytotoxicity of novel water-soluble two-photon photoinitiators for direct 3D microfabrication of hydrogels. RSC Advances, 2013, 3(36), 15939-15946.

[78] Ciba®IRGACURE® 2959. In.: Ciba Specialty Chemicals, 2002.

[79] About The Society of Rheology. In.

[80] MALKIN, A. Y. AND A. I. ISAYEV *Rheology: Concepts, Methods, and Applications*. Edtion ed.: Elsevier Science, 2017. ISBN 9781927885222.

[81] ZUIDEMA, J. M., C. J. RIVET, R. J. GILBERT AND F. A. MORRISON A protocol for rheological characterization of hydrogels for tissue engineering strategies. Journal of Biomedical Materials Research Part B: Applied Biomaterials, 2014, 102(5), 1063-1073.

[82] PEKAŘ, M., KLUČÁKOVÁ, M., VESELÝ M. , ČEPPAN M. *Fyzikální chemie a fotochemie I: praktikum*. Edtion ed. Brno: Vysoké učení technické v Brně, Fakulta chemická, 2003. ISBN 80-214-2470-2.

[83] MALKIN, A. I. A. *Rheology Fundamentals*. Edtion ed.: Elsevier Science Limited, 1994. ISBN 9781895198096.

[84] MEWIS, J. AND N. J. WAGNER Thixotropy. Advances in Colloid and Interface Science, 3// 2009, 147–148, 214-227.

[85] MEZGER, T. G. *The Rheology Handbook: For Users of Rotational and Oscillatory Rheometers*. Edtion ed.: Vincentz Network, 2006. ISBN 9783878701743.

[86] WYSS, H. M., R. J. LARSEN AND D. A. WEITZ Oscillatory rheology. G.I.T. Laboratory Journal, 2007, 3-4, 68-70.

[87] MACOSKO, C. W. *Rheology: Principles, Measurements, and Applications*. Edtion ed.: Wiley, 1994. ISBN 9780471185758.

[88] KHAN, S. A., I. M. PLITZ AND R. A. FRANTZ In situ technique for monitoring the gelation of UV curable polymers. Rheologica Acta, 1992, 31(2), 151-160.

[89] SCHMIDT, C. AND T. SCHERZER Monitoring of the shrinkage during the photopolymerization of acrylates using hyphenated photorheometry/near-infrared spectroscopy. Journal of Polymer Science Part B: Polymer Physics, 2015, 53(10), 729-739.

[90] ORMAN, S. Biocompatible Composite Photopolymers for 3D Printing. Vienna University of Technology, 2015.

[91] MONTEIRO, G. Q. D. M. AND M. A. J. R. MONTES Evaluation of linear polymerization shrinkage, flexural strength and modulus of elasticity of dental composites. Materials Research, 2010, 13, 51-55.

[92] ATAI, M. AND D. C. WATTS A new kinetic model for the photopolymerization shrinkage-strain of dental composites and resin-monomers. Dental Materials, 8// 2006, 22(8), 785-791.

[93] BOTELLA, A., J. DUPUY, A.-A. ROCHE, H. SAUTEREAU, et al. Photo-Rheometry/NIR Spectrometry: An in situ Technique for Monitoring Conversion and Viscoelastic Properties during Photopolymerization. Macromolecular Rapid Communications, 2004, 25(12), 1155-1158.

[94] JUGGERNAUTH, K. A., A. E. GROS, N. A. K. MEZNARICH AND B. J. LOVE In situ photogelation kinetics of Laponite nanoparticle-based photorheological dispersions. Soft Matter, 2011, 7(21), 10108-10115.

[95] BORGES DE COURAÇA, A. Composite Hydrogels for the Replacement of the Nucleus Pulposus. EPFL, 2010.

[96] ACOSTA-VÉLEZ, G., C. LINSLEY, M. CRAIG AND B. WU Photocurable Bioink for the Inkjet 3D Pharming of Hydrophilic Drugs. Bioengineering, 2017, 4(1), 11.

[97] FU, A., K. GWON, M. KIM, G. TAE, et al. Visible-Light-Initiated Thiol–Acrylate Photopolymerization of Heparin-Based Hydrogels. Biomacromolecules, 2015/02/09 2015, 16(2), 497-506.

[98] AIMETTI, A. A., A. J. MACHEN AND K. S. ANSETH Poly(ethylene glycol) hydrogels formed by thiol-ene photopolymerization for enzyme-responsive protein delivery. Biomaterials, 10// 2009, 30(30), 6048-6054.

[99] QIN, X.-H., J. TORGERSEN, R. SAF, S. MÜHLEDER, et al. Three-dimensional microfabrication of protein hydrogels via two-photon-excited thiol-vinyl ester photopolymerization. Journal of Polymer Science Part A: Polymer Chemistry, 2013, 51(22), 4799-4810.

[100] STEEMAN, P. A. M., A. A. DIAS, D. WIENKE AND T. ZWARTKRUIS Polymerization and Network Formation of UV-Curable Systems Monitored by Hyphenated Real-Time Dynamic Mechanical Analysis and Near-Infrared Spectroscopy. Macromolecules, 2004/09/01 2004, 37(18), 7001-7007.

[101] GRIFFIN, D. R. AND A. M. KASKO Photodegradable macromers and hydrogels for live cell encapsulation and release. J Am Chem Soc, Aug 08 2012, 134(31), 13103-13107.

[102] CHAMRADOVÁ, I. Polymeric materials for controlled drug delivery and controlled release of active substances. Brno University of Technology, 2015.

[103] WORKMAN, J. AND L. WEYER *Practical Guide and Spectral Atlas for Interpretive Near-Infrared Spectroscopy, Second Edition*. Edtion ed.: CRC Press, 2012. ISBN 9781439875261.

[104] CHAMRADOVÁ, I., L. VOJTOVÁ, L. MICHLOVSKÁ, P. POLÁČEK, et al. Rheological properties of functionalised thermosensitive copolymers for injectable applications in medicine. Chemical Papers, 2012, 66(10), 977-980.

[105] CHAMRADOVÁ, I. Rheological properties of biodegradable thermosensitive copolymers. Diploma thesis Brno University of Technology, 2012.

[106] Aggregate Particles in Aqueous Solution. In. US.

8 LIST OF ABBREVIATIONS AND SYMBOLS

ATR-IR	attenuated total reflectance–infrared spectroscopy
$CDCl_3$	deuterated chloroform
CGC	critical gel temperature
CGT	critical gel concentration
CQ	camphorquinone
DBC	double bond conversion
DBs	double bonds
DS	degree of substitution
FTIR	Fourier transform infrared spectroscopy
G'	storage modulus
G''	loss modulus
GA	glycolide
G'_{max}	maximal storage modulus
GPC	gel permeatic chromatography
$\dot{\gamma}$	shear rate
^{1}H NMR	proton nuclear magnetic resonance
η	dynamic viscosity
I2959	2-hydroxy-4′-(2-hydroxyethoxy)-2-methyl-propiophenone
ITA	itaconic acid
LA	lactide
LiTPO	lithium phenyl-2,4,6-trimethylbenzoylphosphinate
MALS	multi-angle light scattering method
MAPO	monoacylphosphineoxide

M_n	number average molecular weight
M_w	weight average molecular weight
M_w/M_n	polydispersity index
NIR	near infrared spectroscopy
PDI	polydispersity index
PEG	poly(ethylene glycol)
PEGDA	poly(ethylene glycol) diacrylate
PI	photoinitiator
PLGA	poly(d,l-lactic acid-co-glycolic acid)
PLGA-PEG-PLGA	poly(d,l-lactic acid-co-glycolic acid)-b-poly(ethylene glycol)-bpoly(d,l-lactic acid-co-glycolic acid)
PVA	poly(vinyl alcohol)
RGD	arginyl-glycyl-aspartic acid
ROP	ring opening polymerisation
RT	real time
τ	shear stress
τ_D	delay time
T_{GS}	gel-suspension transition temperature
THF	tetrahydrofurane
TMS	tetramethylsilane
TPO-L	ethyl (2,4,6-trimethylbenzoyl) phenyl phosphinate
T_{SG}	sol-gel transition temperature
UPW	ultra-pure water
UV	ultra-violet
VIS	visible

9 LIST OF FIGURES

10 LIST OF TABLES